



**Calhoun: The NPS Institutional Archive**

---

Theses and Dissertations

Thesis Collection

---

1999-09

**Implementing a low-complexity, adaptive, layered  
video coder for video teleconferencing**

**Skretkowicz, Steven J.**

Monterey, California. Naval Postgraduate School

---

<http://hdl.handle.net/10945/8511>



Calhoun is a project of the Dudley Knox Library at NPS, furthering the precepts and goals of open government and government transparency. All information contained herein has been approved for release by the NPS Public Affairs Officer.

**Dudley Knox Library / Naval Postgraduate School  
411 Dyer Road / 1 University Circle  
Monterey, California USA 93943**

<http://www.nps.edu/library>

**NAVAL POSTGRADUATE SCHOOL  
Monterey, California**



**THESIS**

**IMPLEMENTING A LOW-COMPLEXITY, ADAPTIVE,  
LAYERED VIDEO CODER FOR VIDEO  
TELECONFERENCING**

by  
Steven J. Skretkowicz

September 1999

Thesis Advisor:  
Second Reader:

Murali Tummala  
Robert E. Parker, Jr.

**Approved for public release; distribution is unlimited.**

**19991207 035**

<b>REPORT DOCUMENTATION PAGE</b>			<i>Form Approved</i> OMB No. 0704-0188	
Public reporting burden for this collection of information is estimated to average 1 hour per response, including the time for reviewing instruction, searching existing data sources, gathering and maintaining the data needed, and completing and reviewing the collection of information. Send comments regarding this burden estimate or any other aspect of this collection of information, including suggestions for reducing this burden, to Washington headquarters Services, Directorate for Information Operations and Reports, 1215 Jefferson Davis Highway, Suite 1204, Arlington, VA 22202-4302, and to the Office of Management and Budget, Paperwork Reduction Project (0704-0188) Washington DC 20503.				
<b>1. AGENCY USE ONLY (Leave blank)</b>		<b>2. REPORT DATE</b> September 1999		<b>3. REPORT TYPE AND DATES COVERED</b> Master's Thesis
<b>4. TITLE AND SUBTITLE</b> IMPLEMENTING A LOW-COMPLEXITY, ADAPTIVE, LAYERED VIDEO CODER FOR VIDEO TELECONFERENCING			<b>5. FUNDING NUMBERS</b>	
<b>6. AUTHOR(S)</b> Skretkowitz, Steven J.				
<b>7. PERFORMING ORGANIZATION NAME(S) AND ADDRESS(ES)</b> Naval Postgraduate School Monterey, CA 93943-5000			<b>8. PERFORMING ORGANIZATION REPORT NUMBER</b>	
<b>9. SPONSORING / MONITORING AGENCY NAME(S) AND ADDRESS(ES)</b>			<b>10. SPONSORING / MONITORING AGENCY REPORT NUMBER</b>	
<b>11. SUPPLEMENTARY NOTES</b> The views expressed in this thesis are those of the author and do not reflect the official policy or position of the Department of Defense or the U.S. Government.				
<b>12a. DISTRIBUTION / AVAILABILITY STATEMENT</b> Approved for public release; distribution is unlimited.			<b>12b. DISTRIBUTION CODE</b>	
<b>13. ABSTRACT (Maximum 200 words)</b> Real-time interactive video applications, such as video teleconferencing, present difficult challenges to network designers due to strict quality of service constraints and the limitations of traditional video compression schemes. These limitations reveal themselves notably in two areas: poor error robustness and a lack of flexibility when dealing with multicast scenarios over heterogeneous networks. A more promising approach that improves error robustness while also offering a solution to the network heterogeneity problem is to employ a layered video codec. This thesis presents the implementation of a new layered video codec scheme. Block updating coupled with an aging algorithm is used in this scheme to select macroblocks for transmission. Block updating selects macroblocks that have changed due to scene motion, and the aging algorithm ensures that an entire frame is transmitted within a set time interval. Layering is accomplished through application of the fast Haar transform and/or the discrete cosine transform. Layer assignments are made by grouping bands of coefficients with similar variances. Quantization and encoding for motion video employs both an industry standard and uniform quantization with a custom variable length coding table. For static slides, uniform quantization and a second custom variable length coding table are employed. Rate control is accomplished via the reduction of a four-dimensional operational distortion surface to a one-dimensional optimal curve implemented as a simple table lookup of quantizers.				
<b>14. SUBJECT TERMS</b> Video Teleconference, Layered Video Coder			<b>15. NUMBER OF PAGES</b> 125	
			<b>16. PRICE CODE</b>	
<b>17. SECURITY CLASSIFICATION OF REPORT</b> Unclassified	<b>18. SECURITY CLASSIFICATION OF THIS PAGE</b> Unclassified	<b>19. SECURITY CLASSIFICATION OF ABSTRACT</b> Unclassified	<b>20. LIMITATION OF ABSTRACT</b> UL	



Approved for public release; distribution is unlimited.

**IMPLEMENTING A LOW-COMPLEXITY, ADAPTIVE, LAYERED VIDEO  
CODER FOR VIDEO TELECONFERENCING**

Steven J. Skretkowicz  
Lieutenant, United States Navy  
B.S., Memphis State University, 1992

Submitted in partial fulfillment of the  
requirements for the degree of

**MASTER OF SCIENCE IN ELECTRICAL ENGINEERING**

from the

**NAVAL POSTGRADUATE SCHOOL  
September 1999**

Author: \_\_\_\_\_

Steven J. Skretkowicz

Approved by: \_\_\_\_\_

Murali Tummala, Thesis Advisor

Robert E. Parker Jr., Second Reader

Jeffrey B. Knorr, Chairman  
Department of Electrical and Computer Engineering



## ABSTRACT

Real-time interactive video applications, such as video conferencing, present difficult challenges to network designers due to strict quality of service constraints and the limitations of traditional video compression schemes. These limitations reveal themselves notably in two areas: poor error robustness and a lack of flexibility when dealing with multicast scenarios over heterogeneous networks.

A more promising approach that improves error robustness while also offering a solution to the network heterogeneity problem is to employ a layered video codec. This thesis presents the implementation of a new layered video codec scheme. Block updating coupled with an aging algorithm is used in this scheme to select macroblocks for transmission. Block updating selects macroblocks that have changed due to scene motion, and the aging algorithm ensures that an entire frame is transmitted within a set time interval. Layering is accomplished through application of the fast Haar transform and/or the discrete cosine transform. Layer assignments are made by grouping bands of coefficients with similar variances. Quantization and encoding for motion video employs both an industry standard and uniform quantization with a custom variable length coding table. For static slides, uniform quantization and a second custom variable length coding table are employed. Rate control is accomplished via the reduction of a four-dimensional operational distortion surface to a one-dimensional optimal curve implemented as a simple table lookup of quantizers.





## TABLE OF CONTENTS

<b>I. INTRODUCTION.....</b>	<b>1</b>
<b>A. BACKGROUND.....</b>	<b>1</b>
1. Multimedia Communication and Tactical Video Teleconference (VTC)...	1
2. Video Compression and Robustness .....	2
3. Traditional Video Codecs.....	4
4. Receiver-Based Layered Multicast (RLM) .....	5
<b>B. THESIS OBJECTIVE.....</b>	<b>6</b>
<b>C. THESIS ORGANIZATION.....</b>	<b>7</b>
<b>II. LAYERED VIDEO CODER DESIGN CONSIDERATIONS.....</b>	<b>9</b>
<b>A. VIDEO STREAM STRUCTURAL HIERARCHY.....</b>	<b>9</b>
<b>B. TRANSFORM CODING.....</b>	<b>10</b>
1. Discrete Cosine Transform (DCT).....	11
2. Discrete Wavelet Transform (DWT).....	13
3. Comparison of Transforms.....	15
<b>C. QUANTIZATION TECHNIQUES .....</b>	<b>16</b>
1. Human Visual System (HVS) Weighting .....	17
2. Bit Allocation .....	17
<b>D. ENTROPY ENCODING.....</b>	<b>18</b>
<b>E. FRAME CODING.....</b>	<b>19</b>
<b>F. MEASURING QUALITY .....</b>	<b>20</b>
<b>III. LAYERED VIDEO CODECS.....</b>	<b>23</b>
<b>A. LAYERED CODING SCHEMES .....</b>	<b>23</b>
<b>B. A LOW-COMPLEXITY, ADAPTIVE CODER FOR TACTICAL VTC.....</b>	<b>25</b>
1. Temporal Compression via Block Updating .....	26
2. Aging Algorithm .....	29
3. Layering Strategy .....	32
4. Quantization and Entropy Encoding .....	41

5. Generating Customized VLC Tables .....	44
6. Rate-Distortion Relationship .....	45
7. Bit Rate Control .....	49
8. Scene Change Detection and Scene Type Determination.....	51
<b>IV. RESULTS .....</b>	<b>53</b>
<b>V. CONCLUDING REMARKS .....</b>	<b>61</b>
A. CONCLUSIONS .....	61
B. FUTURE WORK.....	62
<b>APPENDIX A. MOTION VIDEO VARIABLE LENGTH CODING .....</b>	
<b>TABLE (VLC).....</b>	<b>63</b>
<b>APPENDIX B. STATIC SLIDE VARIABLE LENGTH CODING .....</b>	
<b>TABLE (VLC).....</b>	<b>69</b>
<b>APPENDIX C. MATLAB CODE LIBRARY .....</b>	<b>73</b>
<b>LIST OF REFERENCES .....</b>	<b>103</b>
<b>INITIAL DISTRIBUTION LIST .....</b>	<b>107</b>

## LIST OF FIGURES

Figure I-1: Simple VTC Multicast with Two Active and Two Passive Nodes.....	2
Figure I-2: Overview of Layered Coder/Decoder.....	5
Figure I-3: Adapting to Network Heterogeneity Using RLM.....	6
Figure II-1: Basic Components of a Video Coder.....	9
Figure II-2: Organizational Hierarchy for Compressed Video.....	10
Figure II-3: Frequency Interpretation of DCT Coefficients.....	13
Figure II-4: Structural Decomposition of Image Elements [4].....	13
Figure II-5: Octave-Based Wavelet Decomposition.....	15
Figure II-6: HVS-Based Luminance Quantization Matrix [4].....	17
Figure III-1: Sample "Talking Head" Video Frame.....	24
Figure III-2: Basic Layered Video Coder Using the DWT.....	24
Figure III-3: Functional Block Diagram of Proposed Layer Coder.....	26
Figure III-4 Block Search Order; a.) Clockwise and b.) X-pattern.....	28
Figure III-5: Second Order FHT Decomposition of a Macroblock.....	34
Figure III-6: Subband Variances after a First Order Analysis (Motion Video).....	35
Figure III-7: Subband Variances after a Second Order Analysis (Motion Video).....	36
Figure III-8: Partitions Resulting from Merge Algorithm (Motion Video).....	37
Figure III-9 Final Layering Scheme for Motion Video Sequences.....	38
Figure III-10: Subband Variances after a First Order Analysis (Static Slides).....	39
Figure III-11: Subband Variances after a Second Order Analysis (Static Slides).....	39
Figure III-12: Partitions Resulting from Merge Algorithm (Static Slides).....	40
Figure III-13: Final Layering Scheme for Static Slide Sequences.....	40
Figure III-14: Partitions after Merging Similar Non-Contiguous Partitions.....	41
Figure III-15: Partitions for Quantizing Purposes (Static Slides).....	41
Figure III-16: Quantization and Coding for Motion Video Macroblocks.....	42
Figure III-17: Quantization and Coding for Static Macroblocks.....	44
Figure III-18: Rate Distortion Curve with Possible Optimal Solution.....	46
Figure III-19: Operational Rate Distortion Curve (Motion Video).....	47

Figure III-20: Reduced Operational Rate-Distortion Curve (Motion Video). .....	48
Figure III-21: Quantizer Table Triplet Values (Motion Video). .....	48
Figure III-22: Operational Rate-Distortion Curve (Static Slides). .....	49
Figure III-23: Operational Rate Control Curve (Motion Video). .....	50
Figure IV-1: Original and Reconstructed Frames from a Motion Video Sequence. ....	53
Figure IV-2: Original and reconstructed Frames from a Static Video Sequence. ....	54
Figure IV-3: Bit Rates for (a) Fixed Quantization and (b) Bit Rate Control. ....	55
Figure IV-4: pSNR for (a) Fixed Quantization and (b) Bit Rate Control. ....	57
Figure IV-5: Comparison of Error Resilience. ....	58

## LIST OF TABLES

Table I-1: Tactical VTC Multimedia Requirements. ....	7
Table III-1: Significance and Determination of DWT Subbands.....	33
Table III-2: Scan Order for Run-Length Encoding Quantized Coefficients. ....	43
Table IV-1: Rate Controlled and Uncontrolled Motion Video Sequence Statistics.....	57



## LIST OF ABBREVIATIONS, ACRONYMS, AND SYMBOLS

$a_1$	first order FHT average analysis vector
$B$	bit allocation per frame
$\bar{B}$	average bit allocation per frame
$\beta$	bit rate control parameter
$d_1$	first order FHT detail analysis vector
$D$	distortion
$\Delta B_{inter}$	bit allocation error (or deviation)
$\Delta Q_i$	change in quantizer table entry
$\Delta \sigma^2$	variance comparison metric
$f$	frame rate
$f(i,j)$	pixel block
$F(u,v), F_{uv}$	coefficient block
$F_{quv}$	quantized coefficient block
HH	subband via first order FHT analysis; retains diagonal detail of image
HHHH	subband via second order FHT analysis; retains diagonal detail of HH subband
HHHL	subband via second order FHT analysis; retains vertical edge detail of HH subband
HHLH	subband via second order FHT analysis; retains horizontal edge detail of HH subband
HHLL	subband via second order FHT analysis; retains lowpass content of HH subband
HL	subband via first order FHT analysis; retains vertical edge detail of image
HLHH	subband via second order FHT analysis; retains diagonal detail of HL subband
HLHL	subband via second order FHT analysis; retains vertical edge detail of HL subband
HLLH	subband via second order FHT analysis; retains horizontal edge detail of HL subband
HLLL	subband via second order FHT analysis; retains lowpass content of HL subband
$K$	maximum peak-to-peak pixel value
$k_i$	subband $i$
$L$	layer
LH	detail matrix via first order FHT analysis; retains horizontal edge detail
LHHH	subband via second order FHT analysis; retains diagonal detail of LH subband
LHHL	subband via second order FHT analysis; retains vertical edge detail of LH subband

LHLH	subband via second order FHT analysis; retains horizontal edge detail of LH subband
LHLL	subband via second order FHT analysis; retains lowpass content of LL subband
LL	average matrix via first order FHT analysis; retains lowpass content
LLHH	subband via second order FHT analysis; retains diagonal detail of LH subband
LLHL	subband via second order FHT analysis; retains vertical edge detail of LH subband
LLLH	subband via second order FHT analysis; retains horizontal edge detail of LH subband
LLLL	subband via second order FHT analysis; retains lowpass content of LL subband
$M$	total number of macroblocks in a frame
$\bar{M}$	average number of macroblocks chosen per frame in test video sequences
$\bar{M}_{age}$	average number of macroblocks chosen per frame by the aging algorithm
$N_b$	Total number of subbands created by recursive application of FHT
$P$	Partition
$q_1$	first quantizing parameter
$q_2$	second quantizing parameter
$q_3$	third quantizing parameter
$Q_{uv}$	quantizer step size at position $(u,v)$
$R$	bit rate
$R_c$	bit rate constraint
$R_o$	arbitrary bit rate
$R_{target}$	target bit rate
$\sigma^2$	variance
$\sigma_{max}^2$	maximum variance of all subbands
$\sigma_{min}^2$	minimum variance of all subbands
$x$	original image
$\hat{x}$	reconstructed image
$x_0$	original data vector with regard to FHT analysis
$x_{n,m}$	pixel value in current block
$x_{n,m}^R$	pixel value in reference block

1-D	One Dimensional
2-D	Two Dimensional
3-D	Three Dimensional
4-D	Four Dimensional
ASD	Absolute Sum of Differences



ATM	Asynchronous Transfer Mode
bpf	bits per frame
bpp	bits per pixel
CELP	Code Excited Linear Prediction
DCT	Discrete Cosine Transform
DPCM	Differential Pulse Code Modulation
DWT	Discrete Wavelet Transform
EOB	End-Of-Block
FHT	Fast Haar Transform
fps	frames per second
GOB	Group of Macroblocks
HVS	Human Visual System
IP	Internet Protocol
IT-21	Information Technology for the 21 <sup>st</sup> Century
ITU	International Telecommunications Union
ITU-T	ITU Telecommunications Standardization Sector
JPEG	Joint Photographic Experts Group
kbps	kilobits per second
KLT	Karhunen-Loeve Transform
LAN	Local Area Network
M-JPEG	Motion-JPEG
MPEG	Moving Pictures Experts Group
MSE	Mean Squared Error
pSNR	peak Signal-to-Noise Ratio
QCIF	Quarter Common Intermediate Format
QoS	Quality of Service
RLE	Run-Length Encoding
RLM	Receiver-Based Layered Multicast
rt-VBR	real-time Variable Bit Rate
SAD	Sum of Absolute Differences
SNR	Signal-to-Noise Ratio
UD	Uniquely Decipherable
VLC	Variable-Length Code or Variable Length Coding
VOD	Video On Demand
VTC	Video Teleconferencing



## ACKNOWLEDGEMENT

The work presented in this thesis is the culmination of support from many people. I am especially fortunate to have had the opportunity to work with a most dedicated advisor, Murali Tummala. He was instrumental in the completion of this work, and I am grateful for his guidance and insight. I have also had the honor and pleasure to work with another outstanding individual, Robert (Bob) E. Parker, Jr. Throughout the entire process of this work from concept to completion, Bob was forever unselfish with his valuable time. Finally, I acknowledge the support of my wife, Karen, and children, Elizabeth and Christopher. Words cannot express the gratitude I have for their patience and love.

## I. INTRODUCTION

### A. BACKGROUND

Video teleconferencing (VTC) is expected to contribute significantly to the US Navy's Information Technology for the 21<sup>st</sup> Century (IT-21) initiative. IT-21 seeks to change the paradigm to warfighting from a platform-centric approach to a network-centric approach, where information superiority is leveraged with smart weapons in order to achieve the desired result more effectively. The goal of IT-21 is to link all US Forces together in a network that enables transmission of voice, video, and data from individual workstations seamlessly to both local and remote users [1][2]. Employing VTC over a tactical network at the battle group level caters to several useful applications, such as collaborative planning, distance learning, remote maintenance and telemedicine.

#### 1. Multimedia Communication and Tactical Video Teleconference (VTC)

In general, multimedia communications are either unicast or multicast. Unicast represents peer-to-peer communications while multicast represents  $m$  to  $n$  communications where  $m$  ranges from 1 to  $n$ . Unicast includes any client-server applications, such as video on demand (VOD) or IP telephony. Multicast examples include distance learning and remote conferencing. The tactical VTC scenario considered here is inherently a multicast application running over a heterogeneous, wireless network. Here, "heterogeneous" implies that a connection traverses a series of links (each imposing potentially different bandwidths), and the recipient workstations differ in capability and capacity; "wireless" implies an internetwork of wireline local area networks (LANs) connected by at least one wireless channel. As such, each transmitter transmits to multiple receivers in the multicast group. The multicast group consists of some combination of active participants that are allowed to transmit and passive participants that only receive. For example, the problem of transmitting multicast,

multimedia traffic over ATM networks was examined in [3]. This situation is illustrated in Figure I-1.

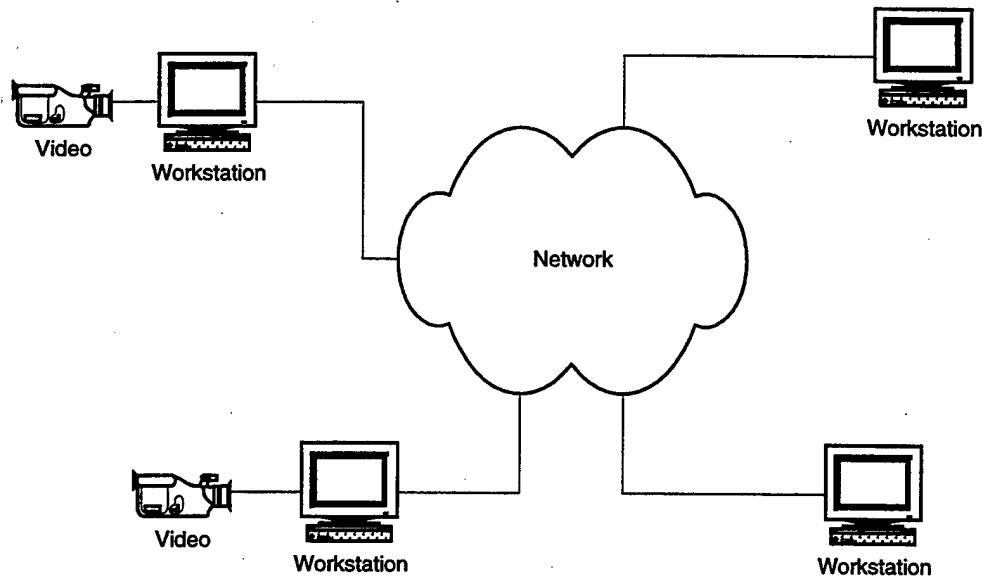


**Figure I-1: Simple VTC Multicast with Two Active and Two Passive Nodes.**

While the network described here affords large bandwidth within each shipboard LAN, VTC realizes its true value only if implemented within the entire battleship. It is because the wireless channel constrains both the bit rate and the bit error rate (each of which, in turn, impacts the robustness of the VTC application) that the tactical VTC network presents challenges not encountered with wireline networks and provides a hostile environment for traditional video codecs.

## **2. Video Compression and Robustness**

Since video and audio, to a lesser degree, are bandwidth intensive, the signals must undergo video coding prior to transmission, trading a reduction in bandwidth for a reduction in quality. Because the human visual system (HVS) places greater relative importance on lower frequencies than higher frequencies, typical motion video is perceived as primarily lowpass [4]. Therefore, lossless two-dimensional (2-D) transform methods are used to create a frequency domain representation of an image. The HVS perceptive properties can then be exploited by quantizing the resulting coefficients to varying degrees of precision with higher precision allotted to the lower frequency

coefficients. Quantization reduces the dynamic range of the coefficients and loses information, but it enables fewer bits to represent the coefficients. Usually, many of the higher frequency coefficients are zeroed out via this quantizing process; runs of zeroes are created. Because zeros need not be explicitly represented, run-length encoding (RLE) is utilized to generate a more compact representation of the quantized coefficients, which is subsequently replaced by a more efficient lossless variable length code (VLC). These techniques are collectively called spatial compression. Spatial compression is the basis of image compression standards like that of the Joint Photographic Experts Group (JPEG).

A video codec may simply treat each frame of a video as a separate still image and subject it to spatial compression independently from the other frames. This approach is known as intraframe coding. An example is Motion-JPEG (M-JPEG). Intraframe coding has the advantage of superior error resilience since decode errors are confined strictly to the current frame. Its disadvantage is that compression gain with acceptable image quality is limited to approximately 0.5 bits per pixel (bpp) [4].

For a given quality, higher compression gains are realized if the video codec exploits the high degree of correlation that video frames tend to exhibit on a frame-to-frame basis. This is called interframe coding, and it eliminates redundancy by coding only the differences in successive frames. The compression gains achieved by interframe coding vary in relation to the degree and type of motion that occurred between successive frames. Nearly static-content frames exhibit high correlation and result in high compression gain while highly dynamic-content frames have little correlation and result in less compression gain. If two successive frames have no correlation, perhaps due to a scene change, interframe coding performs no better than intraframe coding and typically performs worse due to the overhead required to track motion. The disadvantage to interframe coding results from the dependency between frames at the decoder. If errors occur in the current frame, the errors tend to propagate among frames as well as spatially within frames [5][6]. Consequently, video codecs like that of the Moving Pictures

Experts Group (MPEG) incorporate both types of compression techniques in an attempt to increase compression gain and bound error propagation.

### **3. Traditional Video Codecs**

Low bit rate video coding standards such as H.261 and H.263 perform best in homogeneous, unicast environments. The video server negotiates a desired Quality of Service (QoS) consistent with the desired video quality and available bandwidth prior to delivery. Since network conditions are rarely static, the received video quality typically changes due to dropped or incomplete frames caused by losses within the network. With the implementation of a closed loop control scheme via feedback reports from the recipient, the server can react to the changing network conditions and adjust the quantization, frame size, or frame rate in order to vary the bit rate.

However, when traditional video codecs are applied in a wireless, multicast, heterogeneous environment, shortcomings are revealed. First, the traditional scheme relies on guaranteed bandwidth for delivery, trading bandwidth for quality. Selecting an appropriate quality (and therefore required bandwidth) poses a dilemma in a heterogeneous network. Since each user is reached by a different path on the network, each experiences different levels of congestion. Even with feedback, the controllable application is faced with a quandary in determining how to make adjustments. Sending high quality, high bandwidth video supports some users but leaves low bandwidth recipients with degraded video due to high packet loss. If the lowest common denominator is supported instead, all recipients are forced to view lower quality video, and the high bandwidth links are underutilized. Clearly, meeting the varied expectations with a single video stream is impractical and transmitting multiple video streams with gradations in quality demands a much greater bandwidth expense.

Second, the poor error robustness demonstrated by traditional low bit rate video coders is especially troublesome since retransmission is not practical in a real-time application. Finally, feedback itself is undesirable in a low bit rate network. Feedback employed with the goal of mitigating congestion actually consumes available bandwidth, causes an additional load on constrained nodes, and increases congestion further.

#### 4. Receiver-Based Layered Multicast (RLM)

A promising approach that offers a solution to the network heterogeneity problem while offering some improvement in error robustness is the receiver-based layered multicast (RLM) scheme proposed by McCanne et al. [7]. RLM employs a layered video codec that transmits video in scalable layers that progressively refine quality. An independently decodable base layer is generated that guarantees a minimum acceptable quality. Separate enhancement layers increase quality in a hierarchical manner. With RLM, each recipient can decode just the base layer for low, but acceptable, quality or add one or more enhancement layers to improve quality as bandwidth and hardware permit. This idea is illustrated in Figure I-2.

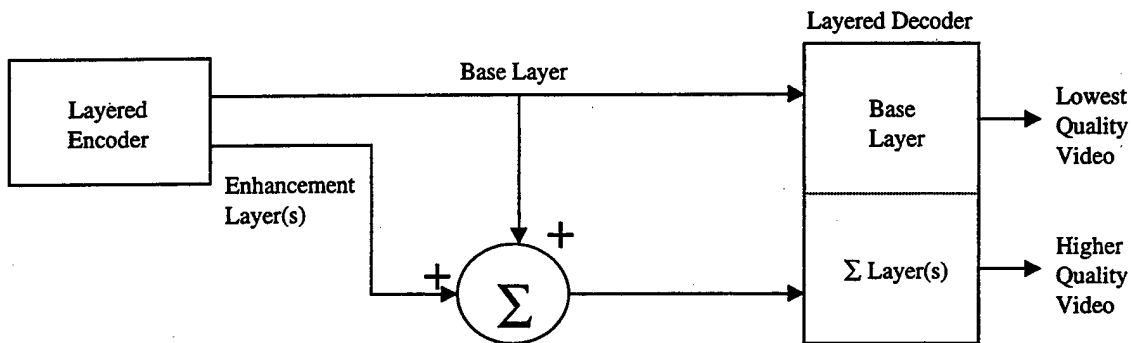


**Figure I-2: Overview of Layered Coder/Decoder.**

RLM represents a starting point for designing an integrated approach to improving robustness. The layered structure slightly reduces the effects of congestion because a particular node only needs to carry subscribed layers. Unsubscribed layers can be dropped. Figure I-3 illustrates this concept. Furthermore, earlier work by Rhee and Gibson indicates that layered video exhibits improved resilience to bit errors introduced during transmission because spreading bit errors across multiple layers has less negative impact on the reconstructed video [8].



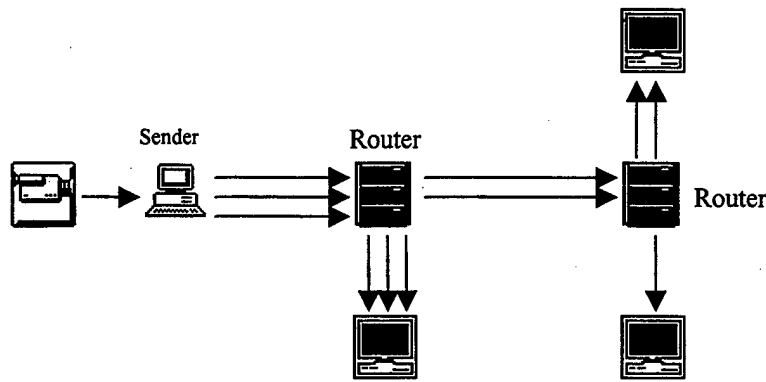


**Figure I-3: Adapting to Network Heterogeneity Using RLM.**

## B. THESIS OBJECTIVE

The main objective of this thesis is to implement in Matlab<sup>1</sup> the new layered video coding scheme for a tactical VTC proposed by Parker [9] [10] for use in multicast, heterogeneous, wireless, asynchronous transfer mode (ATM) networks. The tactical VTC session is assumed to consist of low-motion video, such as a “talking head” in the style of a typical newscast and static displays in the style of an overhead presentation. No assumption is made about the relative proportions of the two types of content; the session could be all low-motion video, a sequence of static displays, or any combination of the two types in any order.

The complete specifications of the coder are detailed in Table I-1 [9]. For the implementation in this thesis, a color depth of 8-bit grayscale is evaluated, but the technique can be expanded to include 4:2:0 sub-sampled 24-bit color. Audio compression to 8 kbps or less may be accomplished via code excited linear prediction (CELP) speech coding, but it is not addressed further in this work. Error robustness is provided via a block updating scheme that limits the impact of decoder errors. Layering is accomplished by judiciously grouping the frequency domain content obtained from the fast Haar transform (FHT) and/or the discrete cosine transform (DCT); the exact method of frequency decomposition depends on the video content. Handling both motion video

<sup>1</sup> Matlab is a registered trademark of The MathWorks, Inc.

and static slides with a single coder requires significant flexibility and compromise since the frequency characteristics of each are different. Therefore, the coder is optimized to handle each type of content separately – separate layering and separate, custom VLC tables. Finally, the bit rate control issue is examined, and an approach that reduces an  $n$ -dimensional rate control problem to a simple table lookup is implemented.

VTC Stream	Parameter	Value
Video	Bandwidth	64-96 kbps
	Resolution	176×144 (QCIF)
	Frame Rate	10 fps
	Color Depth	8-bit gray/4:2:0 24-bit color
Audio	Bandwidth	< 8 kbps

**Table I-1: Tactical VTC Multimedia Requirements.**

### C. THESIS ORGANIZATION

Chapter II considers techniques for coding video. A general discussion of video stream structural hierarchy, transform coding methods, quantization techniques, entropy encoding, frame coding, and quality measurement is presented. Chapter III presents the specific techniques utilized in coding both motion video and static slides. Chapter IV presents results. Conclusions and recommendations for future study are given in Chapter V. Appendix A and Appendix B provide the custom VLC tables used with motion video and static slides, respectively. Appendix C is a Matlab code library of the layered video coder implementation.



## II. LAYERED VIDEO CODER DESIGN CONSIDERATIONS

The basic components of a video coder are shown in Figure II-1. This chapter begins with an explanation of video stream hierarchy and then discusses each of the component parts displayed in Figure II-1. Motion compensation is present only if the coder attempts to exploit frame-to-frame correlation. Otherwise each frame is processed independently. The chapter concludes by addressing a method for quantifying the amount of distortion introduced by the processing.

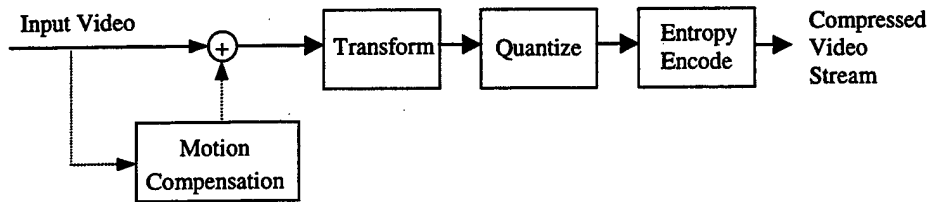


Figure II-1: Basic Components of a Video Coder.

### A. VIDEO STREAM STRUCTURAL HIERARCHY

A video stream is organized into a hierarchy of logical components. Although the specific organizational scheme varies with the particular coder under consideration, some of the most common components are the following.

A frame or picture is the basic display unit. It is a sampled version of the original scene taken at a particular instant in time. Each frame is composed of a rectangular array of pixels or points within the frame. Each pixel contains a data structure indicating its luminosity or color. The dimensions of the array define the picture resolution, given as columns  $\times$  rows, such as the ITU-T defined QCIF resolution of  $176 \times 144$ . Pixels within a frame are organized, in order of increasing size, into blocks, macroblocks, and groups of macroblocks (GOBs). A block is an  $8 \times 8$  array of pixels; a macroblock is a  $16 \times 16$  array of pixels or, equivalently, four blocks. A frame may be considered as rows of

macroblocks. One or more contiguous rows of macroblocks are termed a GOB. This hierarchy is illustrated in Figure II-2.

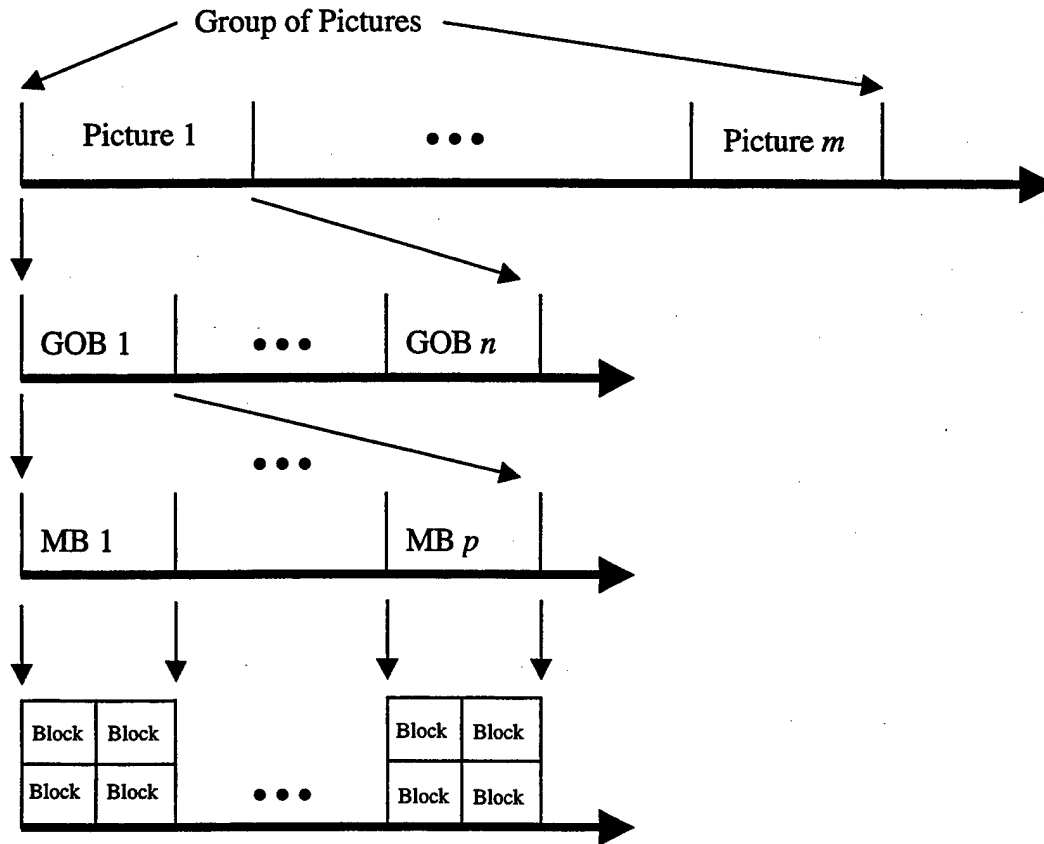


Figure II-2: Organizational Hierarchy for Compressed Video.

## B. TRANSFORM CODING

Although compression through direct scalar quantization of pixel values is possible, it is inefficient. An alternative approach is to use transform coding. Because contiguous pixels within a frame tend to be highly correlated, the application of a suitable linear transform<sup>2</sup> to decorrelate the pixels yields two primary advantages. The first is a property termed “energy packing” efficiency. The second is that the resulting coefficients are more conducive to perceptual-based quantization schemes.

<sup>2</sup> The transform should be lossless and invertible. Lossless means that no information is lost through application of the transform. Invertible means that the original information is recoverable.

A signal is decorrelated if the application of a transform causes the signal's autocorrelation matrix to become diagonal; that is, it uncorrelates the resulting coefficients. The optimal transform tightly packs all the energy (information) into the minimum number of coefficients possible, resulting in the highest energy packing efficiency. Arranging these  $N$  coefficients in decreasing order of magnitude and retaining only the first  $k$  coefficients gives the least distortion as measured by mean squared error (MSE) compared to any other set of  $k$  coefficients. Similarly, a given level of quantization of the decorrelated coefficients results in the least distortion of the original data [11]. Because certain transform coefficients may hold greater perceptual relevance by the HVS, this dependency can be exploited by utilizing a frequency-based transform and then quantizing— a lossy process – with a step size proportional to the perceptual importance of each coefficient.

### **1. Discrete Cosine Transform (DCT)**

Theoretically, the discrete-time Karhunen-Loeve transform (KLT) provides the greatest energy packing efficiency [11]. However, two liabilities preclude the use of the KLT in video compression. First, the KLT is extremely computationally intensive – requiring order  $N^2$  operations. Second, the KLT is signal dependent – requiring a separate eigenvector calculation for each transformed data block. Instead, transforms that approach the energy packing efficiency of the KLT and possess more efficient algorithms are utilized in video coders.

A widely used transform for image processing is the two-dimensional (2-D) discrete cosine transform (DCT). The 2-D DCT provides energy packing performance very close to that of the KLT and can be implemented with fast algorithms that reduce the computational effort to the order of  $N \log_2 N$  [4]. A frame is transformed by partitioning the frame into  $N \times N$  regions of pixels and applying the 2-D DCT to each individual region.  $N$  can be any integer provided that integer multiples of  $N$  equals the overall dimensions of the frame. Because the correlation among contiguous pixels tends to decrease with increasing size of the  $N \times N$  region which, in turn, decreases the resulting compression gain, the typical  $N \times N$  size used with the 2-D DCT is  $8 \times 8$  (a block).

Denoting the original block as  $f(i,j)$  and the coefficient block by  $F(u,v)$ , the 2-D DCT is given by [4]

$$F(u,v) = \frac{2}{N} C(u)C(v) \sum_{i=0}^{N-1} \sum_{j=0}^{N-1} f(i,j) \cos\left(\frac{(2i+1)\pi u}{2N}\right) \cos\left(\frac{(2j+1)\pi v}{2N}\right), \quad (\text{II-1})$$

where

$$C(x) = \begin{cases} \frac{1}{\sqrt{2}}, & x = 0 \\ 1, & \text{otherwise.} \end{cases} \quad (\text{II-2})$$

The inverse DCT is given by

$$f(i,j) = \frac{2}{N} \sum_{u=0}^{N-1} \sum_{v=0}^{N-1} C(u)C(v) \cos\left(\frac{(2i+1)\pi u}{2N}\right) \cos\left(\frac{(2j+1)\pi v}{2N}\right) F(u,v). \quad (\text{II-3})$$

The result is a block of 64 coefficients having a spatial frequency interpretation as shown in Figure II-3. The  $F(0,0)$  coefficient represents the DC contribution and the remaining 63 coefficients represent the AC contribution. The different elements of an image map into the frequency domain as shown in Figure II-4 [4]. The application of the 2-D DCT to an  $8 \times 8$  block, where there is typically little variation from pixel to pixel, leads to a predominance of lowpass content in the frequency domain. Given this condition, the magnitudes of the AC coefficients are largest in the region around the DC coefficient and diminish with increasing spatial frequency.

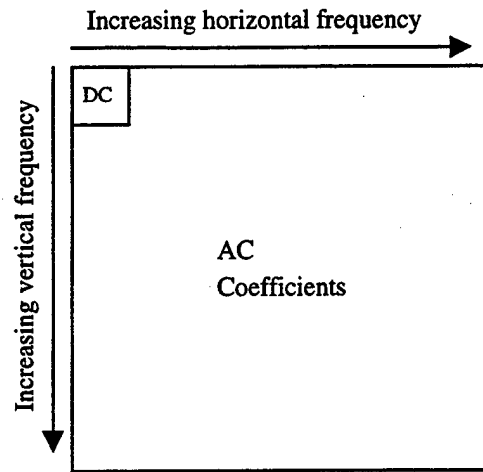


**Figure II-3: Frequency Interpretation of DCT Coefficients.**

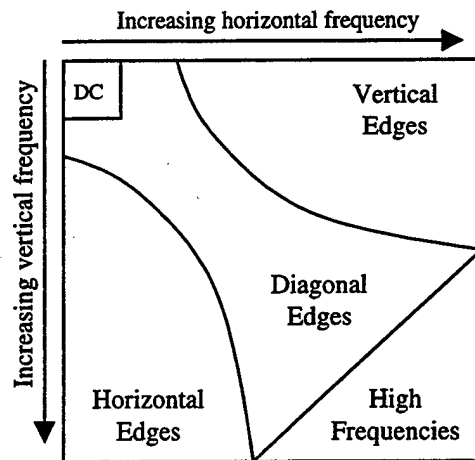


**Figure II-4: Structural Decomposition of Image Elements [4].**

## 2. Discrete Wavelet Transform (DWT)

Wavelet coding is another technique for compressing still images and has been shown to offer slightly better image quality than DCT-based schemes for similar levels of compression at the cost of greater computational complexity [12]. Applying a wavelet transform to an image transforms that image into a “multifrequency component representation,” where each component has its own frequency characteristics and spatial features.<sup>3</sup> A discrete wavelet transform (DWT) filters and decimates an image into

<sup>3</sup> The wavelet transform, like the 2-D DCT, is lossless and invertible.



separate subbands of coefficients containing a mixture of the high frequency and low frequency details. Image decomposition is accomplished via two analysis filters. The first extracts the low frequency content, the signal average; the second extracts the high frequency content, the signal details.

The simplest example of a DWT is the fast Haar transform (FHT) [13]. It is described by its signal average equation,

$$a_1(n) = \frac{1}{2}(x_0(2n) + x_0(2n+1)) \quad (\text{II-4})$$

and its signal detail equation,

$$d_1(n) = \frac{1}{2}(x_0(2n) - x_0(2n+1)), \quad (\text{II-5})$$

where  $x_0$  is the original data vector, and vectors  $a_1$  and  $d_1$  are the first order analysis (decomposition) vectors. If  $x_0$  contains  $2^L$  elements, applying Equations II-4 and II.5 generates analysis vectors of length  $2^{L-1}$ .

Referring to Figure II-5, the LL subband is calculated by applying the average equation to the columns and rows of the image. The LL subband retains the lowpass information from the original image and presents a coarse representation of the original image. Because typical images have lowpass characteristics, most of the energy from the image is represented in this subband. The HL subband is calculated by applying the average equation to the columns of the image and the detail equation to the rows. The HL subband retains the vertical edge details from the original image. Typically, less energy from the original image is represented in the HL subband compared to that of the LL subband. The LH and HH subbands are found analogously with LH retaining horizontal edge details and HH retaining the diagonal edge details. The HH subband typically has the lowest energy content. In fact, in some applications the HH subband is discarded in its entirety [14].

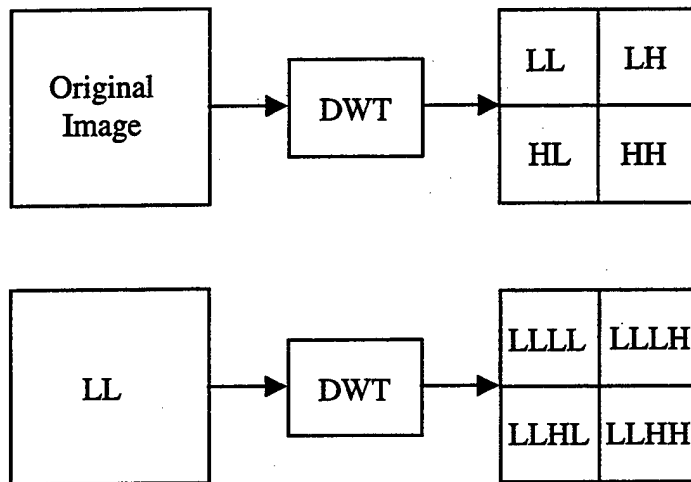


**Figure II-5: Octave-Based Wavelet Decomposition.**

In order to differentiate the frequency content of an image further, a second DWT can be applied. Still referring to Figure II-5, the effect of a second order octave-based decomposition obtained by applying the same analysis filters to the LL subband is illustrated. This increase in the number of subbands allows tailoring additional stages in the coder to emphasize the perceptually important details over less perceptual background noise as will be discussed in greater detail later.

### 3. Comparison of Transforms

Since the 2-D DCT is applied to pixel blocks within a frame that are subsequently quantized, it has a tendency to create “blocking” artifacts that disturb the continuity of the reconstructed frame. The same effect also leads to the presence of “ringing” artifacts around sharp edges. In contrast, the wavelet transforms typically are applied to the entire image and separate the entire image into regions of high and low frequency content. These regions may be quantized and coded independently and result in more efficient bit allocation. This produces a more visually pleasing, smoother reconstructed image compared to that obtained via a 2-D DCT at a comparable peak signal-to-noise ratio (pSNR). In general, at comparable pSNRs, wavelet transform coders offer compression gains superior to that of DCT-based coders [12].

However, several drawbacks have limited the utility of wavelet-based video compression. Wavelets achieve quality superior to DCT-methods by processing the

entire image or frame, but traditional video coders exploit temporal correlation at a subframe (usually macroblock) level. Although the error block could be transformed via a DWT, no significant advantage has been determined over the DCT, and the computational effort is greater [12]. However, the frequency decomposition offered by DWTs provides a powerful basis for layered video coding.

### C. QUANTIZATION TECHNIQUES

After the transform, the coefficients are quantized. Quantization is a lossy process used to reduce precision and zero out some coefficient values. The benefit is that each coefficient can then be represented with fewer bits. However, the information loss is not recoverable, and the loss is manifested as distortion within the reconstructed image. This distortion is termed quantization noise.

The typical quantization scheme, uniform quantization, involves dividing each coefficient  $F_{uv}$  by the quantizer step size  $Q_{uv}$  and rounding the result to the nearest integer to produce a quantized coefficient  $F_{quv}$  as follows [15]:

$$F_{quv} = \text{nearest integer} \left( \frac{F_{uv}}{Q_{uv}} \right). \quad (\text{II-6})$$

The values used in image reconstruction are then  $F_{quv}$  multiplied by the step size. However, as Equation II-6 implies, the step value may be adjusted for each particular coefficient with  $Q_{uv}$  now representing elements of a quantizer matrix. Choosing the appropriate step size involves a trade-off between acceptable error and desired compression. Employing a small step size yields low quantization noise but little compression. The opposite is the case for a large step size. Although uniform quantization is often used, the choice is suboptimal since the individual coefficients are not distributed uniformly [16]. However, two broad approaches are employed to refine the selection of step size: HVS weighting and bit allocation strategies. HVS weighting heuristically refines the step size based on perceptual relevance while bit allocation strategies attempt to spread errors optimally across all coefficients.

## 1. Human Visual System (HVS) Weighting

Because the HVS places greater relative importance on lower frequencies than higher frequencies, step sizes based on HVS modeling are selected such that lower frequencies coefficients are quantized more finely while higher frequency coefficients are quantized more coarsely [4]. The HVS is also more acute to luminous intensity than chromatic intensity. Therefore, different quantizer matrices are developed for each. An example of a luminance quantization matrix widely used in JPEG compression is given in Figure II-6 [4]. The dimensions match the 8×8 block size used with the 2-D DCT. In application of a quantizer matrix, the entire matrix can be scaled by a multiplicative constant in order to scale quantization noise and compression while maintaining the relative importance among the coefficients.

$$\begin{bmatrix} 16 & 11 & 10 & 16 & 24 & 40 & 51 & 61 \\ 12 & 12 & 14 & 19 & 26 & 58 & 60 & 55 \\ 14 & 13 & 16 & 24 & 40 & 57 & 69 & 56 \\ 14 & 17 & 22 & 29 & 51 & 87 & 80 & 62 \\ 18 & 22 & 37 & 56 & 68 & 109 & 103 & 77 \\ 24 & 35 & 55 & 64 & 81 & 104 & 113 & 92 \\ 49 & 64 & 78 & 87 & 103 & 121 & 120 & 101 \\ 72 & 92 & 95 & 98 & 112 & 100 & 103 & 99 \end{bmatrix}$$

Figure II-6: HVS-Based Luminance Quantization Matrix [4].

## 2. Bit Allocation

Using a bit allocation approach, the value of the step size is chosen to minimize distortion within a bit budget. It is a classical resource allocation problem, where the fundamental trade-off in quantization is between rate (number of bits) and distortion (approximation error) formalized as rate-distortion theory. Several sophisticated algorithms utilize Lagrange methods applied to arbitrary rate-distortion curves. Of these, a popular approach is varying the step size in proportion to the variance of the coefficient

[17]. However, bit allocation schemes, regardless of the methodology, do not account for the sensitivity to different spatial frequency characteristics of human visual perception.

#### D. ENTROPY ENCODING

Further compression can be realized through a lossless process called entropy encoding that removes redundant information. The simplest style of entropy encoding is run-length encoding (RLE). With RLE, a data set is parsed to locate sequences of repeated values. Any such sequence is replaced by a codeword consisting of a delimiter, the value, and the number of times the value is repeated. The longer the sequence of the repeated value, the greater the available compression. Following quantization, many elements of a coefficient block typically have a value of zero. Often many high frequency rows and columns are completely composed of zeros. Accordingly, it is advantageous to scan the coefficient block in a manner as to produce the longest runs of zeros. In JPEG compression, scanning the quantized coefficient block as a vector in zigzag fashion starting with the DC coefficient down to the  $F_{8,8}$  coefficient has been shown to increase the run-length of zeros [4]. Since the repeated value here is known (0), an adaptation of the basic codeword scheme cited above consists of the run-length of zeros followed by the magnitude of the next non-zero value. If there is no remaining non-zero value in the block, a special end-of-block (EOB) codeword is used instead.

After RLE, the quantized coefficient block is represented by a set of codewords, where each codeword represents a symbol drawn from a larger source alphabet. Variable-length coding (VLC) minimizes the average codeword length by assigning shorter codewords to the most probable symbols and longer codewords to the least likely occurring symbols while maintaining each uniquely decipherable (UD). Huffman coding is the most widely used entropy-encoding algorithm and is guaranteed to produce a minimum average length, UD code [15]. The Huffman algorithm uses each symbol's probability of occurrence and builds a prefix code using an optimum binary-branching tree. Since both the coder and decoder need to use the same coder and generating a Huffman table is computationally expensive, standard tables are normally pre-defined

using data drawn from test images. Optimal compression is no longer guaranteed, but encoding and decoding are faster, and the need to transmit the VLC table is avoided.

## E. FRAME CODING

As discussed previously, intraframe coding compresses each frame of a video as a separate, still image. Its advantage is superior error resilience; its disadvantage is limited compression gain. Interframe coding exploits frame-to-frame correlation by coding only the difference in successive frames, thereby allowing the potential for higher compression gain than that achieved by intraframe coding alone. The disadvantage to interframe coding is in robustness since decode errors can propagate between frames and spatially within a frame depending on the algorithm.

Because of the compression required for the target VTC scenario, strict intraframe coding is not an option. Therefore, a robust algorithm for interframe coding is needed. Several source-coding techniques used to exploit temporal redundancy, such as motion compensation, differential pulse code modulation (DPCM) and block updating, are discussed in [4]. For a robust application in a real-time, heterogeneous, multicast environment, block updating was judged the most promising and is discussed further.

Interframe coding via block<sup>4</sup> updating is a variation on intraframe coding. With block updating, each block in the current frame is compared to the corresponding block in the previous frame, and a distance metric is calculated. If the metric is above a threshold value, that block is intracoded and transmitted. Otherwise, no further consideration is given to that block; it is skipped. Thus, block updating conserves bandwidth by coding and transmitting only those blocks that have changed perceptually since the previous frame [18]. In low-motion video, such as the "talking head" scenario, motion is confined to a relatively small region within a frame and the background remains static. A significant bandwidth savings is possible.

---

<sup>4</sup> In this context, "block" implies an  $N \times N$  pixel region, not necessarily  $8 \times 8$ .

In order for block updating to be effective, a suitable distance metric must be defined. Common distance metrics employed are MSE, sum of absolute differences (SAD), and absolute sum of differences (ASD) [4] [14].

Utilizing block updating alone for a tactical VTC, where end-users may join a session that is already in progress, has a liability. End-users joining late will never receive a block that does not exceed the selection threshold, thus leaving them with a partially reconstructed video. In order to mitigate this affect, block updating can be combined with an aging algorithm that periodically forces block updates. Such an algorithm guarantees a full scene reception within some set interval [14].

## F. MEASURING QUALITY

Given that video coders trade compression gain for image quality, quantifying the level of distortion introduced is useful in evaluating different coding schemes. A useful measure of image distortion  $D$  is the MSE between the original ( $x$ ) and reconstructed ( $\hat{x}$ ) images [4]:

$$D = \frac{1}{MN} \sum_{n=1}^N \sum_{m=1}^M (x_{n,m} - \hat{x}_{n,m})^2 \quad (\text{II-7})$$

Using distortion  $D$ , the signal-to-noise ratio (SNR) is determined as

$$SNR = 10 \log_{10} \frac{\sigma^2}{D}, \quad (\text{II-8})$$

where  $\sigma^2$  is the variance of the original image. The most widely published measure of image quality is the peak signal-to-noise ratio given by

$$pSNR = 10 \log_{10} \frac{K^2}{D}, \quad (\text{II-9})$$

where  $K$  is the maximum peak-to-peak value in the image, 255 for the typical 8-bit image. For example, a typical peak SNR for a typical JPEG encoded grayscale image is 28 dB at 0.5 bpp.

Using MSE as a measure of image quality does have drawbacks. MSE does not directly define perceptual quality since all errors are given equal weight. Two

compression techniques yielding the same MSE for an image may deliver slight differences in perceptual quality.





### III. LAYERED VIDEO CODECS

#### A. LAYERED CODING SCHEMES

Parker [9] discusses several previous approaches to layered video coding. They can be classified into three fundamental categories: component-based layering, spatial-based layering, and frequency-based layering.

Component-based layered coders transmit a base layer and usually a single enhancement layer. A traditional DCT-based coder (yielding some set quality) supplies the base layer. The enhancement layer improves this quality by either providing augmenting information to the base layer or correcting distortion present within the base layer. Two such schemes are proposed by Rhee and Gibson [8] [20]. Implicit in the component-based approach is that the enhancement layer may duplicate information already present in the base layer.

Spatial-based layered coders partition a frame into hierarchical areas of interest and encode each area separately. For example, the "talking head" frame shown in Figure III-1 may be partitioned into two areas of interest with the speaker being of primary interest and the remainder of the frame being of secondary interest. With spatial-based layering, relatively more bandwidth would be allocated to the region encompassing the speaker with the balance of available bandwidth being apportioned to the rest of the frame. Bahl and Hsu [21] have proposed a coder that incorporates content-sensitive spatial decomposition and multiresolution coding. The difficulty with implementing a spatial-based coder is creating the hierarchical areas of interest dynamically while minimizing the overhead required to identify their shifts relative to the layer assignments.



**Figure III-1: Sample “Talking Head” Video Frame.**

Frequency-based layered coders decompose a frame into subbands and then arrange the subbands into individual layers. The frequency decomposition may be applied to the entire frame or individual macroblocks within the frame. Each layer may contain one or more subbands. The base layer contains at least the low frequency subband but may also contain higher frequency subbands in order to improve base layer quality. Figure III-2 illustrates this concept using the DWT to decompose a frame, where the LL subband alone constitutes the base layer, the LH and HL subbands are combined into a first enhancement layer, and the HH subband constitutes the second enhancement layer.

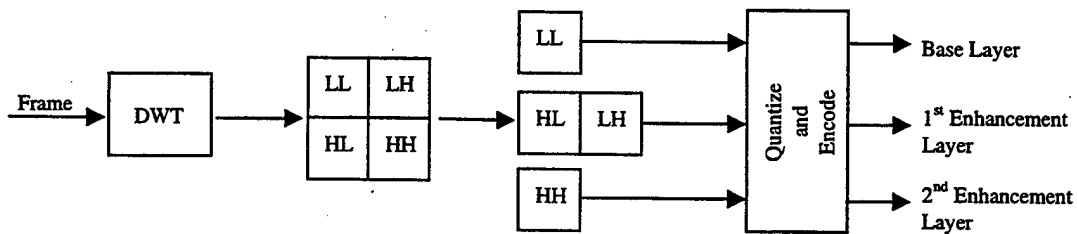


**Figure III-2: Basic Layered Video Coder Using the DWT.**

The principle advantages to frequency-based layering are its extensibility and flexibility. Further decomposing the frame through application of the DWT to each subband depicted in Figure III-2 creates a total of 16 subbands. Repeated application of the DWT to these subbands creates even more subbands. With a larger number of subbands, there is increased flexibility in the manner in which they can be assigned to

layers. This, in turn, facilitates exploiting each subband's perceptual importance. Additionally, a greater number of subbands permits a greater possible number of layers. Three coders that utilize the frequency-based approach are discussed in [14], [22], and [23].

## **B. A LOW-COMPLEXITY, ADAPTIVE CODER FOR TACTICAL VTC**

As cited above, several diverse approaches to designing layered coders have been proposed; each emphasizes different network architectures or applications to varying degrees. However, there is neither a consensus in identifying a preferred, structured approach nor a consensus in quantifying those parameters that make a layered coder *effective*. This section presents the development and implementation of a new layered coder that is specifically tailored for the tactical VTC scenario where limited transmission bandwidth is available, and the robustness of transmission is at a premium.

Both the characteristics of the tactical VTC application and the desire to quantify effectiveness guide the strategy for developing and implementing the new layered coder. Specifically, the application yields five requirements. The coder must 1) provide a video stream characterized by the bandwidth, resolution, frame rate, and color depth detailed in Table I-1, 2) optimize compression adaptively for both low motion video and static slides, 3) provide a low complexity architecture to minimize coding delays and power requirements, 4) provide error resilient decoding at high packet loss rates, and 5) constrain bit rate to a predetermined average.

The guiding factors stemming from the desire to quantify effectiveness are twofold. First, the coder must provide a base layer with acceptable quality and two (or more) enhancement layers that progressively improve *perceptual* quality. Second, the coder must minimize the bitstream overhead required to accommodate the layering structure. A functional diagram of the implemented coder is shown in Figure III-3. Each component is addressed in follow on sections.

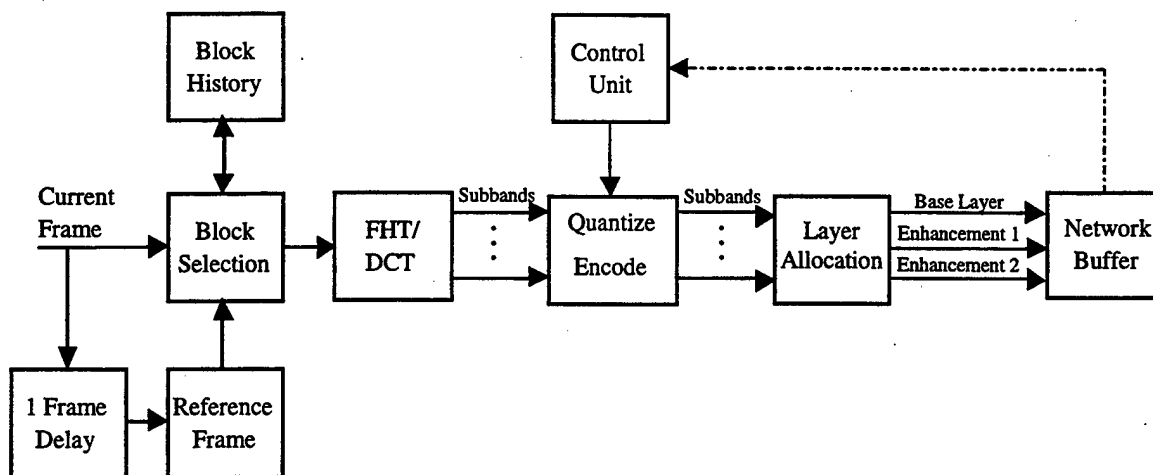


**Figure III-3: Functional Block Diagram of Proposed Layer Coder.**

### 1. Temporal Compression via Block Updating

Temporal compression is accomplished via block updating applied at the macroblock level. Only those macroblocks exhibiting sufficient change on a frame-to-frame basis are encoded. Although block updating has been shown to yield inferior compression performance relative to motion prediction algorithms, block updating was chosen because the performance differential is small when low activity video is considered [24], and greater robustness is realized because temporal error propagation is greatly limited and spatial error propagation is eliminated. Block updating also negates the need for the locally decoded reference frame that is common to motion prediction schemes. This greatly simplifies the coder by eliminating the overhead required by the performance of an inverse quantization/transform at the coder. Block selection, as considered here, is solely with regard to motion video sequences. Since static slide sequences exhibit little or no motion, block selection via motion detection is of limited utility there. Indeed, transmissions during static sequences result from considerations presented in the next section, where macroblock aging is discussed.

Sufficient change between corresponding, frame-successive macroblocks is determined by calculating a distance metric between them and comparing the result to a threshold. The distance metric utilized is the non-normalized ASD given by:

$$ASD = \left| \sum_{m=1}^M \sum_{n=1}^N (x_{m,n} - x_{m,n}^R) \right|, \quad (III-1)$$

where  $x_{n,m}$  represents the pixel value within the current block while  $x_{m,n}^R$  represents the pixel value in the reference block. The primary reasons for choosing ASD over other metrics are twofold. First, the ASD is computationally efficient compared to MSE and SAD. The ASD employs only additions and subtractions and a single absolute value operation. MSE requires expensive multiplication operations – making it ill suited to real-time applications. SAD requires the same number of additions and subtractions as ASD, but it requires  $M \times N - 1$  more absolute value operations. Second, since the ASD takes a single absolute value of a sum, it acts as an accumulator and provides a lowpass filtering effect that removes noise in pixel intensities introduced through video capture. This smoothing prevents the threshold from being exceeded spuriously in otherwise static regions of the frame sequence whereas the nonlinear operations performed on a per-pixel basis in MSE and SAD tend to accumulate this noise energy and yield spurious block selections. Thus, the ASD metric allows bandwidth to be more effectively devoted to regions of interest [14].

Two independent elements affect video quality and, therefore, the required bit rate: adequate motion detection (to prevent “jerky” reconstructed video) and control of distortion introduced through quantization. The goal in motion detection is to select the *maximum* block selection threshold that adequately captures motion. In the video sequences examined, a threshold of 160 (for ASD) proved adequate for detecting perceptual motion and resulted in an average of 24.8 macroblocks selected per frame.

Further considering the issue of computational expense, the ASD metric is applied to individual  $8 \times 8$  blocks within the macroblock; the first block to exceed the threshold triggers macroblock selection and ends the search. This avoids the expense of examining the remaining blocks of the macroblock. Additionally, since the HVS acuity is more sensitive to changes in luminous than chromatic intensity [4], distance calculations are confined to the luminous component of each pixel even if chromatic information were available.

Since motion in VTC scenes tends to be confined to discrete objects within the scene (as opposed to scene motion caused by a camera pan), search efficiency is slightly affected by the order in which the individual blocks are examined. The approach that proved more efficient in the test video sequences considered here is to maximize the distance between the first two blocks examined. As shown in Figure III-4, two search patterns were compared: a clockwise search starting from the upper left block and an X-pattern search that examines the upper left block followed by the lower right. Given that a macroblock was selected for transmission, the X-pattern resulted in a 2.5% decrease in the average number of blocks examined per frame.

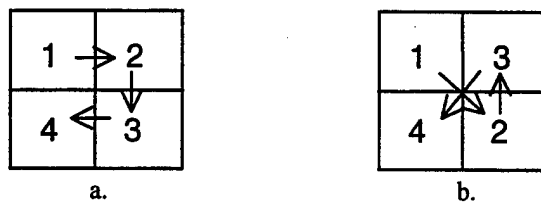


**Figure III-4 Block Search Order; a.) Clockwise and b.) X-pattern.**

Still greater search efficiency is realized by using the X-pattern search and varying the starting block of each macroblock to match the anticipated motion at that point in the frame. Because motion in VTC sequences is fairly confined, macroblocks tend to be selected in the same manner frame-to-frame. For example, a speaker shifts left or right and/or slightly up or down. Therefore, search speed is increased by having the search algorithm remember the identity of the specific block, termed the “anchor”, which caused a particular macroblock to be selected in the previous frame. For the subsequent distance metric calculations, search begins at the anchor. If the anchor again causes selection or if the macroblock is not selected, the anchor identity is unchanged. If another block causes selection, the anchor identity is updated. Using this search scheme produced an additional 20% reduction in the number of blocks examined for selected macroblocks. A more complex approach not examined here is to remember the two blocks that most frequently cause selection and tailor the search accordingly.

## 2. Aging Algorithm

Utilizing this block updating scheme alone for macroblock refreshment exposes some undesirable performance characteristics. One such consequence is termed hysteresis. Consider an arbitrary macroblock whose content is changing temporally due to the movement of an item within its spatial bounds. The item travels from its initial position along some trajectory to its final position. At some point in the trajectory, let the change in the macroblock's content be sufficient to exceed the motion-detection threshold, so the macroblock is selected for update. If the final position of the item has not yet been reached at the time of macroblock selection, the item continues movement to its destiny. Once the final position is reached, hysteresis occurs if the distance between this final position and the item's position at the last macroblock update is insufficient to force another macroblock selection; that is, the distance is less than the threshold. In this case, the displayed macroblock at the receiver is left with a persistent error. As another illustration of hysteresis, consider a frame sequence depicting only slight motion contained within an arbitrary macroblock's spatial position. If the change between successive macroblocks as calculated by the distance metric is below the threshold value, the macroblock is not selected for encoding. If several frames in the video sequence continue to depict similar slight motion below the threshold, the displayed macroblock at the receiver eventually shows a persistent error.

Another problem is in the duration the error artifacts (introduced by the channel through dropped or corrupted packets) are maintained in a receiver's reconstructed video. Error artifacts in the dynamic portion of a scene tend to last only a single frame because block updates occur frequently. However, any such error in a relatively static region tends to persist longer due to the much lower frequency of block updating there.

A final problem occurs when new participants are allowed to join a VTC already in progress (dynamic multicast). Since only those macroblocks depicting motion above the perceptual threshold are transmitted, new participants receive only a portion of the current scene. Although the portion received is the most dynamic region of frame (e.g.



the speaker), a speaker completely disassociated from the background yields an awkward reconstruction.

Complementing the block updating scheme with an aging algorithm that intermittently forces macroblock updates alleviates these problems. The general principle is that the coder monitors the number of frames since each macroblock was last encoded – its “age.” If a macroblock’s age exceeds a predetermined interval, that macroblock is flagged for encoding and transmission. Thus, the aging algorithm guarantees a maximum period between macroblock updates and bounds both the duration of hysteresis errors and the persistence of visual artifacts caused by the channel. Such bounding also ensures that new participants to a dynamic multicast session can construct an entire frame in a timely fashion.

Obviously, forcing selection of macroblocks for transmission that would not have been selected otherwise increases the bandwidth requirement, but this impact can be mitigated by the manner in which the aging algorithm is implemented. Important considerations are the following. Simply increasing the interval for macroblock selection by aging decreases the required bandwidth but increases the persistence of decode errors at receivers and prolongs the time required for new participants to receive a full frame. Merely forcing a macroblock update after  $n$  frames have passed without selection leads to an undesirable correlation in updates following scene changes. Although motion within a scene tends to disperse updates to some extent, a sufficiently static background region would still lead to correlation of a significant fraction of the block updates. The worst case is realized by a scene change where the new scene is entirely static, such as an overhead slide. In this case, the bit rate would spike every  $n$  frames. In order to avoid undesirable spikes in bit rate, it is advantageous to spread the number of macroblocks selected by aging evenly over time. This, in turn, requires a scheme that ages each block independently.

The aging algorithm developed for the coder implemented here tracks the age of each macroblock *indirectly*. Instead of counting the frames since a given macroblock was last updated, the coder maintains an update vector identifying the number of frames

remaining until each macroblock must be updated. Each value,  $m$ , in the update vector is chosen from a discrete uniform distribution in the range  $[1, n]$  and is interpreted as an update scheduled  $m$  frames in the future. Using a uniform distribution to schedule updates smoothes macroblock selection over  $n$  frames and decorrelates the selections due to aging. Choosing the aging intervals randomly also prevents events, such as scene changes, from correlating updates and causing periodic spikes in bit rate. The specific value chosen for  $n$  controls the tradeoff between the additional bandwidth required and coder responsiveness. For a given value of  $n$ , the average number of macroblocks selected through aging per frame,  $\bar{M}_{age}$ , is

$$\bar{M}_{age} = \frac{2M}{(n+1)}, \quad (\text{III-2})$$

where  $M$  is the total number of macroblocks in a frame.

The final block selection algorithm is performed by the function,  $m\_blk\_id\_xr.m$ .  $m\_blk\_id\_xr.m$  is provided in Appendix C, and it incorporates motion detection and aging as follows. As each frame is captured, the update vector entry corresponding to each macroblock is decremented by one. As each macroblock is processed for selection in a given frame, the coder examines the macroblock's entry in the update vector. If its corresponding entry has reached zero, the macroblock is selected for transmission. Otherwise, the distance metric is applied to determine if the macroblock should be selected due to motion. If either criterion is met, a new random entry is generated for that update vector position. The order of these two events is important. Since the distance metric need not be calculated if the macroblock is selected by aging, there is net decrease in the number of calculations required to select a macroblock for transmission.

For the assumed VTC video format of 176×144 QCIF,  $M$  is 99. At the assumed frame rate of 10 fps, setting  $n$  to 20 guarantees all macroblocks are encoded within two seconds and yields 9.43 as the average number of macroblocks selected through aging per frame. However, the true bandwidth impact is less than this value since some of the macroblocks selected via aging would have been selected by motion. For the test motion video sequences considered here, the average number of macroblocks selected per frame

increased to 31.4 (from 24.8 without aging). The payoff for this modest increase in bandwidth is that all the problems encountered by using the distance metric alone for macroblock selection are bounded to this duration. The duration of two seconds represents a compromise judged acceptable between the additional bandwidth required and the desired coder responsiveness.

### **3. Layering Strategy**

Macroblocks selected for transmission are decomposed in frequency using a DWT. Performing the selection process prior to the transform reduces computational cost because the transform is only applied to those macroblocks requiring transmission. The DWT was chosen since frequency decomposition, as discussed earlier, offers the most flexibility in the subsequent populating of layers. However, the task of determining a consistent, extendable scheme for determining an appropriate number of layers and the manner in which the frequency content within each macroblock was to be apportioned across those layers remains.

Parker [9] proposes a set of heuristic guidelines to determine the appropriate layer assignments and bit allocation. First, as layers are to be hierarchical in importance, layer assignments should map frequency content to that hierarchy in a manner consistent with perceptual importance. Second, the base layer must provide acceptable quality, and the addition of each enhancement layer must provide a perceptual improvement in quality. Since the broad goal in image or video coding is to remove information that is not perceptually relevant, transmitting a layer that provides no perceptual improvement in quality wastes bandwidth and is, therefore, undesirable. Third, the number of bits assigned to each layer should be substantive so that dropping a layer potentially decreases congestion in the network. Finally, the bandwidth consumed by the image data should also be sufficient to avoid an excessive relative consumption by network control symbols and overhead. This is especially critical for low bit rate video.

The DWT chosen was the fast Haar transform (FHT). The FHT has several desirable properties with regard to minimizing coder complexity. First, the FHT, as a real transform, avoids the necessity for complex arithmetic and simplifies storage.

Second, the FHT is not computationally demanding, requiring only addition, subtraction, and left- and right-shifts [13]. Finally, unlike more sophisticated wavelet transforms, the FHT does not require extending or padding the data set. However, the simplicity of the FHT may lead to blocking artifacts at high compression levels since the average and detail calculations are confined only to contiguous pixels.

Since the defining equations of the FHT and their manner of application to affect a first order frequency decomposition were discussed previously in Section II.B.2, only a summary of the first order FHT decomposition is detailed in Table III-1. The operation is accomplished via the function *fht.m* as provided in Appendix C. Again, higher order frequency decompositions may be accomplished by recursively applying the FHT to each of the subbands created by the next lower order decomposition.

Array	Detail	Horizontal Operation	Vertical Operation
LL	Lowpass	Average	Average
LH	Horizontal	Average	Detail
HL	Vertical	Detail	Average
HH	Diagonal	Detail	Detail

**Table III-1: Significance and Determination of DWT Subbands.**

Although a greater number of layers would offer more flexibility in managing quality and congestion, the coder restricts the number of layers to three. The decision to limit the number of layers to three was driven primarily by the constraint of a target bit rate in range of 64-96 kbps. At these bit rates and with each layer consuming an equal amount of bandwidth overhead, three layers appeared to be the limit in terms of producing enhancement layers that provided a perceptual improvement in quality while maintaining a base layer that rendered an acceptable quality.

Establishing a suitable layered structure for motion video sequences can be posed as the following conditional, two-part problem. Given that  $n$  layers are desired, determine the degree to which a selected macroblock is decomposed in frequency and the manner in which the resulting subbands are assigned into layers. Parker [9] proposes using a variant of a split-and-merge algorithm, which was originally proposed by Diab, et

al. [25] to identify regions of equivalent activity in the spatial domain, and applying it at the macroblock level in the frequency domain to identify region of similar energy and perceptual content. The particulars of the implementation follow, but the essence of the approach is that a selected macroblock is uniformly decomposed in frequency via the FHT, subbands of approximately equal variance are merged, and the resulting regions are apportioned into individual layers. These steps were performed on representative video sequences, and the ensuing layering structure is implemented within the coder.

Utilizing representative video sequences, each selected macroblock is uniformly decomposed in frequency by recursively applying the FHT until the desired number of subbands is obtained. The first order analysis creates four 8x8 subbands; the second order analysis produces sixteen 4x4 subbands. The third order analysis results in sixty-four 2x2 subbands. Extending the recursion to its limit yields 128 subbands consisting of a single point. In practical terms, a second order analysis as shown in Figure III-5 proved sufficient for three layers.

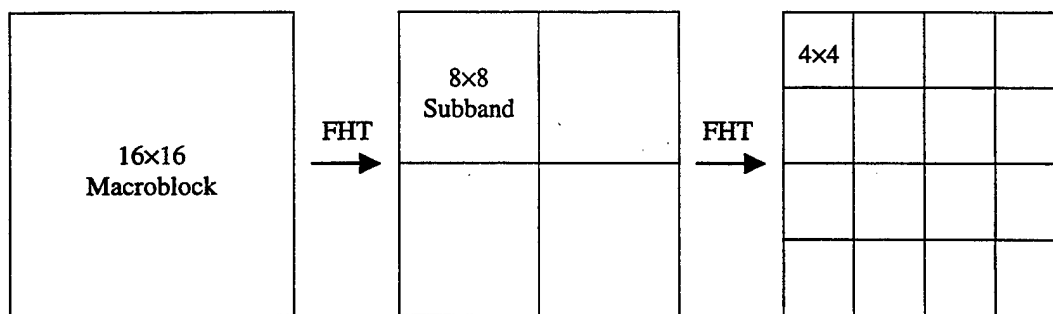


**Figure III-5: Second Order FHT Decomposition of a Macroblock.**

Next, the variance of the coefficient set composing each subband was determined across all frames of video. These variances were then used as a subband merging metric. Two benefits are afforded by employing subband variance as the merging metric. First, with motion video, the variance of coefficient sets appear to possess an inverse relationship to spatial frequency and, by extension, to perceptual importance. That is, the more perceptually relevant subbands at lower frequencies exhibit higher variances. Consequently, differences in variance provide a convenient mechanism for assigning

subbands to a layered hierarchy. Second, grouping subbands with similar variances simplifies coder architecture since each group can employ a common quantizer. Several quantization algorithms use variance as an indication of the dynamic range exhibited by coefficients and allocate bits by varying quantizer step size in inverse proportion to variance. The particulars of the quantization scheme employed are discussed in more detail later.

The subband variances calculated from a first order analysis of the test video sequences are shown in Figure III-6. Those from a second order analysis are shown in Figure III-7. As Figure III-6 illustrates, subband variance provides a good indication of the energy concentration within each subband. For instance, since motion video is characteristically lowpass, the variance is largest in the LL subband and smallest in the HH subband. By extension, subband variance therefore serves as a relative indicator of the perceptual importance among subbands – an observation that suggests subband variance should dictate layer assignments. As Figure III-7 illustrates, a second order analysis further separates the frequency content of the subband to which it is applied. The LL subband decomposes into the LLLL, LLLH, LLHL, and LLHH subbands containing the lowpass, horizontal, vertical, and diagonal edge details, respectively, which were previously lumped into the LL subband alone. Performing the second order analysis of the LH (horizontal detail) subband apportions energy in a manner symmetrical to the original first order analysis; that is, as the LH subband is found in the northeast quadrant of Figure III-6, the energy distribution attained by the second order analysis is concentrated in the northeast and northwest sub-quadrants with a slightly greater energy in the northeast sub-quadrant as shown in Figure III-7. Similar observations can be made for the HL and HH subbands. These characteristics further leverage the argument for using subband variances to make layer assignments in a hierarchical manner.

$\sigma_{LL}^2$	$\sigma_{LH}^2$	=	2891	52.0
$\sigma_{HL}^2$	$\sigma_{HH}^2$		73.3	12.4

**Figure III-6: Subband Variances after a First Order Analysis (Motion Video).**

$\sigma_{LLL}^2$	$\sigma_{LLH}^2$	$\sigma_{LHLL}^2$	$\sigma_{LHLH}^2$	2702.0	57.7	19.2	21.6
$\sigma_{LLHL}^2$	$\sigma_{LLHH}^2$	$\sigma_{LHHL}^2$	$\sigma_{LHHH}^2$	117.4	12.5	4.5	6.8
$\sigma_{HLLL}^2$	$\sigma_{HLLH}^2$	$\sigma_{HHLL}^2$	$\sigma_{HHLH}^2$	27.7	6.0	2.2	2.8
$\sigma_{HLHL}^2$	$\sigma_{HLHH}^2$	$\sigma_{HHHL}^2$	$\sigma_{HHHH}^2$	31.5	8.0	3.2	4.2

**Figure III-7: Subband Variances after a Second Order Analysis (Motion Video).**

After variance data had been gathered for each subband at the desired order of analysis, the next step was to merge adjacent subbands exhibiting similar variances into an entity termed a "partition." The criterion outlined by [9] is to merge adjacent subbands  $k_1$  and  $k_2$  when

$$\left| \log \left( \frac{\sigma_{k_1}^2}{\sigma_{k_2}^2} \right) \right| \leq \Delta\sigma^2, \quad (\text{III-3})$$

where

$$\Delta\sigma^2 = \frac{1}{N_b} \log \left( \frac{\sigma_{\max}^2}{\sigma_{\min}^2} \right), \quad (\text{III-4})$$

where  $N_b$  is the total number of subbands created by successive application of the FHT, and  $\sigma_{\min}^2$  and  $\sigma_{\max}^2$  are the minimum and maximum variances, respectively, found among all the subbands. Applying the merge algorithm to the subbands listed in Figure III-7 results in the partitions shown in Figure III-8. Assuming that subbands are statistically independent, the variance of each partition  $P_k$  is now simply the sum of the variances for the subbands  $k_i$  comprising that partition:

$$\sigma_{P_k}^2 = \sum_{k_i \in P_k} \sigma_{k_i}^2. \quad (\text{III-5})$$

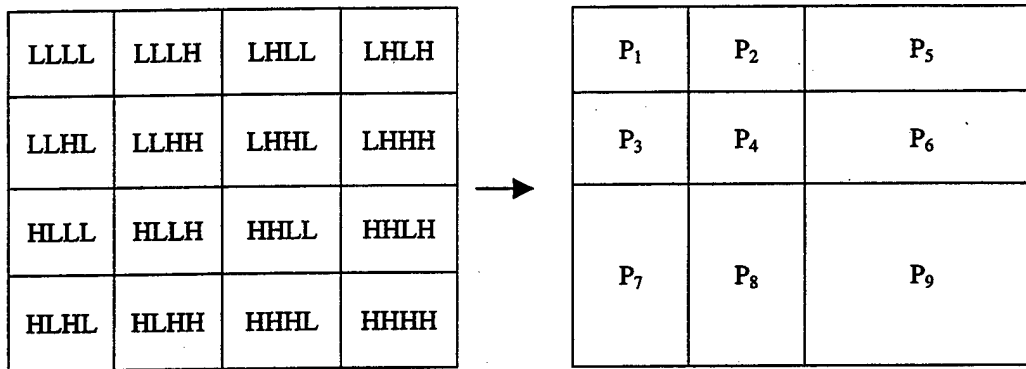


**Figure III-8: Partitions Resulting from Merge Algorithm (Motion Video).**

Next, these partitions are assigned to layers  $L_j$  until the requisite number of layers were created using the set of heuristic rules proposed in [9].

**Rule 1:** No layer may have a greater variance than a lower layer. That is, given  $N$  layers,

$$\sigma_{L_1}^2 > \sigma_{L_2}^2 > \dots > \sigma_{L_N}^2. \quad (\text{III-6})$$

**Rule 2:** Layers must be populated in order of increasing frequency. A layer may not contain a partition of lower frequency content than any layer below it.

**Rule 3:** Partitions that meet the criterion given by Equation III-3 are assigned to the same layer even if the partitions are non-contiguous.

**Rule 4:** Partitions are applied to layers in a symmetric fashion.

**Rule 5:** If more than two subbands comprising a coarser subband remain as partitions after merging and applying the above rules, all of the partitions comprising the coarser subband are merged together into one partition.



**Rule 6:** If one or more partitions is moved between layers, as required to achieve a more balanced distribution of bit rates or quality, move the partition(s) with the lowest variance if promoting to a higher layer and the partition(s) with highest variance if demoting to a lower layer.

Application of these rules to the partitions shown in Figure III-8 culminated in the final layering scheme for motion video sequences shown in Figure III-9. The base layer is essentially a lowpass-filtered version of the original macroblock, and the two enhancement layers progressively added higher frequency details. Additionally, since the LL subband retains many of the perceptual properties of the original macroblock, it was further transformed using the 2-D DCT via the function, *dct\_of\_fht.m*. This additional transform allowed the LL subband to be processed using JPEG-based quantization and encoding techniques to maximize retention of the most perceptually relevant information.

Summarizing the process as implemented in the coder, each macroblock selected for transmission is decomposed in frequency using the FHT. The LL subband is further transformed via the 2-D DCT as previously discussed and assigned to layer I. The HH subband is assigned to layer III in its entirety. The HL and LH subbands are decomposed with a second application of the FHT. The resulting subbands are then partitioned and assigned to layers II and III as appropriate.

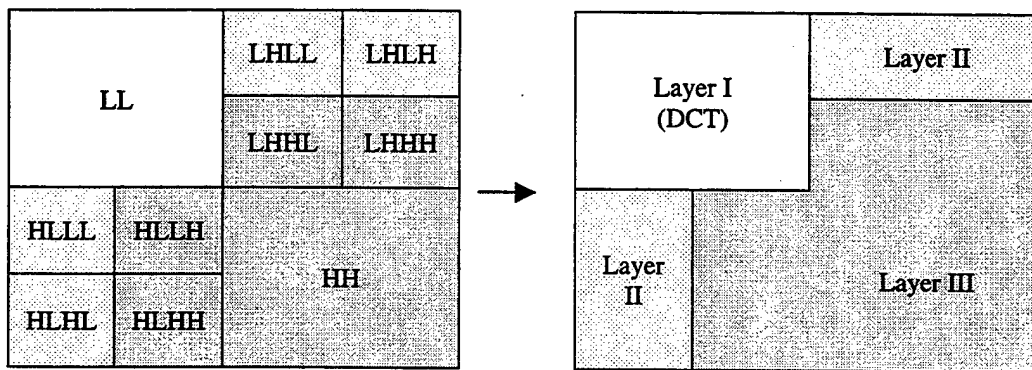


**Figure III-9 Final Layering Scheme for Motion Video Sequences.**

The situation with static slide sequences consisting of text and line drawings is much different. Sequences such as these demonstrate a greater dependency on their

higher frequency components for perceptual recognition. A hierarchical layering scheme based on the lowpass characteristics of motion video yields blurred, indistinct reconstructions until the higher frequency components are included as well. Such a structure, of course, is contrary to the principle of layered video transmission. Therefore, a separate layering scheme is needed if the video stream is to include both types of sequences.

The foregoing remarks notwithstanding, pursuing the split-and-merge algorithm still provides valuable insight. The variances of the subbands produced by a first order FHT analysis of the text and line drawing static sequences are shown in Figure III-10; those of a second order FHT analysis are shown in Figure III-11. Compared to Figure III-6 and Figure III-7 – the analogous results for motion video sequences – it is clear that energy is much more evenly distributed among subbands of static slides. In practical terms, this implies a much more complex relationship between variance and perceptual importance.

$\sigma_{LL}^2$	$\sigma_{LH}^2$	=	2613	1216
$\sigma_{HL}^2$	$\sigma_{HH}^2$		1209	610

**Figure III-10: Subband Variances after a First Order Analysis (Static Slides).**

$\sigma_{LLL}^2$	$\sigma_{LLH}^2$	$\sigma_{LHL}^2$	$\sigma_{LHH}^2$	=	1392	600.5	404.4	441.3
$\sigma_{LLL}^2$	$\sigma_{LLH}^2$	$\sigma_{LHL}^2$	$\sigma_{LHH}^2$		456.7	159.2	184.3	185.7
$\sigma_{HLL}^2$	$\sigma_{HLH}^2$	$\sigma_{HHL}^2$	$\sigma_{HHL}^2$		536.2	128.3	162.2	148.1
$\sigma_{HLH}^2$	$\sigma_{HLH}^2$	$\sigma_{HHL}^2$	$\sigma_{HHH}^2$		423.3	121.1	141.7	157.8

**Figure III-11: Subband Variances after a Second Order Analysis (Static Slides).**

Applying the split-and-merge as before results in the partitions identified in Figure III-12. Using the rules of layer assignment as before, a reasonable layering scheme might assign partitions  $P_1$ ,  $P_2$ , and  $P_4$  to layer I. However, this implementation led to a poor reconstruction. Even adding  $P_3$ ,  $P_5$ , and  $P_6$  so that the vast majority of the energy was included in the reconstructed image failed to provide acceptable quality.

Clearly contrary to the motion video case, variance alone is a poor guide to determining perceptual relevance.

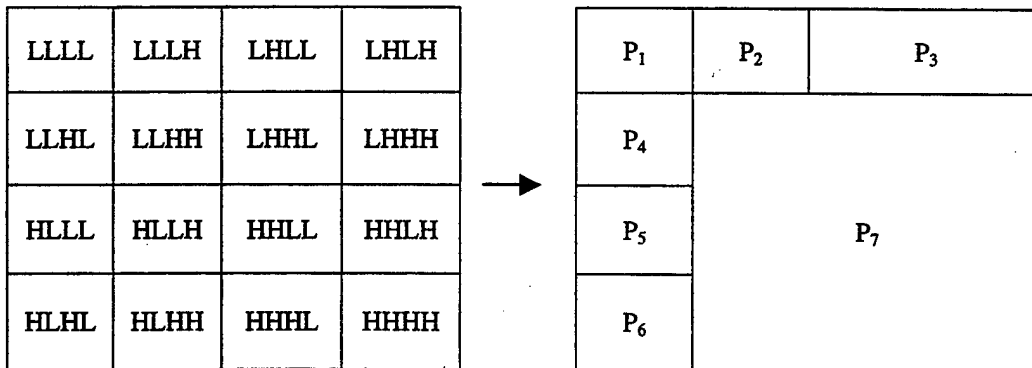


**Figure III-12: Partitions Resulting from Merge Algorithm (Static Slides).**

Producing an “effective” base layer required allocating a portion of the frequency content from each of the 8x8 subbands to it. Therefore, while maintaining symmetry in assignment, those 4x4 subbands that exhibited comparatively larger variances among the four subbands derived from the same parent subband were allocated to layer I. The remaining subbands were divided between the remaining layers in order of increasing frequency. The final layering scheme for static slide sequences is shown in Figure III-13.

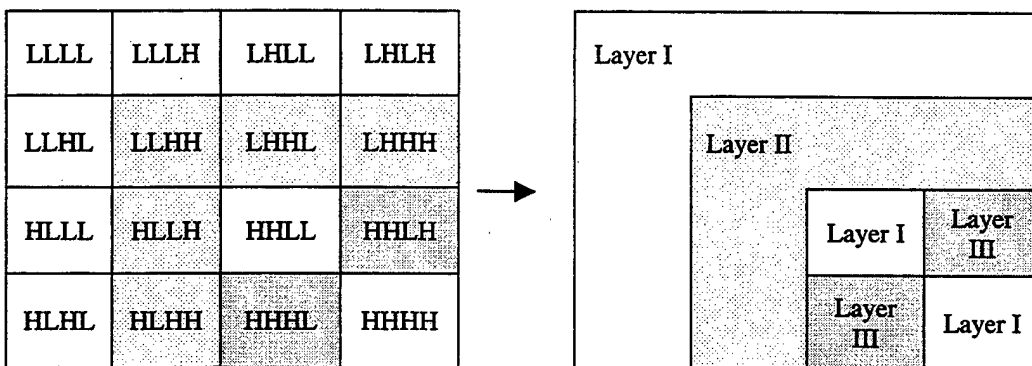


**Figure III-13: Final Layering Scheme for Static Slide Sequences.**

Although the final layering scheme does not stem directly from the partitions in Figure III-12, continued analysis on them is insightful nonetheless. Merging partitions with similar variance reduces the partitions to those shown in Figure III-14. The difference in variances of partitions P<sub>1</sub> and P<sub>2</sub> is only slightly too large to permit their

merging by the criterion of Equation III-3. The difference is small enough, however, to justify quantizing both bands with the same step size. The simplicity gained in quantizing both bands together balances any potentially suboptimal bit allocation. Therefore, the final partitions for quantization purposes are as given in Figure III-15.

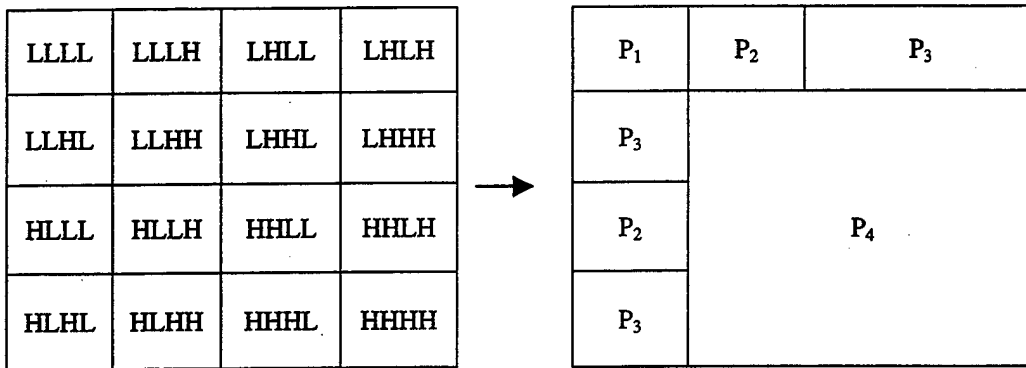


**Figure III-14: Partitions after Merging Similar Non-Contiguous Partitions.**

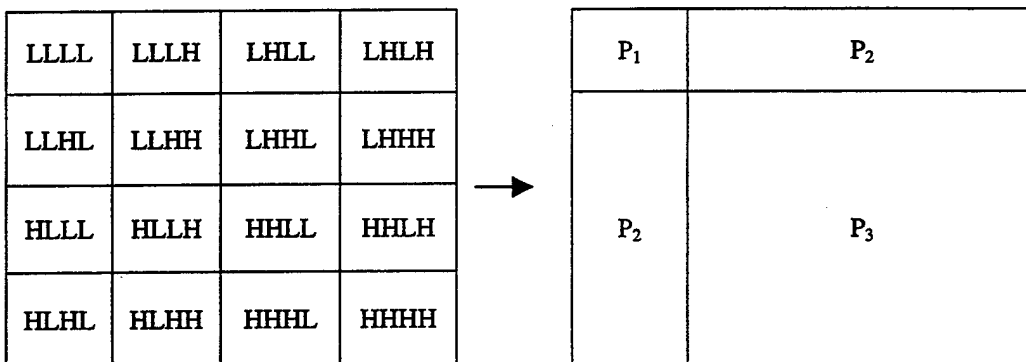


**Figure III-15: Partitions for Quantizing Purposes (Static Slides).**

#### 4. Quantization and Entropy Encoding

After the transform stage, the coefficients are quantized and subjected to entropy encoding. For motion video sequences, the process is depicted in Figure III-16. The base layer (LL subband) is quantized using the luminance matrix (Figure II-6) via the function, *quantizer\_ll.m*, run-length encoded using a zigzag scan via the function *zz\_b.m*, and converted to a VLC using the luminance VLC table suggested in [4]. The conversion to a

VLC is accomplished stepwise via three functions: *make\_it\_compact.m*, *parse\_Huff.m*, and *get\_bits\_Huff.m*. This approach leverages the LL subband's retention of the lowpass characteristics of the original macroblock. The implementation is as discussed previously in Sections II.C and II.D with the scaling factor of the quantization matrix designated as  $q_1$ <sup>5</sup>. The remaining subbands are each quantized uniformly using a common step size for all its coefficients. Using variance as an indication of the dynamic range of the coefficients within a given subband and comparing to Figure III-9, it is reasonable to quantize all the subbands composing each enhancement layer with the same step size. Therefore, the quantizer step size for layer II is set to  $q_2$ ; that of layer III is set to  $q_3$ .

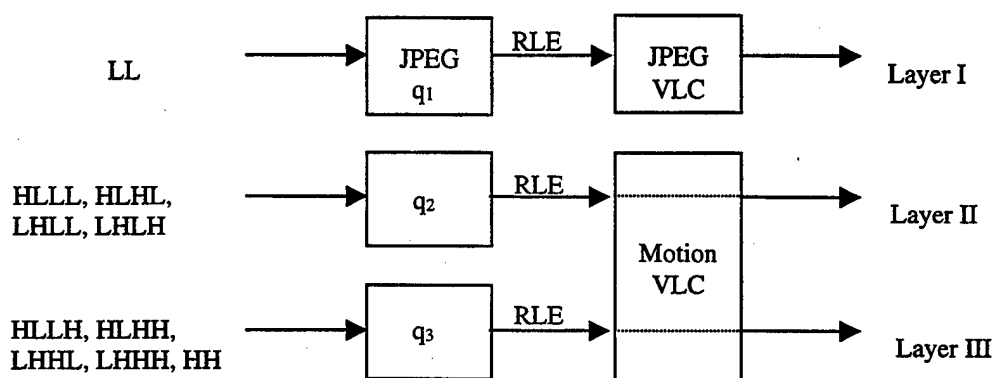


**Figure III-16: Quantization and Coding for Motion Video Macroblocks.**

Unlike the JPEG based coding of the LL subband, zigzag scanning of the quantized FHT coefficients provided no apparent coding gain. Instead, trials indicated a simpler horizontal raster scan was adequate for all subbands except HL. The HL showed a slight preference for a vertical raster scan. This seems rational given the frequency detail represented in this band. The scan orders are summarized in Table III-2 where the scan order applies to the indicated subband as well as its child subbands. (The LL entry pertains only to the coding of the static content macroblocks as discussed later, but it is included here for completeness.) Horizontal raster scans are performed by the function,

<sup>5</sup> As executed in the code, the scaling factor  $q_1$  is a parameter in *quantizer\_ll.m*. A value of 16 for  $q_1$  means no scaling of the values in Figure II-6. A value smaller than 16 results in finer quantization and less quantization noise.  $q_1$  must be positive.

*raster.m*; vertical raster scans are performed by the function, *vertical.m*. Upon completion of the run-length encoding accomplished by the functions *make\_it\_compact.m* and *parse\_3D.m*, each coefficient is represented by a set of codewords. Each codeword is then mapped to an entry in a custom VLC table via the function *get\_bits2.m*. The VLC table is provided in Appendix A. Its structure mirrors the three-dimensional (3-D) event structure employed by the H.263 coding standard [26], and the methodology of its creation is presented in the next section.

Parent Subband	Raster Scan Order
LL	Horizontal
LH	Horizontal
HL	Vertical
HH	Horizontal

**Table III-2: Scan Order for Run-Length Encoding Quantized Coefficients.**

The quantization and encoding process for selected macroblocks from static sequences is shown in Figure III-17. This process differs from the motion video process in three ways. JPEG-based quantization is not used; all sixteen subbands are supplied to one of three independent uniform quantizers with fixed step sizes of  $q_1$ ,  $q_2$ , and  $q_3$ . Contrary to the motion macroblock scheme, the step sizes are not associated with layers, but with the partitions depicted in Figure III-15. Finally, the VLC table that is provided in Appendix B and customized for static slides is used. The same three functions cited above accomplish these steps with the appropriate VLC table being employed via the argument *kind* in the function *get\_bits2.m* signaling the type of frame under consideration – motion video or static slide.

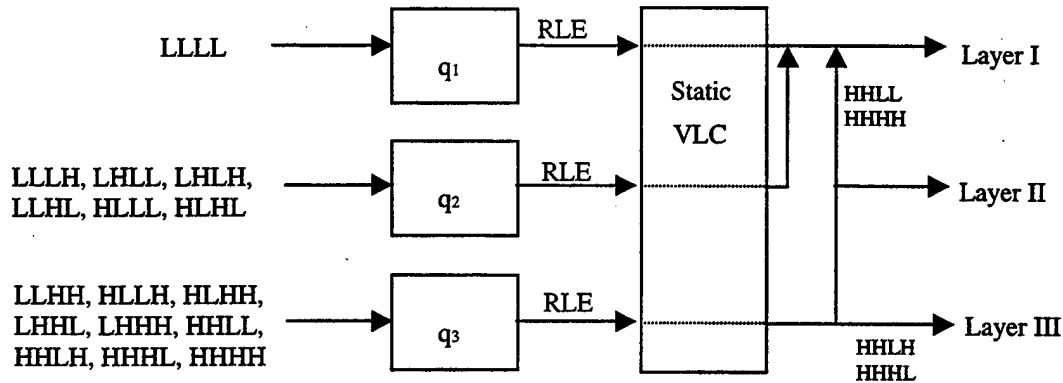


**Figure III-17: Quantization and Coding for Static Macroblocks.**

Neither Figure III-16 nor Figure III-17 indicates the presence of the control signal from the Control Unit shown in Figure III-3. The control signal allows manipulation of  $q_1$ ,  $q_2$ , and  $q_3$  as required by a bit rate control scheme. Rate control is covered later.

### 5. Generating Customized VLC Tables

The VLC coding scheme mirrors the 3-D event structure employed by the H.263 standard. Each non-zero coefficient is replaced by an equivalent event described by three RLE parameters [26]: {LAST, RUN, LEVEL}, where LAST indicates whether there are any more non-zero coefficients in the current subband, RUN indicates the number of successive zeros that precede the non-zero coefficient, and LEVEL represents the non-zero magnitude of the quantized coefficient. Each event maps to a VLC codeword to which a sign bit is appended to represent the sign of the coefficient.

Using various combinations of  $q_1$ ,  $q_2$ , and  $q_3$ , a series of representative motion video test sequences was processed. The processing followed the implementation as discussed thus far (except for the last step of mapping each codeword obtained from RLE to a VLC table.) The relative frequency of occurrence of each RLE codeword was then used to create a Huffman VLC utilizing an optimal binary-branching tree. Since every possible {LAST, RUN, LEVEL} event is not guaranteed to be formed by the set of test video sequences, the custom VLC table further mirrors the H.263 standard in that a default codeword length of 22 bits is used for any event not contained elsewhere in the table.

A Huffman code offers the following advantages. The average codeword length is minimized because the more frequently occurring events are assigned shorter codewords (fewer bits) while the less frequently occurring codewords are assigned longer codewords (more bits). Additionally, each codeword is uniquely decipherable ensuring that no codeword can be a prefix to a longer codeword.

This same procedure is used here for both motion video sequences and static slide sequences. Again, using different VLC tables for the two basic types of video content is advantageous because of the inherent difference between their frequency content and, consequently, the different makeup of the RLE codeword population.

## 6. Rate-Distortion Relationship

Compressed video is inherently variable bit rate since compression gain varies with scene activity and complexity. However, transmission channels inevitably require a constraint on bit rate due to finite channel capacity or QoS guarantees. Most commonly, bit rate is constrained to maintain a constant rate or to maintain a constant local-average bit rate over time. Many factors affect bit rate, but the most important is the tradeoff made between quantizer step size and image fidelity. A larger step size results in a lower bit rate and a larger amount of distortion. Reducing the step size increases the bit rate but reduces the amount of distortion. Rate control therefore requires evaluation of the rate-distortion relationship created by a particular coder design.

The rate control problem may be posed as a resource allocation problem in terms of the rate-distortion relationship, where the goal is to minimize distortion  $D$  for a bit rate  $R$  subject to a bit rate constraint  $R_c$  [24], i.e.,  $\min\{D\}$ , subject to  $R < R_c$ . The corresponding optimization problem is solved using Lagrangian methods and yields the optimal solution for a particular rate constraint as a point along the rate-distortion curve. Figure III-18 shows a typical rate-distortion curve and an optimal solution for a bit rate of  $R_0$ . While the true rate-distortion curve is guaranteed to be convex [17], the operational curve is influenced by the coder design including the motion-detection scheme, the quantizer design, and lossless coding gains. Therefore, rate control schemes tend to only



approximate the true rate-distortion relationship when determining a method for varying quantizer step size to achieve the desired bit rate.

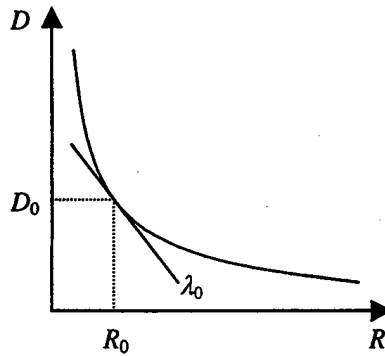


**Figure III-18: Rate Distortion Curve with Possible Optimal Solution.**

Additionally, for a layered coder where multiple quantizer parameters are employed, the corresponding multi-dimensional aspect of the rate-distortion curve complicates the rate-control problem. Assuming distortion for each layer  $i$  is additive, the rate control problem becomes minimizing

$$D = \sum_{i=0}^{N-1} D_i \quad (\text{III-7})$$

subject to

$$\sum_{i=0}^{N-1} R_i \leq R_c, \quad (\text{III-8})$$

where  $N$  is the total number of layers. The assumption of additive distortion implies that a decrease in rate requires a suitable decrease in all quantizer parameters to yield an optimal solution. However, since the rate-distortion curves in the operational coder are not necessarily convex, the approach above does not necessarily give optimal results. An alternate, albeit heuristic, approach proposed by Parker [9] is to simplify the control problem by creating a simplified, operational rate-distortion curve.

Considering the test motion video sequences, an operational distortion curve is created by first plotting total bit rate and distortion (measured by pSNR) separately through a three-dimensional space spanned by the set of candidate quantizers. This process captures the operational effect of the coder design, such as the values of the

quantizer parameters  $\{q_1, q_2, q_3\}$  and the VLC coding gain as well as any interdependence between layers, on the rate-distortion relationship. The result is best described as a four-dimensional (4-D) surface wherein both rate and distortion are functions of a triplet of quantizer parameters  $\{q_1, q_2, q_3\}$ . Recall that the first parameter represents the JPEG scaling factor while the remaining parameters represent the actual quantizer step sizes.

Next, the points representing the pSNR surface are sorted in a descending order and associated with their corresponding average bit rates and quantizer triplets. Any triplet set yielding a higher average bit rate for the same or lower pSNR is discarded. The result is an implicit vector quantization of the operational 3-D rate-distortion space. The dimensionality of the operational rate-distortion curve is therefore reduced to 1-D as shown in Figure III-19. Each point on the curve represents results from a single optimal triplet. Considering only those quantizer triplets associated with average bit rates about the target bit rates of 64-96 kbps and considering a 5% change in the average bit rate of the coarsest quantizer triplet as a reasonable control step, the operational rate-distortion curve of Figure III-19 reduces to that shown in Figure III-20. The corresponding quantizer triplets are plotted in Figure III-21. These results indicate that an optimal rate control scheme does not necessarily increase/decrease each quantizer parameter in lockstep as would be expected if distortion in each layer were independent.

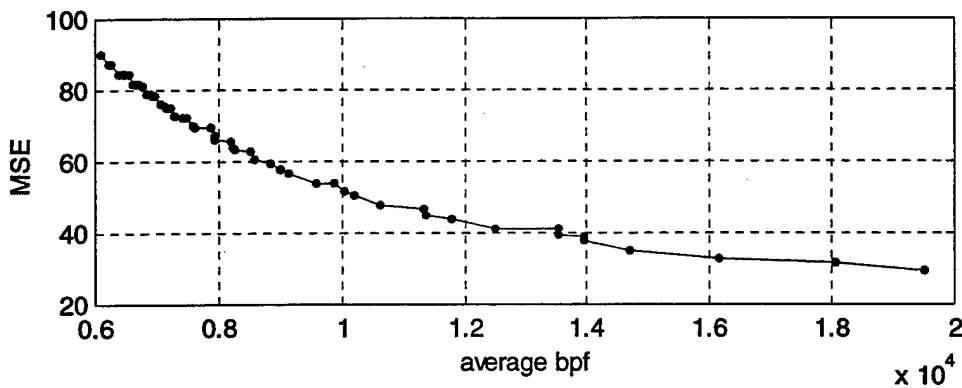


**Figure III-19: Operational Rate Distortion Curve (Motion Video).**

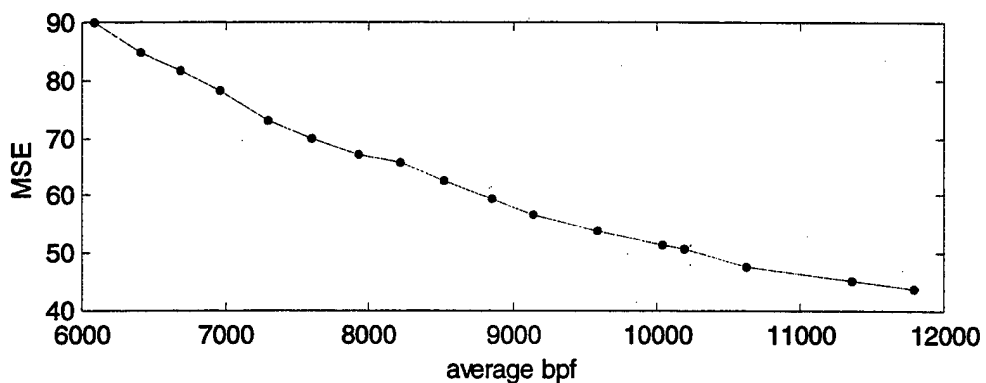


**Figure III-20: Reduced Operational Rate-Distortion Curve (Motion Video).**

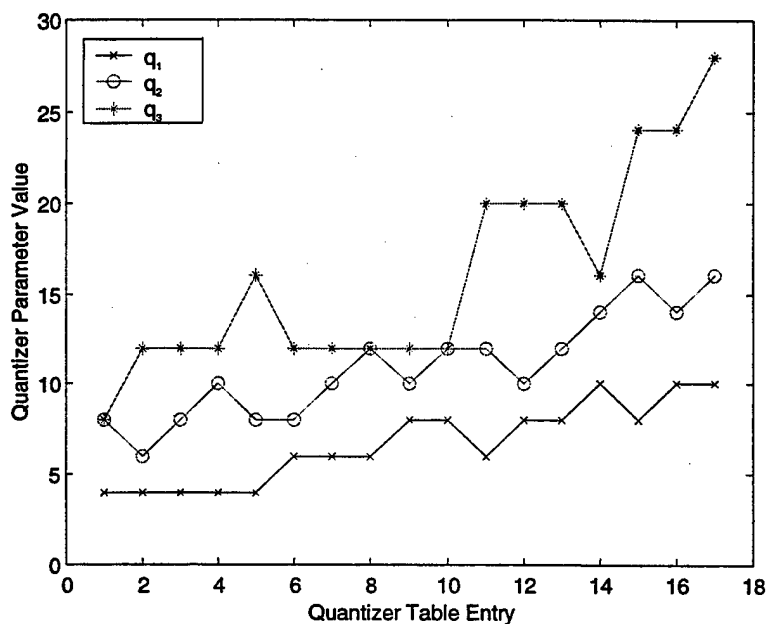


**Figure III-21: Quantizer Table Triplet Values (Motion Video).**

The same approach was followed for static slide sequences. However, a slightly different behavior was observed. Instead of the expected continued decrease in MSE as bit rate increased with finer quantization, the behavior was as depicted in Figure III-22. Past a limiting value of MSE, finer quantization and the related increase in bit rate yielded no increase in image fidelity. After reconstructing the custom VLC table with the

quantizer triplet at that limiting point ( $\{q_1:q_2:q_3\}$  equal to  $\{4:16:16\}$ ) the average bit rate became approximately 44 kbps as shown. Since this bit rate is below 64 kbps, no additional bit rate control scheme was deemed necessary; all static slide sequences are quantized with the same triplet.

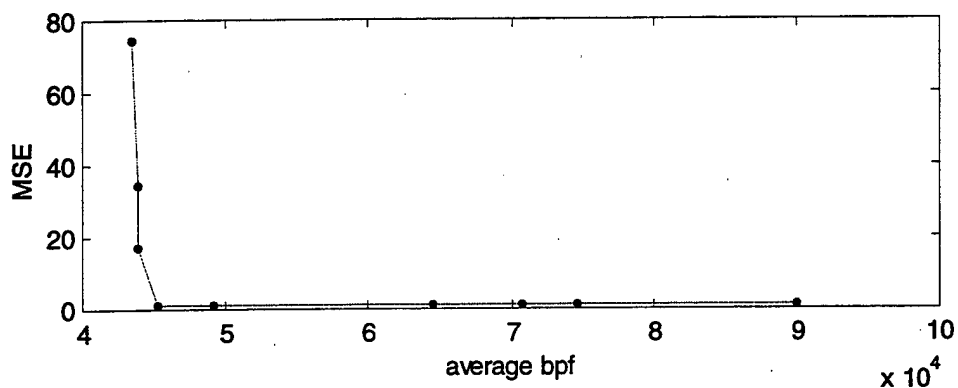


**Figure III-22: Operational Rate-Distortion Curve (Static Slides).**

## 7. Bit Rate Control

This approach to the rate-distortion problem provides a potential method for a simplified layered rate control scheme since the set of possible quantizer parameters is reduced to a far smaller set of parameters. Considering each triplet as an optimal quantizer state, any control scheme would manipulate the quantizers for each layer of a motion video sequence by selecting only entries from this set via a simple table lookup. Parker [9] proposes two such schemes. One functions at the frame level; the other operates at the macroblock level. The former was examined and implemented for this thesis in the coder.

Using the operational rate-distortion curve, a linear control curve relating bits per frame  $B$  to quantizer setting  $Q$  is created as shown in Figure III-23. The slope  $\Delta B/\Delta Q$  represents the average increment or decrement in bits per frame with a step change in the quantizer table. Dividing this quantity by the average number of macroblocks selected per frame in the test sequences,  $\bar{M}$ , yields the desired control parameter  $\beta$ :

$$\beta = \frac{\Delta B}{\Delta Q} \frac{1}{\bar{M}} \quad (\text{III-9})$$

The calculated value of  $\beta$  resulting from the test motion video sequences was  $-11.346$ . This control parameter was then used to adjust the coder quantizer setting in accordance with the following scheme.

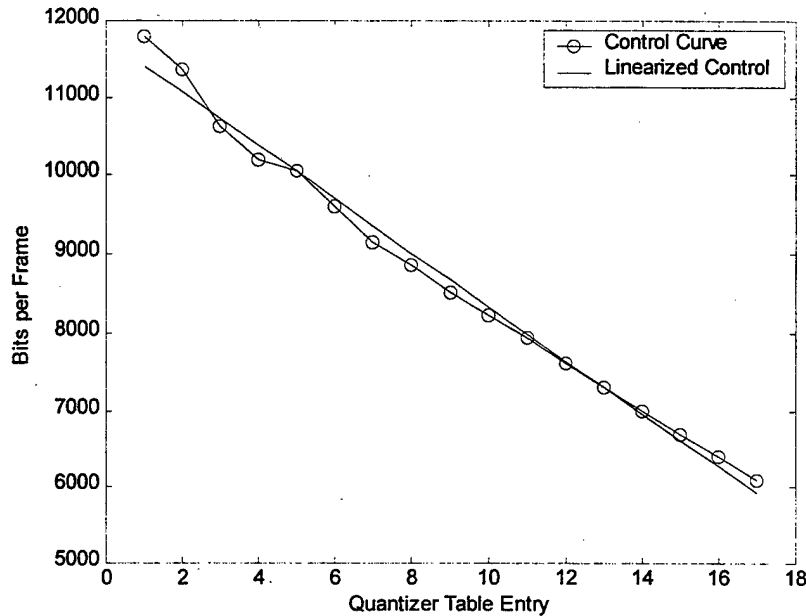


**Figure III-23: Operational Rate Control Curve (Motion Video).**

At call setup, the average bit allocation per frame  $\bar{B}$  is set to

$$\bar{B} = \frac{R_{\text{target}}}{f}, \quad (\text{III-10})$$

where  $R_{\text{target}}$  is the channel bit rate, and  $f$  is the frame rate. For each new frame  $i$ , the actual bit allocation from the last frame ( $i-1$ ) is used to estimate the bit allocation error or deviation expected to result from the current frame  $i$  if the quantizer setting used in the previous frame is not changed. Accounting for the change in the number of macroblocks selected between the last and current frames, the deviation expected is:

$$\Delta B_{\text{inter}} = \bar{B} - \left( \frac{M_i}{M_{i-1}} \right) B_{i-1}, \quad (\text{III-11})$$

where  $M_i$  is the number of macroblocks selected for transmission in the current frame,  $M_{i-1}$  is the number of macroblocks selected for transmission in the previous frame, and  $B_{i-1}$  is the number of bits used in the transmission of the previous frame. The required change in the quantizer setting is calculated using the deviation  $\Delta B_{\text{inter}}$ , the number of macroblocks selected for transmission in the current frame  $M_i$ , and the control parameter  $\beta$ :

$$\Delta Q_i = \left\lfloor \frac{\Delta B_{\text{inter}}}{M_i \beta} \right\rfloor. \quad (\text{III-12})$$

Here,  $\lfloor \ ]$  is the fixed integer operator that discards the decimal portion of the result. The result indicates the quantizer setting from the last frame should be incremented or decremented by  $\Delta Q_i$ . If the quantizer has reached the upper or lower limit of the table, the value is not changed. This quantizer triplet selection scheme is accomplished via the function, *get\_qd\_entryf.m*.

This control scheme is only applicable for motion video; a single quantizer parameter triplet is used for static slides. The only exception is due to a scene change. When a scene change is detected by the coder (as defined in the next section), so much of the frame is selected for transmission that a spike in bit rate would occur if quantized with any of the triplets available in the control table. To avoid this undesirable spike, the first frame of a new scene is heavily compressed. Following this initial frame, the appropriate quantization technique ensues.

## 8. Scene Change Detection and Scene Type Determination

Since the bit rate must be suppressed during a scene change and the coder must determine which of two possible layering schemes to employ following a scene change, these criteria must be defined. The coder concludes that a scene change has occurred if the number of macroblocks selected exceeds a threshold. This threshold was determined from the block selection statistics of the test video sequence containing the most highly

active content (though still considered low-motion video) of all the test video sequences examined. For this sequence, the average number of macroblocks selected per frame was 34.61 and their standard deviation was 10.19. The threshold was set at three standard deviations above the mean (65). The comparison operation is performed in the main code block, *thesis.m*. A frame sequence is determined to be static when macroblocks chosen for transmission result solely from aging. In this case, the fixed quantizer triplet and the static VLC table from Appendix B are used. Otherwise, the sequence is deemed motion video, and the bit rate control scheme discussed above is employed with its associated custom VLC table from Appendix B. This determination is performed within the function, *m\_blk\_id\_xr.m*:

This chapter began with a presentation of the three basic techniques available for layered video coding. The approach implemented here, as proposed by Parker [9], is frequency-based and utilizes the FHT and the 2-D DCT for motion video sequences and the FHT alone for static slide sequences. Different frequency transforms are used due to the inherent differences in the perceptual frequency content within the two types of sequences. The method of implementing frame refreshment was detailed as a block selection scheme applied at the macroblock level that captures perceptual changes due to motion within a scene and limits the duration of decoder errors at receivers by forcing macroblock updates via an aging algorithm. Quantization and encoding techniques were presented with the implementation including the use of the JPEG standard and uniform quantization coupled with one of two custom VLC tables. The issue of rate control was addressed, and the implementation of a scheme that reduces a 4-D rate control surface to a simple quantizer table lookup to control bit rate at the frame level was discussed. Finally, the manner by which the coder detects a scene change and determines the type of sequence under consideration was delineated.

## IV. RESULTS

This chapter presents some results from a short video segment consisting of 100 frames of a single speaker followed by 50 frames of a presentation slide filled with line diagrams and text. The Matlab code is contained in Appendix C. A sample frame from each sequence is shown in Figure IV-1 and Figure IV-2. Each shows the original frame and the reconstructed frame with only the base layer received, with the base layer and the first enhancement layer received, and with all layers received.

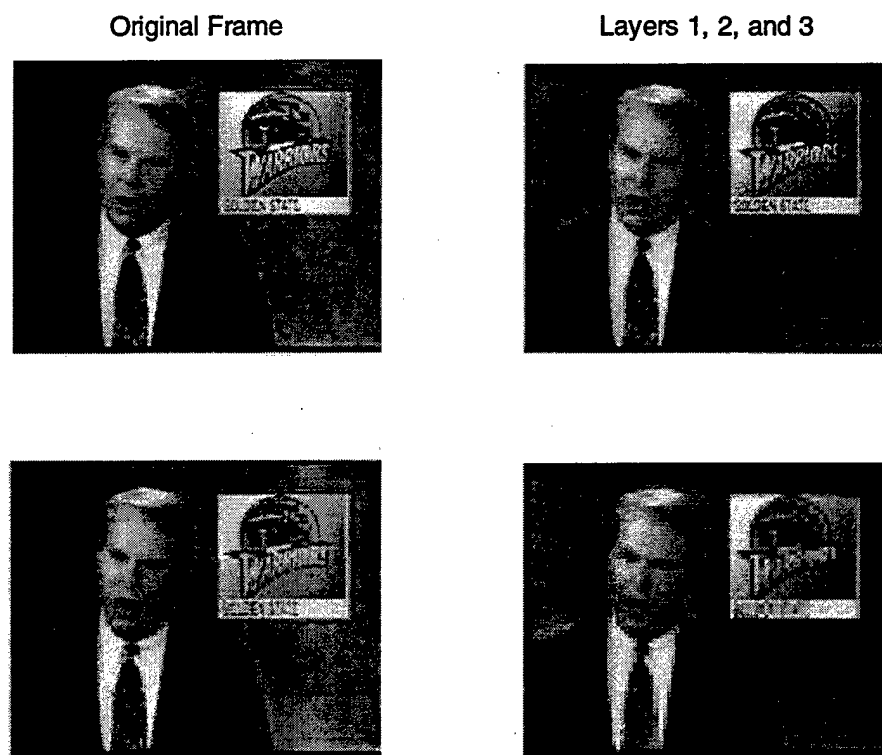


**Figure IV-1: Original and Reconstructed Frames from a Motion Video Sequence.**



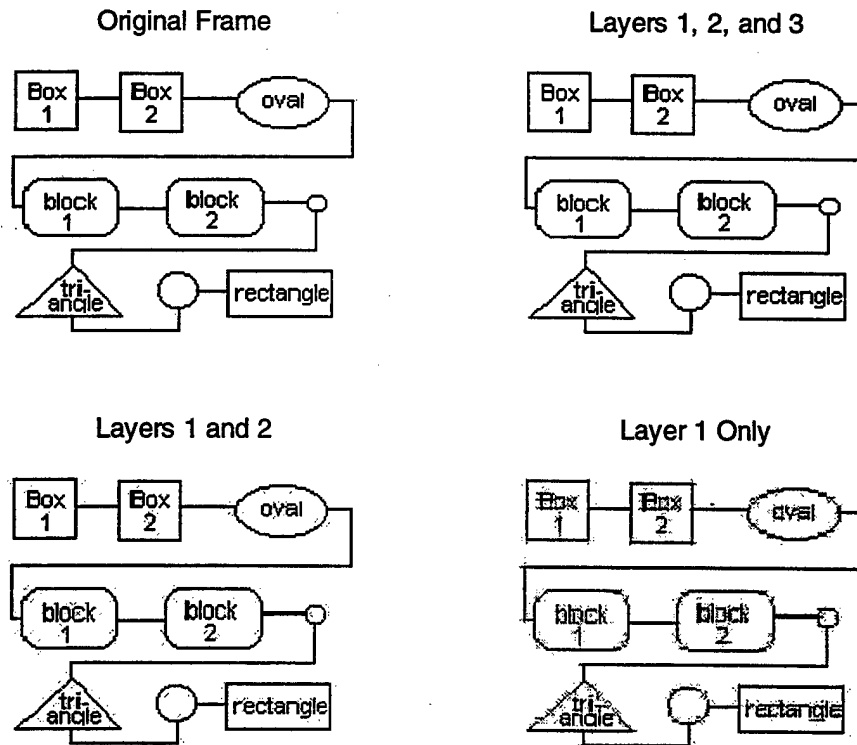


**Figure IV-2: Original and reconstructed Frames from a Static Video Sequence.**

Figure IV-3 shows the bit rate traces for the 150-frame layered video segment. Part (a) displays the traces resulting from the constant motion video quantizer triplet  $(\{6,12,20\})$  expected to yield 80 kbps based on the average bit rate resulting from all test motion video sequences and the fixed static sequence quantizer triplet. Part (b) displays the traces resulting from the bit rate control scheme for the motion video frames with the coder attempting to achieve an average 80 kbps and the fixed static sequence quantizer triplet. Bit rate spike suppression is employed for the initial frame of each scene as discussed previously. The distribution of bit rate offered by a layered video coder is evident with the bit rate ratio among layers being approximately 5:3:2 for both sequences. As congestion occurs in the network, the higher layers can be dropped to combat the congestion while maintaining much of the quality as illustrated in Figure IV-1 and Figure IV-2. Neglecting the initial frame, the average bits per frame for the motion video

sequence without the control scheme is 7454 bpf with a standard deviation of 1362 bpf. With the control scheme, the average and standard deviation are 7988 bpf and 942 bpf, respectively. As expected, the bit rate from the static sequence is much lower since the bit rate results solely from macroblock aging. This illustrates that rate control is not of significant benefit for static sequences.

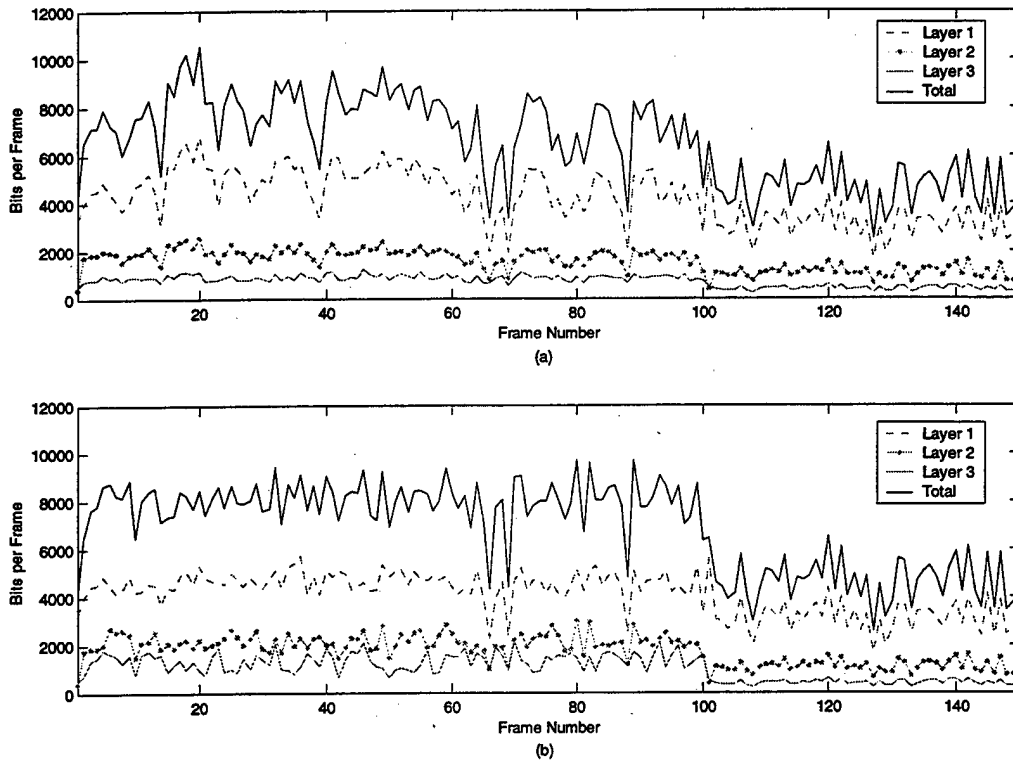


**Figure IV-3: Bit Rates for (a) Fixed Quantization and (b) Bit Rate Control.**

Figure IV-4 quantifies the progressive improvement in quality of the reconstructed video based on pSNR for the same 150-frame layered video segment illustrated in Figure IV-1 and Figure IV-2. At the beginning of each sequence, quality ramps up over the aging interval following a scene change. After this period, quality is observed to remain relatively flat for each sequence regardless of the number of layers. For the motion video sequence, the base layer provides a smoothed but acceptable display. Text is not readable but the speaker's movements are easy to follow. Adding the first enhancement layer improves sharpness and adds a 4 dB improvement in pSNR

although small text is still difficult to discern. The second enhancement layer only adds 1-2 dB improvement, but small text is clearly readable and other features with fine edges are sharper. With static video, the role of the enhancement layers is even more dramatic. Even though most of the macroblock's energy is included in the base layer and contributions from each frequency band are included, the base layer still shows much softness although the shapes are readily identifiable. The first enhancement layer adds a 7 dB improvement and dramatically improves sharpness. The final layer, even though the bit rate contribution is the smallest of the three layers, almost doubles the pSNR, and the reconstructed frame is virtually identical to the original frame. Neglecting the initial frame, the average pSNR utilizing all layers for the motion video sequence without the control scheme is 29.5 dB with a standard deviation of 1.7 dB. With the control scheme, the average and standard deviation are 29.8 dB and 1.9 dB, respectively. Note that these values include the ramp up in quality following the initial scene change. These average pSNR values are not directly comparable, however, because of the difference in average bit rates; the higher quality, rate control approach uses approximately 500 more bits per frame. But since this quality is achieved within the desired bit budget of 80 kbps, the rate controller allows more effective utilization of the available bandwidth to better image fidelity. The statistics obtained from the motion video sequence traces in Figure IV-3 and Figure IV-4 are summarized in Table IV-1.

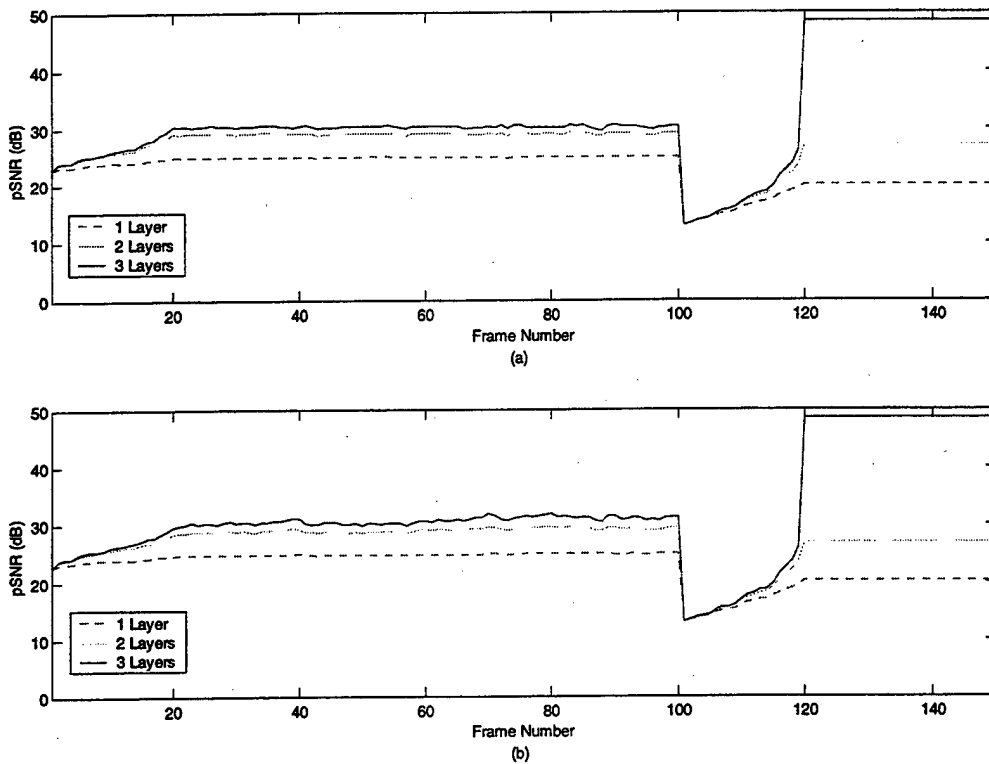


**Figure IV-4: pSNR for (a) Fixed Quantization and (b) Bit Rate Control.**

Parameter	With Rate Control	Without Rate Control
Mean Bit Rate (bpf)	7998	7454
Bit Rate STD (bpf)	942	1362
Mean pSNR (dB)	29.83	29.51
pSNR STD (dB)	1.92	1.74

**Table IV-1: Rate Controlled and Uncontrolled Motion Video Sequence Statistics.**

Additionally, the issue of the layered video codec's resilience to bit errors introduced during transmission was examined using the same motion video sequence as above. Using loss rates of 10%, 25%, and 50%, four different case were tested. Case one distributed the bit errors across the layers in proportion to their contribution to the total bit rate and utilized zero-order error concealment; the reconstructed frame retained the content of the previous frame for that portion lost during transmission. If the loss

occurred in the base layer, the enhancement layers were neglected. If the loss occurred in an enhancement layer, the reconstruction was performed utilizing the base layer and the other enhancement layer. Case two treated all layers as a single video stream and utilized zero-order error concealment; that is, a transmission loss was a loss for all layers. Cases three and four are identical to cases one and two, respectively, except that no error concealment was used. Instead an information loss caused the decoder to assign the value of zero to all coefficients in the affected layers. As Figure IV-5 illustrates, spreading bit errors across multiple layers has less negative impact on the reconstructed image at high loss rates.

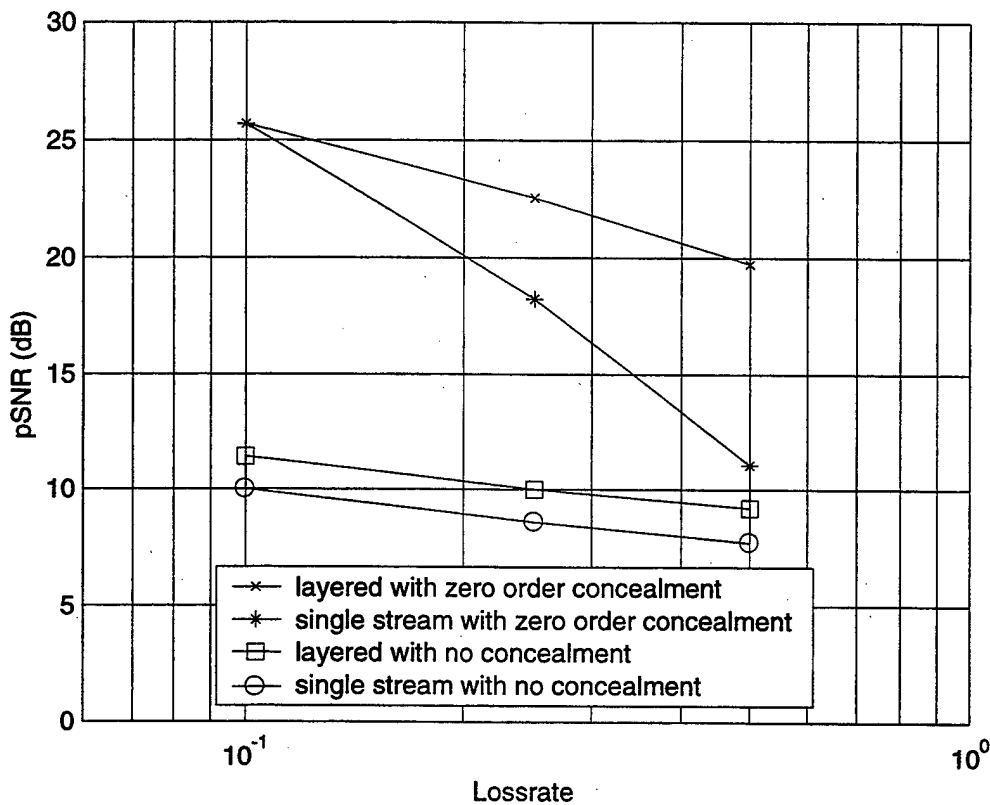


**Figure IV-5: Comparison of Error Resilience.**

Considering static slide sequences, the relationship is more complicated. In general, since the frame content is entirely static, the best reconstruction in an error prone environment is to forgo a macroblock update if the update would be made with fewer

layers than the present reconstruction of that macroblock. Further study into the implementation of such a scheme is warranted.

This chapter presented representative frames from a video segment consisting of motion video and static slides. For each type of content, the original frame and the reconstructions with one, two, and three layers were given. Also presented were plots of the bits per frame and pSNR as a function of the frame sequence for both fixed quantization and variable quantization using the bit rate control scheme. These plots served to quantify the quality depicted in the reconstructions and to illustrate the bit allocation among the layers. Finally, the effect of spreading bit errors across layers compared to confining them to a single video stream was presented.



## V. CONCLUDING REMARKS

### A. CONCLUSIONS

This thesis has presented the development and implementation of a new layered video codec proposed by Parker [9] that emphasizes robust transmission of a video teleconference (VTC) at low bit rates. The dual nature of the targeted scene content – low-motion video and static slide sequences consisting of text and line drawings – and the assumed application in a multicast, heterogeneous, wireless network environment required significant flexibility in the implementation. The essential features of the coder are summarized as follows.

Frame refreshment is accomplished via block updating and an aging algorithm, both applied at the macroblock level. This approach promotes greater robustness because spatial error propagation is eliminated and temporal error propagation is greatly limited. The combined technique captures perceptual changes due to motion within the scene, limits the duration of error artifacts in the reconstruction at receivers, and ensures that new participants in a VTC session that is already in progress receive a complete frame in a timely manner.

The macroblocks selected for transmission are decomposed in frequency using the fast Haar transform (FHT). For motion video sequences, the lowpass subband is further processed with the two-dimensional discrete cosine transform. The horizontal and vertical edge detail subbands are further decomposed with a repeated application of the FHT. Static slide sequences are decomposed solely by a second order FHT analysis.

The lowpass subband of motion video is quantized and encoded using the JPEG standard in order to exploit the human visual system perceptive characteristics. The remaining subbands of motion video sequences are subjected to uniform quantization and encoding with a custom variable length coding (VLC) table. All subbands of static slides are subjected to uniform quantization and encoding with a separate custom VLC table. All quantization is performed using a triplet of quantizers, and each subband is quantized with one of the triplet parameters based on the variance of subband coefficients.



Subbands are assigned to layers by grouping bands of coefficients with similar variances into a common layer. Three layers are used in the coder. The base layer is independently decodable and yields an acceptable, minimum-quality reconstruction; each enhancement layer progressively improves the quality of the reconstruction.

Bit rate is controlled at the frame level by selecting the quantizer triplet to be used in the current frame based on the number of bits used in the previous frame, the desired average bit rate, and the number of macroblocks selected for transmission. The implementation involves a simple table lookup, which resulted from the optimal one-dimensional reduction of a four-dimensional control surface.

## **B. FUTURE WORK**

The implementation and the results presented here suggest that the layered video codec has potential practical utility to video teleconferencing in multicast, heterogeneous, wireless networks. Now, several aspects of the coder can be pursued further. For example, although three layers were used in the present implementation, the techniques employed can be used to scale the coder to include an arbitrary number of layers. Work on techniques to dynamically change the layering scheme within a sequence is desirable. The ability to handle color and audio needs to be incorporated into the code. Further refinement of the block search pattern utilized for macroblock selection and the possibility of rate control at the macroblock level can be evaluated. Also, with regard to static slide sequences, investigation of the ability to detect and reconstruct slight movement within such a frame, such as the movement of a cursor, is warranted. Finally, implementation in a high level language or hardware is another potential future task.

## APPENDIX A. MOTION VIDEO VARIABLE LENGTH CODING TABLE (VLC)

The following is the custom VLC table used with motion video sequences. The last character in the codeword *s* indicates the appended sign bit.

INDEX	LAST	RUN	LEVEL	BITS	CODEWORD
1	0	0	1	3	11s
2	0	0	2	5	0101s
3	0	0	3	6	10010s
4	0	0	4	9	10100011s
5	0	0	5	12	101110011101s
6	0	0	6	14	1011111001110s
7	0	1	1	5	0100s
8	0	1	2	7	100111s
9	0	1	3	10	001000101s
10	0	1	4	12	10111110000s
11	0	1	5	17	1011010010000111s
12	0	1	6	14	1011010010100s
13	0	2	1	5	0000s
14	0	2	2	8	1011001s
15	0	2	3	12	01110001010s
16	0	2	4	13	001000110110s
17	0	3	1	6	01111s
18	0	3	2	9	01100100s
19	0	3	3	11	1011100101s
20	0	3	4	13	101101011001s
21	0	4	1	6	00011s
22	0	4	2	9	01110010s
23	0	4	3	10	101101010s
24	0	4	4	15	00101101001111s
25	0	5	1	6	10010s
26	0	5	2	10	000101101s
27	0	5	3	12	10111110001s
28	0	5	4	16	101101001000111s
29	0	6	1	7	011101s
30	0	6	2	10	000101110s
31	0	6	3	14	0111000100000s
32	0	6	4	16	101101001000110s
33	0	7	1	7	011011s
34	0	7	2	10	001000100s
35	0	7	3	14	1011111001111s
36	0	7	4	16	101101001000001s
37	0	8	1	7	011000s
38	0	8	2	9	00100100s
39	0	8	3	10	001011011s
40	0	8	4	13	011100010001s
41	0	9	1	8	0010111s
42	0	9	2	11	0010011010s
43	0	9	3	14	1001101011000s
44	0	10	1	8	1011011s
45	0	10	2	11	1001101001s
46	0	10	3	14	0010011011010s
47	0	10	5	16	101101001000000s

48	0	11	1	9	00101100s
49	0	11	2	12	00100011100s
50	0	11	3	14	1011010010101s
51	0	12	1	8	0010000s
52	0	12	2	10	011100011s
53	0	12	3	13	101111100100s
54	0	12	4	15	00010110011101s
55	0	13	1	9	10111000s
56	0	13	2	12	10111111111s
57	0	13	3	15	00101101001100s
58	0	14	1	9	00100101s
59	0	14	2	13	001000110111s
60	0	14	3	17	1011010010011010s
61	0	15	1	10	011001010s
62	0	15	2	14	1011010001011s
63	0	16	1	10	101000100s
64	0	16	2	15	10011011110010s
65	0	17	1	11	0001011110s
66	0	17	2	17	0110010110011111s
67	0	18	1	11	1010001011s
68	0	19	1	11	1010001010s
69	0	20	1	11	1011010011s
70	0	20	2	17	0110010110011110s
71	0	21	1	12	01100101101s
72	0	22	1	12	01110001011s
73	0	22	2	16	101101001011101s
74	0	23	1	12	00010111111s
75	0	23	2	15	00101101001101s
76	0	24	1	11	0010001100s
77	0	24	2	16	101101001011100s
78	0	24	3	17	1011010010000100s
79	0	25	1	12	00100110011s
80	0	25	2	16	101101001011111s
81	0	26	1	12	10111111001s
82	0	26	2	17	1011010000101000s
83	0	27	1	12	00010110000s
84	0	27	2	17	1011010000101011s
85	0	28	1	12	00100011110s
86	0	28	2	17	1011010000101010s
87	0	29	1	12	10111111000s
88	0	29	2	17	1011010010010101s
89	0	30	1	12	10110101110s
90	0	30	2	15	10110100001000s
91	0	31	1	12	10011011100s
92	0	31	2	17	1011010010010100s
93	0	32	1	12	10011010101s
94	0	32	2	14	1011010001010s
95	0	33	1	13	101111111100s
96	0	33	2	17	1011010010010001s
97	0	34	1	13	001000111110s
98	0	34	2	17	1011010010010000s
99	0	35	1	13	101111110100s
100	0	35	2	17	1011010010010011s
101	0	36	1	12	10011010100s
102	0	36	2	17	1011010010010010s
103	0	37	1	13	000101111100s

104	0	38	1	12	10111001110s
105	0	39	1	12	10110100011s
106	0	40	1	13	101111111001s
107	0	40	2	16	001011010010100s
108	0	41	1	13	101110011110s
109	0	41	2	17	1011010010011101s
110	0	42	1	14	0111000100100s
111	0	43	1	13	011001011000s
112	0	43	2	17	1011010010011100s
113	0	44	1	13	101110010001s
114	0	45	1	12	10110101101s
115	0	46	1	14	0111000100111s
116	0	46	2	16	101101001011110s
117	0	47	1	13	100110111011s
118	0	48	1	12	10011010000s
119	0	48	2	15	00010110010000s
120	0	49	1	13	011001011111s
121	0	50	1	13	101101000011s
122	0	51	1	14	1011100110010s
123	0	52	1	14	0111000100110s
124	0	53	1	14	1001101011100s
125	0	53	2	16	101101001011001s
126	0	54	1	14	1011111001100s
127	0	54	2	16	001011010010111s
128	0	55	1	14	0001011001101s
129	0	56	1	13	101111111000s
130	0	56	2	15	00010110010011s
131	0	57	1	14	0001011001100s
132	0	57	2	16	001011010010001s
133	0	58	1	15	10011011110011s
134	0	59	1	16	011001011001110s
135	0	60	1	16	000101100111000s
136	0	61	1	17	0001011001110010s
137	0	62	1	15	00101101000000s
138	1	0	1	5	0011s
139	1	0	2	7	011010s
140	1	0	3	8	1011000s
141	1	0	4	11	0010011000s
142	1	0	5	15	00101101001001s
143	1	1	1	6	10001s
144	1	1	2	10	101111101s
145	1	1	3	13	101111110101s
146	1	1	4	15	10110100001011s
147	1	1	5	17	1011010010000110s
148	1	2	1	7	001010s
149	1	2	2	11	0010110101s
150	1	2	3	13	100110111101s
151	1	2	4	16	101101001000101s
152	1	3	1	6	10101s
153	1	3	2	10	100110110s
154	1	3	3	13	001001100100s
155	1	3	4	16	001011010010000s
156	1	4	1	7	101001s
157	1	4	2	12	00100110111s
158	1	4	3	16	101101001011000s
159	1	4	4	16	101101001000100s

160	1	5	1	8	1011110s
161	1	5	2	15	00010110010001s
162	1	5	3	15	00010110010010s
163	1	6	1	8	0001001s
164	1	6	2	13	100110101101s
165	1	7	1	8	0110011s
166	1	7	2	12	10011011111s
167	1	7	3	14	1001101011001s
168	1	8	1	8	0001010s
169	1	8	2	13	101110010010s
170	1	8	3	16	101101001011011s
171	1	9	1	9	01110011s
172	1	9	2	15	00101101000011s
173	1	9	3	17	1011010010011000s
174	1	10	1	8	1001100s
175	1	10	2	15	00101101000010s
176	1	11	1	8	1010000s
177	1	11	2	14	1001101011110s
178	1	11	3	17	1011010010011011s
179	1	12	1	8	1011101s
180	1	12	2	13	001011010001s
181	1	12	3	16	101101001011010s
182	1	13	1	9	00100111s
183	1	13	2	14	0111000100001s
184	1	14	1	9	01110000s
185	1	14	2	18	00010110011100111s
186	1	14	3	17	1011010010000101s
187	1	15	1	8	0001000s
188	1	15	2	13	011001011110s
189	1	15	3	14	0001011111011s
190	1	15	4	15	00101101001110s
191	1	16	1	12	10110101111s
192	1	16	2	16	001011010010101s
193	1	17	1	13	011001011100s
194	1	18	1	14	0001011111010s
195	1	19	1	13	001000110101s
196	1	20	1	13	001001101100s
197	1	20	2	18	00010110011100110s
198	1	21	1	14	1011111111011s
199	1	22	1	13	001000111111s
200	1	23	1	12	00010110001s
201	1	23	2	15	10110100001001s
202	1	24	1	14	0110010110010s
203	1	24	2	17	1011010000101001s
204	1	25	1	13	101101011000s
205	1	26	1	14	0110010111011s
206	1	27	1	14	1011100110011s
207	1	28	1	14	1011010000011s
208	1	29	1	13	101101000000s
209	1	30	1	13	100110100011s
210	1	31	1	13	101110011000s
211	1	31	2	17	1011010010010111s
212	1	32	1	14	1011111111010s
213	1	32	2	17	1011010010010110s
214	1	33	1	15	01100101100110s
215	1	34	1	14	0110010111010s

216	1	35	1	14	0111000100101s
217	1	36	1	14	0010001110101s
218	1	37	1	14	0010011011011s
219	1	38	1	13	101110011111s
220	1	39	1	13	001001100101s
221	1	40	1	14	0010001110100s
222	1	41	1	13	100110100010s
223	1	42	1	14	1001101111000s
224	1	43	1	14	0010001110111s
225	1	44	1	15	00010110010101s
226	1	45	1	14	1011010000010s
227	1	46	1	13	101110010000s
228	1	47	1	13	101111100101s
229	1	48	1	13	001000110100s
230	1	48	2	17	1011010010011111s
231	1	49	1	14	1001101011101s
232	1	50	1	15	00101101000001s
233	1	51	1	14	1011111001101s
234	1	52	1	15	00010110010100s
235	1	53	1	13	100110111010s
236	1	54	1	14	1011010001001s
237	1	54	2	17	1011010010011110s
238	1	55	1	12	10111111011s
239	1	55	2	17	1011010010011001s
240	1	56	1	12	10111111101s
241	1	56	2	16	001011010010110s
242	1	57	1	13	101110010011s
243	1	58	1	14	0001011001111s
244	1	59	1	15	00010110010111s
245	1	60	1	15	00010110010110s
246	1	61	1	14	1011010001000s
247	1	62	1	14	1001101011111s
248	1	63	1	14	0010001110110s



## APPENDIX B. STATIC SLIDE VARIABLE LENGTH CODING TABLE (VLC)

The following is the custom VLC table used with static slide sequences. The last character in the codeword *s* indicates the appended sign bit.

INDEX	LAST	RUN	LEVEL	BITS	CODEWORD
1	0	0	1	4	101s
2	0	0	2	4	110s
3	0	0	3	5	1000s
4	0	0	4	7	111100s
5	0	0	5	7	001110s
6	0	0	6	6	00110s
7	0	0	7	13	011011010011s
8	0	0	8	10	011101011s
9	0	0	10	11	1111101011s
10	0	0	11	11	1001000100s
11	0	0	13	11	1001101000s
12	0	0	20	15	00111101111100s
13	0	0	24	12	00111101100s
14	0	0	28	11	0110110101s
15	0	0	32	9	00001100s
16	0	0	36	9	01111100s
17	0	0	40	8	0000100s
18	0	0	44	8	1001100s
19	0	0	48	6	00011s
20	0	0	52	8	0110011s
21	0	0	56	8	0010101s
22	0	0	60	9	00100010s
23	0	0	64	4	010s
24	0	1	1	6	11100s
25	0	1	2	6	00010s
26	0	1	3	8	0111011s
27	0	1	4	10	111111111s
28	0	1	5	10	001111110s
29	0	1	6	9	00100001s
30	0	1	7	16	0011110111110010s
31	0	1	8	12	10010010111s
32	0	1	10	14	0111101001000s
33	0	1	13	15	11111110000101s
34	0	2	1	7	011100s
35	0	2	2	7	011010s
36	0	2	3	8	0010011s
37	0	2	4	11	0111101100s
38	0	2	5	9	10010011s
39	0	2	6	9	10011110s
40	0	2	7	17	0011110111111110s
41	0	2	8	12	00101001110s
42	0	2	10	14	1111111000001s
43	0	2	11	15	11111110011000s
44	0	2	13	14	1111111000011s
45	0	3	1	8	0111100 s
46	0	3	2	8	0110000s
47	0	3	3	9	00001101s



48	0	3	4	11	0000111000s
49	0	3	5	10	001001010s
50	0	3	6	10	001111101s
51	0	3	7	17	0011110111111001s
52	0	3	8	13	100100010111s
53	0	3	10	15	11111110011100s
54	0	3	11	15	11111110011011s
55	0	3	13	16	011011010010111s
56	0	4	1	8	0110001s
57	0	4	2	8	0111111s
58	0	4	3	9	00100100s
59	0	4	4	10	100110101s
60	0	4	5	11	0000111001s
61	0	4	6	9	00100011s
62	0	4	8	15	11111110010000s
63	0	5	1	10	011111010s
64	0	5	2	9	01101100s
65	0	5	3	10	011110101s
66	0	5	4	12	10011111001s
67	0	5	5	12	00111100010s
68	0	5	6	11	1111101000s
69	0	5	8	15	11111110010011s
70	0	6	1	9	11111011s
71	0	6	2	9	00001010s
72	0	6	3	10	100110111s
73	0	6	4	13	111111101111s
74	0	6	5	11	1001001000s
75	0	6	6	12	01111011011s
76	0	6	10	15	11111110011111s
77	0	7	1	10	111101000s
78	0	7	2	10	001000000s
79	0	7	3	11	1001101001s
80	0	7	4	15	01101101001010s
81	0	7	5	16	001001011000011s
82	0	7	6	13	011101010000s
83	0	7	7	16	001111011111101s
84	0	7	10	15	11111110011110s
85	0	8	1	9	00101000s
86	0	8	2	9	00101111s
87	0	8	3	10	100110110s
88	0	8	4	11	0010010111s
89	0	8	5	12	10011111000s
90	0	8	6	10	011110111s
91	0	8	8	15	11111110010010s
92	0	8	10	15	11111110011001s
93	0	9	1	9	11110101s
94	0	9	2	9	10010000s
95	0	9	3	11	0010100110s
96	0	9	4	15	00111101110001s
97	0	9	5	11	1111010010s
98	0	9	6	13	111111101110s
99	0	10	1	12	00111101101s
100	0	10	2	11	0010000011s
101	0	10	3	13	001000001011s
102	0	10	4	15	00111101110011s
103	0	10	5	13	001111010011s

104	0	10	6	13	111110101001s
105	0	10	8	15	11111110011101s
106	0	11	1	14	1001111111111s
107	0	11	2	11	0110110111s
108	0	11	3	12	11110100111s
109	0	11	4	15	11111110010110s
110	0	11	5	15	00111101111101s
111	0	11	6	15	11111110010001s
112	0	12	1	12	00111100011s
113	0	12	2	12	01111010000s
114	0	12	3	14	0011110100011s
115	0	12	4	13	100100010101s
116	0	12	5	16	001111011110001s
117	0	12	6	13	011101010010s
118	0	13	1	13	100111111110s
119	0	13	2	12	00101001111s
120	0	13	3	13	001000001010s
121	0	13	4	15	00111101110010s
122	0	13	5	16	001111011110011s
123	0	14	3	15	11111110010100s
124	0	14	5	14	0111010100011s
125	1	0	1	6	11101s
126	1	0	2	6	00000s
127	1	0	3	7	100101s
128	1	0	4	9	00001011s
129	1	0	5	9	00001111s
130	1	0	6	8	0110111s
131	1	0	7	14	1001000101100s
132	1	0	8	12	00100000100s
133	1	0	10	12	11111010010s
134	1	0	11	13	111110101011s
135	1	0	13	14	1111111000000s
136	1	0	32	13	001111010010s
137	1	0	36	13	001111011101s
138	1	0	40	12	10010010110s
139	1	0	44	14	0011110111101s
140	1	0	48	10	001111100s
141	1	0	52	12	00100101101s
142	1	0	56	12	01111010011s
143	1	0	60	13	111110101010s
144	1	0	64	8	0110010s
145	1	1	1	8	1111100s
146	1	1	2	8	1111110s
147	1	1	3	10	000011101s
148	1	1	4	14	0011110100010s
149	1	1	5	13	001111010000s
150	1	1	6	13	001001011001s
151	1	1	7	17	001111011111111s
152	1	2	1	9	01110100s
153	1	2	2	9	10011101s
154	1	2	3	11	0011110010s
155	1	2	4	15	01111011010010s
156	1	2	5	13	011101010011s
157	1	2	6	14	0111010100010s
158	1	2	8	14	0010010110001s
159	1	2	13	15	11111110000100s

160	1	3	1	8	0010110s
161	1	3	2	8	1111011s
162	1	3	3	9	10011100s
163	1	3	4	12	01111101100s
164	1	3	5	11	1001111101s
165	1	3	6	11	0011111110s
166	1	3	7	17	0011110111111000s
167	1	3	11	15	11111110011010s
168	1	4	1	11	0011110000s
169	1	4	2	10	001010010s
170	1	4	3	13	011110110101s
171	1	4	4	14	1001000101101s
172	1	4	5	17	0011110111111101s
173	1	4	6	14	0111101001001s
174	1	5	1	10	001011100s
175	1	5	2	10	111111110s
176	1	5	3	14	1001111111110s
177	1	6	1	11	1001001010s
178	1	6	2	12	11111110110s
179	1	6	3	15	01111011010011s
180	1	6	5	14	1111111000111s
181	1	7	1	10	001011101s
182	1	7	2	10	100100011s
183	1	7	3	14	0111101101000s
184	1	8	1	11	1001111110s
185	1	8	2	12	01110101010s
186	1	8	4	16	011011010010110s
187	1	8	6	14	111111000110s
188	1	9	1	11	0111110111s
189	1	9	2	12	01111010001s
190	1	9	3	14	0110110100100s
191	1	9	4	15	00111101110000s
192	1	9	5	16	001001011000010s
193	1	10	1	11	0011110011s
194	1	10	2	15	00100101100000s
195	1	11	1	11	1111111010s
196	1	11	2	11	0011110101s
197	1	11	3	12	10011111110s
198	1	11	4	14	1111111000100s
199	1	11	5	17	0011110111111100s
200	1	11	6	13	111110101000s
201	1	12	1	11	0011111111s
202	1	12	2	11	0110110110s
203	1	12	3	12	11110100110s
204	1	12	4	13	100100010100s
205	1	12	5	16	001111011110000s
206	1	12	6	13	011110100101s
207	1	13	1	12	01101101000s
208	1	13	2	12	11111010011s
209	1	13	3	15	1111110010101s
210	1	14	1	12	01110101011s
211	1	14	2	11	1001001001s
212	1	14	3	15	11111110010111s
213	1	15	2	12	01111101101s
214	1	15	3	14	1111111000101s

## APPENDIX C. MATLAB CODE LIBRARY

This appendix contains the Matlab code used in the layered video codec. The main code block, *thesis.m*, is provided first, and the supporting functions follow in alphabetical order. As provided, *thesis.m* processes four video sequences: two motion video sequences of 100 frames each, followed by two, static slide sequences of 50 frames each.

```

% thesis

format compact
clear all
close all

global QD_TABLE VLC_DYN VLC_STA RV HUFF_TABLE LAST

load('g:\QD_TABLE')
load('g:\VLC_dyn')
load('g:\VLC_sta')

VLC_DYN = VLC_dyn; clear VLC_dyn           % gets custom VLC table for motion video
VLC_STA = VLC_sta; clear VLC_sta           % gets custom VLC table for static
slides

rand('state',0)                             % seed for reproductivity
RV = floor(21*rand(99,1));                    % for aging algorithm
HUFF_TABLE = make_HAC_table;                 % gets JPEG standard table
LAST = ones(99,1);                          % sets block selection to 1 initially
threshold = 160;                            % for use with asd
count = -1;                                  % where is it in the loop?
mse = 1;                                     % calculate MSE?
display = 1;                                 % show the images?
write = 1;                                   % write to file for evaluation?
last = 299;                                  % last frame # to consider
tOff = 0;                                    % initialize (used with scene change)
frame_type = 0;                              % initialize (zero means dynamic scene)
m_mat_ndx = [];                              % initialize (track macroblocks
selected)
f_vec = zeros(1584,16);                      % initialize (reshaped frame)

f_far_ll = double(zeros(792,8));             % initialize for decoder
f_far_lh = double(zeros(792,8));             % initialize for decoder
f_far_hl = double(zeros(792,8));             % initialize for decoder
f_far_hh = double(zeros(792,8));             % initialize for decoder

f_far_ll_p1 = double(zeros(792,8));          % initialize for decoder
f_far_lh_p1 = double(zeros(792,8));          % initialize for decoder
f_far_hl_p1 = double(zeros(792,8));          % initialize for decoder
f_far_hh_p1 = double(zeros(792,8));          % initialize for decoder

f_far_ll_p2 = double(zeros(792,8));          % initialize for decoder
f_far_lh_p2 = double(zeros(792,8));          % initialize for decoder
f_far_hl_p2 = double(zeros(792,8));          % initialize for decoder
f_far_hh_p2 = double(zeros(792,8));          % initialize for decoder

f_1 = double(zeros(1584,16));                % initialize for decoder
f_2 = double(zeros(1584,16));                % initialize for decoder
f_3 = double(zeros(1584,16));                % initialize for decoder

```

```

beta = -11.346; % slope of rate control curve

br = input('Enter the target bitrate (Kbps) \n >> ');
B_bar = br * 1024/10;
qd_entry = min(find(B_bar > QD_TABLE(:,4))); % intial triplet based on test averages

for i = 0:last % loop through frames

    count = count+1

    if (i<=99)
        i_present = get_next_image(i); % read head#.bmp
    elseif ( (i>=100) & (i<=199) )
        i_present = get_next_image_2(i-100); % read ncaa#.bmp
    elseif (i==200)
        i_present = get_next_image(101); % read busy text slide
    elseif (i==250)
        i_present = get_next_image(102); % read line drawing slide
    else
        i_present;
    end

    if display % diplays original if desired
        figure;
        subplot(2,2,1)
        image(i_present)
        colormap(gray(256))
        title(['Original'])
        axis off
    end

    %*****
    %***** Coder %*****
    %*****

    %***** Change dimensions of image and identify macroblocks by threshold %*****

    f_last = f_vec; % buffers previous frame
    f_vec = shape(i_present); % shapes current frame
    [m_vec_ndx,frame_type] = m_blk_id_xr(f_last,f_vec,threshold); % compare current to
last
    m_mat_ndx = [m_mat_ndx,m_vec_ndx]; % matrix of MB's selected

    if (sum(m_vec_ndx) >= 65) % triggers a scene change
        tOff = 1; % "trigger" flag set "on"
    end

    if (tOff) % scene change just occurred
        tOff = 0; % resets "trigger" flag
        flag = 1; % "flag" for 1st frame after scene change
        q1 = 64; % heavily compressed scene change
        q2 = 1000;
        q3 = 1000;
    elseif frame_type
        q1 = 4; % triplet for static sequence
        q2 = 16;
        q3 = 16;
    else % a dynamic frame sequence
        delta_Binter = B_bar - (sum(m_vec_ndx)/sum(m_mat_ndx(:,i))) * total(i);
        qd_entry = get_qd_entryf(flag,B_bar,qd_entry,delta_Binter,sum(m_vec_ndx),beta);
        flag = 0; % resets flag
        q1 = QD_TABLE(qd_entry,1); % rate control triplets fetched
        q2 = QD_TABLE(qd_entry,2);
        q3 = QD_TABLE(qd_entry,3);
    end

    Q = get_Q1_matrix(q1); % quantizer matrix (via JPEG standard)

    if ~frame_type % if dynamic frame sequence

```

```

***** Transforms *****
[f_fht_ll,f_fht_lh,f_fht_hl,f_fht_hh ] = fht(f_vec,m_vec_ndx,16); % FHT of frame

f_fht_ll = f_fht_ll - 128; % level shift of LL
f_fht_ll = dct_of_fht(f_fht_ll,m_vec_ndx); % 2_D DCT of LL

[f_fht_lh_ll,f_fht_lh_lh,f_fht_lh_hl,f_fht_lh_hh] = ...
    fht(f_fht_lh,m_vec_ndx,8); % subband LH FHT

[f_fht_hl_ll,f_fht_hl_lh,f_fht_hl_hl,f_fht_hl_hh] = ...
    fht(f_fht_hl,m_vec_ndx,8); % subband HL FHT

***** Quantizing *****

f_fht_ll_q = quantizer_ll(f_fht_ll,Q,m_vec_ndx); % quantize LL

f_fht_hh_q = round(f_fht_hh/q3); % quantize HH

f_fht_lh_ll_q = round(f_fht_lh_ll/q2); % quantize of LH subbands
f_fht_lh_lh_q = round(f_fht_lh_lh/q2);
f_fht_lh_hl_q = round(f_fht_lh_hl/q3);
f_fht_lh_hh_q = round(f_fht_lh_hh/q3);

f_fht_hl_ll_q = round(f_fht_hl_ll/q2); % quantize of HL subbands
f_fht_hl_lh_q = round(f_fht_hl_lh/q3);
f_fht_hl_hl_q = round(f_fht_hl_hl/q2);
f_fht_hl_hh_q = round(f_fht_hl_hh/q3);

***** Working on LL *****
% zig-zag scans each LL 8x8 (Results are one 6336x1 vector [ll_zz] and the index
% of the last non-zero entity [last_ll_zz]. Get "inf" if a group of
% 64 is all zeros.)
[last_ll_zz,ll_zz] = zzb(f_fht_ll_q,8);

% gets rid of trailing zeros (one big vector of varying size.)
a_ll_zz = make_it_compact(ll_zz,last_ll_zz,8);

% parsing LL with Huffman routine
parsed_ll_zz = parse_Huff(a_ll_zz,last_ll_zz);

% gets bits per frame due to LL
bits_ll_zz(i+1) = get_bits_Huff(parsed_ll_zz);

***** Working on HH *****
% scans each HH 8x8 (Results are one 6336x1 vector [hh_r] and the index of the last
% non-zero entity [last_hh_r], where r indicates horizontal raster
% the scan method. Get "inf" if a group of 64 is all zeros.)
[last_hh_r,hh_r] = raster(f_fht_hh_q,8);

% gets rid of trailing zeros (one big vector of varying size)
a_hh_r = make_it_compact(hh_r,last_hh_r,8);

% parsing HH and getting the number of parsings for later used in eval_thesis to
% get the percent of time that the default bit number is used.
parsed_hh_r_3D = parse_3D(a_hh_r,last_hh_r);
l_p_hh_r_3D(i+1) = length(parsed_hh_r_3D(:,1));

% gets bits per frame and number of times the default is chosen
% (includes 99 COD bits)
[bits_hh_r_3D(i+1), hh_r_22(i+1)] = get_bits2(parsed_hh_r_3D,frame_type);

***** Working on LH subbands *****

```

```

*****
***** Doing the LH_LL subband *****
% scans each LH_LL 4x4 (Results are one 1584x1 vector [lh_ll_r] and the index of
% the last non-zero entity [last_lh_ll_r], where the r indicates
% horizontal raster scan method. Get "inf" if a group of 16 is all
% zeros.)
[last_lh_ll_r,lh_ll_r] = raster(f_fht_lh_ll_q,4);

% gets rid of trailing zeros (one big vector of varying size)
a_lh_ll_r = make_it_compact(lh_ll_r,last_lh_ll_r,4);

% parsing LH_LL and getting the number of parsings for later used in eval_thesis to
% get the percent of time that the default bit number is used.
parsed_lh_ll_r_3D = parse_3D(a_lh_ll_r,last_lh_ll_r);
l_p_lh_ll_r_3D(i+1) = length(parsed_lh_ll_r_3D(:,1));

% gets bits per frame and number of times the default is chosen
% (includes 99 COD bits)
[bits_lh_ll_r_3D(i+1), lh_ll_r_22(i+1)] = get_bits2(parsed_lh_ll_r_3D,frame_type);

***** Doing the LH_LH subband *****
% scans each LH_LH 4x4 (Results are one 1584x1 vector [lh_lh_r] and the index of
% the last non-zero entity [last_lh_lh_r], where the r indicates
% horizontal raster scan method. Get "inf" if a group of 16 is all
% zeros.)
[last_lh_lh_r,lh_lh_r] = raster(f_fht_lh_lh_q,4);

% gets rid of trailing zeros (one big vector of varying size)
a_lh_lh_r = make_it_compact(lh_lh_r,last_lh_lh_r,4);

% parsing LH_LH and getting the number of parsings for later used in eval_thesis to
% get the percent of time that the default bit number is used.
parsed_lh_lh_r_3D = parse_3D(a_lh_lh_r,last_lh_lh_r);
l_p_lh_lh_r_3D(i+1) = length(parsed_lh_lh_r_3D(:,1));

% gets bits per frame and number of times the default is chosen
% (includes 99 COD bits)
[bits_lh_lh_r_3D(i+1), lh_lh_r_22(i+1)] = get_bits2(parsed_lh_lh_r_3D,frame_type);

***** Doing the LH_HL subband *****
% scans each LH_HL 4x4 (Results are 1584x1 vector [lh_hl_r] and the index of
% the last non-zero entity [last_lh_hl_r], where the r indicates
% horizontal raster scan method. Get "inf" if a group of 16 is all
% zeros.)
[last_lh_hl_r,lh_hl_r] = raster(f_fht_lh_hl_q,4);

% gets rid of trailing zeros (one big vector of varying size)
a_lh_hl_r = make_it_compact(lh_hl_r,last_lh_hl_r,4);

% parsing LH_HL and getting the number of parsings for later used in eval_thesis to
% get the percent of time that the default bit number is used.
parsed_lh_hl_r_3D = parse_3D(a_lh_hl_r,last_lh_hl_r);
l_p_lh_hl_r_3D(i+1) = length(parsed_lh_hl_r_3D(:,1));

% gets bits per frame and number of times the default is chosen
% (includes 99 COD bits)
[bits_lh_hl_r_3D(i+1), lh_hl_r_22(i+1)] = get_bits2(parsed_lh_hl_r_3D,frame_type);

***** Doing the LH_HH subband *****
% scans each LH_HH 4x4 (Results are 1584x1 vector [lh_hh_r] and the index of
% the last non-zero entity [last_lh_hh_r], where the r indicates
% horizontal raster scan method. Get "inf" if a group of 16 is all
% zeros.)
[last_lh_hh_r,lh_hh_r] = raster(f_fht_lh_hh_q,4);

% gets rid of trailing zeros (one big vector of varying size)

```

```

a_lh_hh_r = make_it_compact(lh_hh_r,last_lh_hh_r,4);

% parsing LH_HH and getting the number of parsings for later used in eval_thesis to
% get the percent of time that the default bit number is used.
parsed_lh_hh_r_3D = parse_3D(a_lh_hh_r,last_lh_hh_r);
l_p_lh_hh_r_3D(i+1) = length(parsed_lh_hh_r_3D(:,1));

% gets bits per frame and number of times the default is chosen
% (includes 99 COD bits)
[bits_lh_hh_r_3D(i+1), lh_hh_r_22(i+1)] = get_bits2(parsed_lh_hh_r_3D,frame_type);

*****
***** Working on HL subbands *****
*****

***** Doing the HL_LL subband *****

% scans each HL_LL 4x4 (Results are a 1584x1 vector [hl_ll_v] and the index of
% the last non-zero entity [last_hl_ll_v], where the v indicates
% vertical raster scan method. Get "inf" if a group of 16 is all
% zeros.)
[last_hl_ll_v,hl_ll_v] = vertical(f_fht_hl_ll_q,4);

% gets rid of trailing zeros (one big vector of varying size)
a_hl_ll_v = make_it_compact(hl_ll_v,last_hl_ll_v,4);

% parsing HL_LL and getting the number of parsings for later used in eval_thesis to
% get the percent of time that the default bit number is used.
parsed_hl_ll_v_3D = parse_3D(a_hl_ll_v,last_hl_ll_v);
l_p_hl_ll_v_3D(i+1) = length(parsed_hl_ll_v_3D(:,1));

% gets bits per frame and number of times the default is chosen
% (includes 99 COD bits)
[bits_hl_ll_v_3D(i+1), hl_ll_v_22(i+1)] = get_bits2(parsed_hl_ll_v_3D,frame_type);

***** Doing the HL_LH subband *****

% scans each HL_LH 4x4 (Results are a 1584x1 vector [hl_lh_v] and the index of
% the last non-zero entity [last_hl_lh_v], where the v indicates
% vertical raster scan method. Get "inf" if a group of 16 is all
% zeros.)
[last_hl_lh_v,hl_lh_v] = vertical(f_fht_hl_lh_q,4);

% gets rid of trailing zeros (one big vector of varying size)
a_hl_lh_v = make_it_compact(hl_lh_v,last_hl_lh_v,4);

% parsing HL_LH and getting the number of parsings for later used in eval_thesis to
% get the percent of time that the default bit number is used.
parsed_hl_lh_v_3D = parse_3D(a_hl_lh_v,last_hl_lh_v);
l_p_hl_lh_v_3D(i+1) = length(parsed_hl_lh_v_3D(:,1));

% gets bits per frame and number of times the default is chosen
% (includes 99 COD bits)
[bits_hl_lh_v_3D(i+1), hl_lh_v_22(i+1)] = get_bits2(parsed_hl_lh_v_3D,frame_type);

***** Doing the HL_HL subband *****

% scans each HL_HL 4x4 (Results are a 1584x1 vector [hl_hl_v] and the index of
% the last non-zero entity [last_hl_hl_v], where the v indicates
% vertical raster scan method. Get "inf" if a group of 16 is all
% zeros.)
[last_hl_hl_v,hl_hl_v] = vertical(f_fht_hl_hl_q,4);

% gets rid of trailing zeros (one big vector of varying size)
a_hl_hl_v = make_it_compact(hl_hl_v,last_hl_hl_v,4);

% parsing HL_HL and getting the number of parsings for later used in eval_thesis to
% get the percent of time that the default bit number is used.
parsed_hl_hl_v_3D = parse_3D(a_hl_hl_v,last_hl_hl_v);
l_p_hl_hl_v_3D(i+1) = length(parsed_hl_hl_v_3D(:,1));

```



```

% gets bits per frame and number of times the default is chosen
% (includes 99 COD bits)
[bits_hl_hl_v_3D(i+1), hl_hl_v_22(i+1)] = get_bits2(parsed_hl_hl_v_3D,frame_type);

%%%%%%%%%%%%%%%%%%%%%%%%%%%%%%%%%%%%%%%%%%%%%%%%%%%%%%%%%%%%%%%%%%%%%%%%% Doing the HL_HH subband %%%%%%%%%%%%%%%%%%%%%%%%%%%%%%%%%%%%%%%%%%%%%%%%%%%%%%%%%%%%%%%%%%%%%%%%%%

% scans each HL_HL 4x4 (Results are a 1584x1 vector [hl_hh_v] and the index of
% the last non-zero entity [last_hl_hh_v], where the v indicates
% vertical raster scan method. Get "inf" if a group of 16 is all
% zeros.)
[last_hl_hh_v,hl_hh_v] = vertical(f_fht_hl_hh_q,4);

% gets rid of trailing zeros (one big vector of varying size)
a_hl_hh_v = make_it_compact(hl_hh_v,last_hl_hh_v,4);

% parsing HL_HH and getting the number of parsings for later used in eval_thesis to
% get the percent of time that the default bit number is used.
parsed_hl_hh_v_3D = parse_3D(a_hl_hh_v,last_hl_hh_v);
l_p_hl_hh_v_3D(i+1) = length(parsed_hl_hh_v_3D(:,1));

% gets bits per frame and number of times the default is chosen
% (includes 99 COD bits)
[bits_hl_hh_v_3D(i+1), hl_hh_v_22(i+1)] = get_bits2(parsed_hl_hh_v_3D,frame_type);

% getting bits per frame per layer
layer1(i+1) = bits_ll_zz(i+1);
layer2(i+1) = bits_lh_ll_r_3D(i+1) + bits_lh_lh_r_3D(i+1) + ...
             bits_hl_ll_v_3D(i+1) + bits_hl_hl_v_3D(i+1);
layer3(i+1) = bits_hh_r_3D(i+1) + bits_lh_hl_r_3D(i+1) + bits_lh_hh_r_3D(i+1) + ...
             bits_hl_lh_v_3D(i+1) + l_p_hl_hh_v_3D(i+1);
total(i+1) = layer1(i+1) + layer2(i+1) + layer3(i+1);

%%%%%%%%%%%%%%%%%%%%%%%%%%%%%%%%%%%%%%%%%%%%%%%%%%%%%%%%%%%%%%%%%%%%%%%%%
%
% Channel
%
%%%%%%%%%%%%%%%%%%%%%%%%%%%%%%%%%%%%%%%%%%%%%%%%%%%%%%%%%%%%%%%%%%%%%%%%%

%%%%%%%%%%%%%%%%%%%%%%%%%%%%%%%%%%%%%%%%%%%%%%%%%%%%%%%%%%%%%%%%%%%%%%%%% Unquantize %%%%%%%%%%%%%%%%%%%%%%%%%%%%%%%%%%%%%%%%%%%%%%%%%%%%%%%%%%%%%%%%%%%%%%%%%%

f_fht_ll_uq = unquantize_ll(f_fht_ll_q,Q,m_vec_ndx); % unquantize LL

f_fht_hh_uq = f_fht_hh_q * q3; % unquantize HH

f_fht_lh_ll_uq = f_fht_lh_ll_q * q2; % unquantize of LH subbands
f_fht_lh_lh_uq = f_fht_lh_lh_q * q2;
f_fht_lh_hl_uq = f_fht_lh_hl_q * q3;
f_fht_lh_hh_uq = f_fht_lh_hh_q * q3;

f_fht_hl_ll_uq = f_fht_hl_ll_q * q2; % unquantize of HL subbands
f_fht_hl_lh_uq = f_fht_hl_lh_q * q3;
f_fht_hl_hl_uq = f_fht_hl_hl_q * q2;
f_fht_hl_hh_uq = f_fht_hl_hh_q * q3;

%%%%%%%%%%%%%%%%%%%%%%%%%%%%%%%%%%%%%%%%%%%%%%%%%%%%%%%%%%%%%%%%%%%%%%%%% Inverse Transform %%%%%%%%%%%%%%%%%%%%%%%%%%%%%%%%%%%%%%%%%%%%%%%%%%%%%%%%%%%%%%%%%%%%%%%%%%

f_far_ll = invdct_of_fht(f_fht_ll_uq,m_vec_ndx); % inv 2-D dct of LL
f_far_ll = f_far_ll + 128; % level shift
f_far_lh = remake_3(f_far_lh,f_fht_lh_ll_uq,f_fht_lh_lh_uq,f_fht_lh_hl_uq, ...
                  f_fht_lh_hh_uq,m_vec_ndx,8); % LH subband inv FHT
f_far_hl = remake_3(f_far_hl,f_fht_hl_ll_uq,f_fht_hl_lh_uq,f_fht_hl_hl_uq, ...
                  f_fht_hl_hh_uq,m_vec_ndx,8); % HL subband inv FHT
f_far_hh = f_fht_hh_uq;

f_far_ll_p2 = f_far_ll; % LL p2 assignment
f_far_lh_p2 = remake_3(f_far_lh_p2,f_fht_lh_ll_uq,f_fht_lh_lh_uq,...
                    0,0,m_vec_ndx,8); % LH p2 subband inv FHT
f_far_hl_p2 = remake_3(f_far_hl_p2,f_fht_hl_ll_uq,0,...
                    f_fht_hl_hl_uq,0,m_vec_ndx,8); % HL p2 subband inv FHT

```

```

f_far_hh_p2 = 0; % HH p2 assignment

f_far_ll_p1 = f_far_ll; % LL p1 assignment
f_far_lh_p1 = 0; % HH p1 assignment
f_far_hl_p1 = 0; % HH p1 assignment
f_far_hh_p1 = 0; % HH p1 assignment

f_3 = remake_3(f_3,f_far_ll,f_far_lh,f_far_hl,... % frame inv FHT with 3 layers
    f_far_hh,m_vec_ndx,16);
f_2 = remake_3(f_2,f_far_ll_p2,f_far_lh_p2,f_far_hl_p2,... % frame inv FHT with 2 layers
    f_far_hh_p2,m_vec_ndx,16);
f_1 = remake_3(f_1,f_far_ll_p1,f_far_lh_p1,f_far_hl_p1,... % frame inv FHT with 1 layer
    f_far_hh_p1,m_vec_ndx,16);

else % a static frame sequence

***** Transforms *****
[f_fht_ll,f_fht_lh,f_fht_hl,f_fht_hh] = fht(f_vec,m_vec_ndx,16); % FHT of frame

[f_fht_ll_ll,f_fht_ll_lh,f_fht_ll_hl,f_fht_ll_hh] = ... % subband LL FHT
    fht(f_fht_ll,m_vec_ndx,8);
[f_fht_lh_ll,f_fht_lh_lh,f_fht_lh_hl,f_fht_lh_hh] = ... % subband LH FHT
    fht(f_fht_lh,m_vec_ndx,8);
[f_fht_hl_ll,f_fht_hl_lh,f_fht_hl_hl,f_fht_hl_hh] = ... % subband HL FHT
    fht(f_fht_hl,m_vec_ndx,8);
[f_fht_hh_ll,f_fht_hh_lh,f_fht_hh_hl,f_fht_hh_hh] = ... % subband HH FHT
    fht(f_fht_hh,m_vec_ndx,8);

***** Quantizing *****

f_fht_ll_ll_q = round(f_fht_ll_ll/q1); % quantize of LL subbands
f_fht_ll_lh_q = round(f_fht_ll_lh/q2);
f_fht_ll_hl_q = round(f_fht_ll_hl/q2);
f_fht_ll_hh_q = round(f_fht_ll_hh/q3);

f_fht_lh_ll_q = round(f_fht_lh_ll/q2); % quantize of LH subbands
f_fht_lh_lh_q = round(f_fht_lh_lh/q2);
f_fht_lh_hl_q = round(f_fht_lh_hl/q3);
f_fht_lh_hh_q = round(f_fht_lh_hh/q3);

f_fht_hl_ll_q = round(f_fht_hl_ll/q2); % quantize of HL subbands
f_fht_hl_lh_q = round(f_fht_hl_lh/q3);
f_fht_hl_hl_q = round(f_fht_hl_hl/q2);
f_fht_hl_hh_q = round(f_fht_hl_hh/q3);

f_fht_hh_ll_q = round(f_fht_hh_ll/q3); % quantize of HL subbands
f_fht_hh_lh_q = round(f_fht_hh_lh/q3);
f_fht_hh_hl_q = round(f_fht_hh_hl/q3);
f_fht_hh_hh_q = round(f_fht_hh_hh/q3);

*****
***** Working on LL *****
*****

***** Doing the LL_LL subband *****

% scans each LL_LL 4x4 (Results are one 1584x1 vector [ll_ll_r] and the index of
% the last non-zero entity [last_ll_ll_r], where the r indicates
% horizontal raster scan method. Get "inf" if a group of 16 is all
% zeros.)
[last_ll_ll_r,ll_ll_r] = raster(f_fht_ll_ll_q,4);

% gets rid of trailing zeros (one big vector of varying size)
a_ll_ll_r = make_it_compact(ll_ll_r,last_ll_ll_r,4);

```

```

% parsing LL_LL and getting the number of parsings for later used in eval_thesis to
%     get the percent of time that the default bit number is used.
parsed_ll_ll_r_3D = parse_3D(a_ll_ll_r,last_ll_ll_r);
l_p_ll_ll_r_3D(i+1) = length(parsed_ll_ll_r_3D(:,1));

% gets bits per frame and number of times the default is chosen
%     (includes 99 COD bits)
[bits_ll_ll_r_3D(i+1), ll_ll_r_22(i+1)] = get_bits2(parsed_ll_ll_r_3D,frame_type);

***** Doing the LL_LH subband *****

% scans each LL_LH 4x4 (Results are one 1584x1 vector [ll_lh_r] and the index of
%     the last non-zero entity [last_ll_lh_r], where the r indicates
%     horizontal raster scan method. Get "inf" if a group of 16 is all
%     zeros.)
[ll_lh_r,last_ll_lh_r] = raster(f_fht_ll_lh_q,4);

% gets rid of trailing zeros (one big vector of varying size)
a_ll_lh_r = make_it_compact(ll_lh_r,last_ll_lh_r,4);

% parsing LL_LH and getting the number of parsings for later used in eval_thesis to
%     get the percent of time that the default bit number is used.
parsed_ll_lh_r_3D = parse_3D(a_ll_lh_r,last_ll_lh_r);
l_p_ll_lh_r_3D(i+1) = length(parsed_ll_lh_r_3D(:,1));

% gets bits per frame and number of times the default is chosen
%     (includes 99 COD bits)
[bits_ll_lh_r_3D(i+1), ll_lh_r_22(i+1)] = get_bits2(parsed_ll_lh_r_3D,frame_type);

***** Doing the LL_HL subband *****

% scans each LL_HL 4x4 (Results are 1584x1 vector [ll_hl_r] and the index of
%     the last non-zero entity [last_ll_hl_r], where the r indicates
%     horizontal raster scan method. Get "inf" if a group of 16 is all
%     zeros.)
[ll_hl_r,last_ll_hl_r] = raster(f_fht_ll_hl_q,4);

% gets rid of trailing zeros (one big vector of varying size)
a_ll_hl_r = make_it_compact(ll_hl_r,last_ll_hl_r,4);

% parsing LL_HL and getting the number of parsings for later used in eval_thesis to
%     get the percent of time that the default bit number is used.
parsed_ll_hl_r_3D = parse_3D(a_ll_hl_r,last_ll_hl_r);
l_p_ll_hl_r_3D(i+1) = length(parsed_ll_hl_r_3D(:,1));

% gets bits per frame and number of times the default is chosen
%     (includes 99 COD bits)
[bits_ll_hl_r_3D(i+1), ll_hl_r_22(i+1)] = get_bits2(parsed_ll_hl_r_3D,frame_type);

***** Doing the LL_HH subband *****

% scans each LL_HH 4x4 (Results are 1584x1 vector [ll_hh_r] and the index of
%     the last non-zero entity [last_ll_hh_r], where the r indicates
%     horizontal raster scan method. Get "inf" if a group of 16 is all
%     zeros.)
[ll_hh_r,last_ll_hh_r] = raster(f_fht_ll_hh_q,4);

% gets rid of trailing zeros (one big vector of varying size)
a_ll_hh_r = make_it_compact(ll_hh_r,last_ll_hh_r,4);

% parsing LL_HH and getting the number of parsings for later used in eval_thesis to
%     get the percent of time that the default bit number is used.
parsed_ll_hh_r_3D = parse_3D(a_ll_hh_r,last_ll_hh_r);
l_p_ll_hh_r_3D(i+1) = length(parsed_ll_hh_r_3D(:,1));

% gets bits per frame and number of times the default is chosen
%     (includes 99 COD bits)
[bits_ll_hh_r_3D(i+1), ll_hh_r_22(i+1)] = get_bits2(parsed_ll_hh_r_3D,frame_type);

```

```

*****
***** Working on LH subbands *****
*****

***** Doing the LH_LL subband *****

% scans each LH_LL 4x4 (Results are one 1584x1 vector [lh_ll_r] and the index of
% the last non-zero entity [last_lh_ll_r], where the r indicates
% horizontal raster scan method. Get "inf" if a group of 16 is all
% zeros.)
[last_lh_ll_r,lh_ll_r] = raster(f_fht_lh_ll_q,4);

% gets rid of trailing zeros (one big vector of varying size)
a_lh_ll_r = make_it_compact(lh_ll_r,last_lh_ll_r,4);

% parsing LH_LL and getting the number of parsings for later used in eval_thesis to
% get the percent of time that the default bit number is used.

parsed_lh_ll_r_3D = parse_3D(a_lh_ll_r,last_lh_ll_r);
l_p_lh_ll_r_3D(i+1) = length(parsed_lh_ll_r_3D(:,1));

% gets bits per frame and number of times the default is chosen
% (includes 99 COD bits)
[bits_lh_ll_r_3D(i+1), lh_ll_r_22(i+1)] = get_bits2(parsed_lh_ll_r_3D,frame_type);

***** Doing the LH_LH subband *****

% scans each LH_LH 4x4 (Results are one 1584x1 vector [lh_lh_r] and the index of
% the last non-zero entity [last_lh_lh_r], where the r indicates
% horizontal raster scan method. Get "inf" if a group of 16 is all
% zeros.)
[last_lh_lh_r,lh_lh_r] = raster(f_fht_lh_lh_q,4);

% gets rid of trailing zeros (one big vector of varying size)
a_lh_lh_r = make_it_compact(lh_lh_r,last_lh_lh_r,4);

% parsing LH_LH and getting the number of parsings for later used in eval_thesis to
% get the percent of time that the default bit number is used.
parsed_lh_lh_r_3D = parse_3D(a_lh_lh_r,last_lh_lh_r);
l_p_lh_lh_r_3D(i+1) = length(parsed_lh_lh_r_3D(:,1));

% gets bits per frame and number of times the default is chosen
% (includes 99 COD bits)
[bits_lh_lh_r_3D(i+1), lh_lh_r_22(i+1)] = get_bits2(parsed_lh_lh_r_3D,frame_type);

***** Doing the LH_HL subband *****

% scans each LH_HL 4x4 (Results are 1584x1 vector [lh_hl_r] and the index of
% the last non-zero entity [last_lh_hl_r], where the r indicates
% horizontal raster scan method. Get "inf" if a group of 16 is all
% zeros.)
[last_lh_hl_r,lh_hl_r] = raster(f_fht_lh_hl_q,4);

% gets rid of trailing zeros (one big vector of varying size)
a_lh_hl_r = make_it_compact(lh_hl_r,last_lh_hl_r,4);

% parsing LH_HL and getting the number of parsings for later used in eval_thesis to
% get the percent of time that the default bit number is used.
parsed_lh_hl_r_3D = parse_3D(a_lh_hl_r,last_lh_hl_r);
l_p_lh_hl_r_3D(i+1) = length(parsed_lh_hl_r_3D(:,1));

% gets bits per frame and number of times the default is chosen
% (includes 99 COD bits)
[bits_lh_hl_r_3D(i+1), lh_hl_r_22(i+1)] = get_bits2(parsed_lh_hl_r_3D,frame_type);

***** Doing the LH_HH subband *****

% scans each LH_HH 4x4 (Results are 1584x1 vector [lh_hh_r] and the index of
% the last non-zero entity [last_lh_hh_r], where the r indicates
% horizontal raster scan method. Get "inf" if a group of 16 is all

```

```

%          zeros.)
[last_lh_hh_r, lh_hh_r] = raster(f_fht_lh_hh_q, 4);

% gets rid of trailing zeros (one big vector of varying size)
a_lh_hh_r = make_it_compact(lh_hh_r, last_lh_hh_r, 4);

% parsing LH_HH and getting the number of parsings for later used in eval_thesis to
%          get the percent of time that the default bit number is used.
parsed_lh_hh_r_3D = parse_3D(a_lh_hh_r, last_lh_hh_r);
l_p_lh_hh_r_3D(i+1) = length(parsed_lh_hh_r_3D(:, 1));

% gets bits per frame and number of times the default is chosen
%          (includes 99 COD bits)
[bits_lh_hh_r_3D(i+1), lh_hh_r_22(i+1)] = get_bits2(parsed_lh_hh_r_3D, frame_type);

%%%%%%%%%%%%%%%%%%%%%%%%%%%%%%%%%%%%%%%%%%%%%%%%%%%%%%%%%%%%%%%%%%%%%%%%
%%%%%%%%%%%%%%%%%%%%%%%%%%%%%%%%%%%%%%%%%%%%%%%%%%%%%%%%%%%%%%%%%%%%%%%% Working on HL subbands %%%%%%%%%%%%%%%%%%%%%%%%%%%%%%%%%%%%%%%%%%%%%%%%%%%%%%%%%%%%%%%%%%%%%%%%%
%%%%%%%%%%%%%%%%%%%%%%%%%%%%%%%%%%%%%%%%%%%%%%%%%%%%%%%%%%%%%%%%%%%%%%%%

%%%%%%%%%%%%%%%%%%%%%%%%%%%%%%%%%%%%%%%%%%%%%%%%%%%%%%%%%%%%%%%%%%%%%%%% Doing the HL_LL subband %%%%%%%%%%%%%%%%%%%%%%%%%%%%%%%%%%%%%%%%%%%%%%%%%%%%%%%%%%%%%%%%%%%%%%%%%

% scans each HL_LL 4x4 (Results are a 1584x1 vector [hl_ll_v] and the index of
%          the last non-zero entity [last_hl_ll_v], where the v indicates
%          vertical raster scan method. Get "inf" if a group of 16 is all
%          zeros.)
[last_hl_ll_v, hl_ll_v] = vertical(f_fht_hl_ll_q, 4);

% gets rid of trailing zeros (one big vector of varying size)
a_hl_ll_v = make_it_compact(hl_ll_v, last_hl_ll_v, 4);

% parsing HL_LL and getting the number of parsings for later used in eval_thesis to
%          get the percent of time that the default bit number is used.
parsed_hl_ll_v_3D = parse_3D(a_hl_ll_v, last_hl_ll_v);
l_p_hl_ll_v_3D(i+1) = length(parsed_hl_ll_v_3D(:, 1));

% gets bits per frame and number of times the default is chosen
%          (includes 99 COD bits)
[bits_hl_ll_v_3D(i+1), hl_ll_v_22(i+1)] = get_bits2(parsed_hl_ll_v_3D, frame_type);

%%%%%%%%%%%%%%%%%%%%%%%%%%%%%%%%%%%%%%%%%%%%%%%%%%%%%%%%%%%%%%%%%%%%%%%% Doing the HL_LH subband %%%%%%%%%%%%%%%%%%%%%%%%%%%%%%%%%%%%%%%%%%%%%%%%%%%%%%%%%%%%%%%%%%%%%%%%%

% scans each HL_LH 4x4 (Results are a 1584x1 vector [hl_lh_v] and the index of
%          the last non-zero entity [last_hl_lh_v], where the v indicates
%          vertical raster scan method. Get "inf" if a group of 16 is all
%          zeros.)
[last_hl_lh_v, hl_lh_v] = vertical(f_fht_hl_lh_q, 4);

% gets rid of trailing zeros (one big vector of varying size)
a_hl_lh_v = make_it_compact(hl_lh_v, last_hl_lh_v, 4);

% parsing HL_LH and getting the number of parsings for later used in eval_thesis to
%          get the percent of time that the default bit number is used.
parsed_hl_lh_v_3D = parse_3D(a_hl_lh_v, last_hl_lh_v);
l_p_hl_lh_v_3D(i+1) = length(parsed_hl_lh_v_3D(:, 1));

% gets bits per frame and number of times the default is chosen
%          (includes 99 COD bits)
[bits_hl_lh_v_3D(i+1), hl_lh_v_22(i+1)] = get_bits2(parsed_hl_lh_v_3D, frame_type);

%%%%%%%%%%%%%%%%%%%%%%%%%%%%%%%%%%%%%%%%%%%%%%%%%%%%%%%%%%%%%%%%%%%%%%%% Doing the HL_HL subband %%%%%%%%%%%%%%%%%%%%%%%%%%%%%%%%%%%%%%%%%%%%%%%%%%%%%%%%%%%%%%%%%%%%%%%%%

% scans each HL_HL 4x4 (Results are a 1584x1 vector [hl_hl_v] and the index of
%          the last non-zero entity [last_hl_hl_v], where the v indicates
%          vertical raster scan method. Get "inf" if a group of 16 is all
%          zeros.)
[last_hl_hl_v, hl_hl_v] = vertical(f_fht_hl_hl_q, 4);

% gets rid of trailing zeros (one big vector of varying size)
a_hl_hl_v = make_it_compact(hl_hl_v, last_hl_hl_v, 4);

```

```

% parsing HL_HL and getting the number of parsings for later used in eval_thesis to
% get the percent of time that the default bit number is used.
parsed_hl_hl_v_3D = parse_3D(a_hl_hl_v,last_hl_hl_v);
l_p_hl_hl_v_3D(i+1) = length(parsed_hl_hl_v_3D(:,1));

% gets bits per frame and number of times the default is chosen
% (includes 99 COD bits)
[bits_hl_hl_v_3D(i+1), hl_hl_v_22(i+1)] = get_bits2(parsed_hl_hl_v_3D,frame_type);

***** Doing the HL_HH subband *****

% scans each HL_HL 4x4 (Results are a 1584x1 vector [hl_hh_v] and the index of
% the last non-zero entity [last_hl_hh_v], where the v indicates
% vertical raster scan method. Get "inf" if a group of 16 is all
% zeros.)
[last_hl_hh_v,hl_hh_v] = vertical(f_fht_hl_hh_q,4);

% gets rid of trailing zeros (one big vector of varying size)
a_hl_hh_v = make_it_compact(hl_hh_v,last_hl_hh_v,4);

% parsing HL_HH and getting the number of parsings for later used in eval_thesis to
% get the percent of time that the default bit number is used.
parsed_hl_hh_v_3D = parse_3D(a_hl_hh_v,last_hl_hh_v);
l_p_hl_hh_v_3D(i+1) = length(parsed_hl_hh_v_3D(:,1));

% gets bits per frame and number of times the default is chosen
% (includes 99 COD bits)
[bits_hl_hh_v_3D(i+1), hl_hh_v_22(i+1)] = get_bits2(parsed_hl_hh_v_3D,frame_type);

***** Working on HH subbands *****

***** Doing the HH_LL subband *****

% scans each HH_LL 4x4 (Results are one 1584x1 vector [hh_ll_r] and the index of
% the last non-zero entity [last_hh_ll_r], where the r indicates
% horizontal raster scan method. Get "inf" if a group of 16 is all
% zeros.)
[last_hh_ll_r,hh_ll_r] = raster(f_fht_hh_ll_q,4);

% gets rid of trailing zeros (one big vector of varying size)
a_hh_ll_r = make_it_compact(hh_ll_r,last_hh_ll_r,4);

% parsing HH_LL and getting the number of parsings for later used in eval_thesis to
% get the percent of time that the default bit number is used.
parsed_hh_ll_r_3D = parse_3D(a_hh_ll_r,last_hh_ll_r);
l_p_hh_ll_r_3D(i+1) = length(parsed_hh_ll_r_3D(:,1));

% gets bits per frame and number of times the default is chosen
% (includes 99 COD bits)
[bits_hh_ll_r_3D(i+1), hh_ll_r_22(i+1)] = get_bits2(parsed_hh_ll_r_3D,frame_type);

***** Doing the HH_LH subband *****

% scans each HH_LH 4x4 (Results are one 1584x1 vector [hh_lh_r] and the index of
% the last non-zero entity [last_hh_lh_r], where the r indicates
% horizontal raster scan method. Get "inf" if a group of 16 is all
% zeros.)
[last_hh_lh_r,hh_lh_r] = raster(f_fht_hh_lh_q,4);

% gets rid of trailing zeros (one big vector of varying size)
a_hh_lh_r = make_it_compact(hh_lh_r,last_hh_lh_r,4);

% parsing HH_LH and getting the number of parsings for later used in eval_thesis to
% get the percent of time that the default bit number is used.
parsed_hh_lh_r_3D = parse_3D(a_hh_lh_r,last_hh_lh_r);
l_p_hh_lh_r_3D(i+1) = length(parsed_hh_lh_r_3D(:,1));

% gets bits per frame and number of times the default is chosen
% (includes 99 COD bits)

```

```

[bits_hh_lh_r_3D(i+1), hh_lh_r_22(i+1)] = get_bits2(parsed_hh_lh_r_3D,frame_type);
***** Doing the HH_HL subband *****

% scans each HH_HL 4x4 (Results are 1584x1 vector [hh_hl_r] and the index of
% the last non-zero entity [last_hh_hl_r], where the r indicates
% horizontal raster scan method. Get "inf" if a group of 16 is all
% zeros.)
[last_hh_hl_r,hh_hl_r] = raster(f_fht_hh_hl_q,4);

% gets rid of trailing zeros (one big vector of varying size)
a_hh_hl_r = make_it_compact(hh_hl_r,last_hh_hl_r,4);

% parsing HH_HL and getting the number of parsings for later used in eval_thesis to
% get the percent of time that the default bit number is used.
parsed_hh_hl_r_3D = parse_3D(a_hh_hl_r,last_hh_hl_r);
l_p_hh_hl_r_3D(i+1) = length(parsed_hh_hl_r_3D(:,1));

% gets bits per frame and number of times the default is chosen
% (includes 99 COD bits)
[bits_hh_hl_r_3D(i+1), hh_hl_r_22(i+1)] = get_bits2(parsed_hh_hl_r_3D,frame_type);
***** Doing the HH_HH subband *****

% scans each HH_HH 4x4 (Results are 1584x1 vector [hh_hh_r] and the index of
% the last non-zero entity [last_hh_hh_r], where the r indicates
% horizontal raster scan method. Get "inf" if a group of 16 is all
% zeros.)
[last_hh_hh_r,hh_hh_r] = raster(f_fht_hh_hh_q,4);

% gets rid of trailing zeros (one big vector of varying size)
a_hh_hh_r = make_it_compact(hh_hh_r,last_hh_hh_r,4);

% parsing HH_HH and getting the number of parsings for later used in eval_thesis to
% get the percent of time that the default bit number is used.
parsed_hh_hh_r_3D = parse_3D(a_hh_hh_r,last_hh_hh_r);
l_p_hh_hh_r_3D(i+1) = length(parsed_hh_hh_r_3D(:,1));

% gets bits per frame and number of times the default is chosen
% (includes 99 COD bits)
[bits_hh_hh_r_3D(i+1), hh_hh_r_22(i+1)] = get_bits2(parsed_hh_hh_r_3D,frame_type);

% getting bits per frame per layer and total
layer1(i+1) = bits_ll_ll_r_3D(i+1) + bits_ll_lh_r_3D(i+1) + ...
    bits_lh_ll_r_3D(i+1)+ bits_lh_lh_r_3D(i+1) + ...
    bits_ll_hl_r_3D(i+1)+ bits_hl_ll_v_3D(i+1) + ...
    bits_hh_ll_r_3D(i+1)+ bits_hl_hl_v_3D(i+1) + ...
    bits_hh_hh_r_3D(i+1);
layer2(i+1) = bits_ll_hh_r_3D(i+1) + bits_lh_hl_r_3D(i+1) + ...
    bits_lh_hh_r_3D(i+1) + bits_hl_lh_v_3D(i+1) + ...
    bits_hl_hh_v_3D(i+1);
layer3(i+1) = bits_hh_lh_r_3D(i+1) + bits_hh_hl_r_3D(i+1);
total(i+1) = layer1(i+1) + layer2(i+1) + layer3(i+1);

*****
%
% Channel
%
*****

***** Unquantize *****

f_fht_ll_ll_uq = f_fht_ll_ll_q * q1; % unquantize of LH subbands
f_fht_ll_lh_uq = f_fht_ll_lh_q * q2;
f_fht_ll_hl_uq = f_fht_ll_hl_q * q2;
f_fht_ll_hh_uq = f_fht_ll_hh_q * q3;

f_fht_lh_ll_uq = f_fht_lh_ll_q * q2; % unquantize of LH subbands
f_fht_lh_lh_uq = f_fht_lh_lh_q * q2;
f_fht_lh_hl_uq = f_fht_lh_hl_q * q3;

```

```

f_fht_lh_hh_uq = f_fht_lh_hh_q * q3;

f_fht_hl_ll_uq = f_fht_hl_ll_q * q2;           % unquantize of HL subbands
f_fht_hl_lh_uq = f_fht_hl_lh_q * q3;
f_fht_hl_hl_uq = f_fht_hl_hl_q * q2;
f_fht_hl_hh_uq = f_fht_hl_hh_q * q3;

f_fht_hh_ll_uq = f_fht_hh_ll_q * q3;           % unquantize of HH subbands
f_fht_hh_lh_uq = f_fht_hh_lh_q * q3;
f_fht_hh_hl_uq = f_fht_hh_hl_q * q3;
f_fht_hh_hh_uq = f_fht_hh_hh_q * q3;

***** Inverse Transform *****

f_far_ll = remake_3(f_far_ll, f_fht_ll_ll_uq, f_fht_ll_lh_uq, f_fht_ll_hl_uq, ...
    f_fht_ll_hh_uq, m_vec_ndx, 8);           % LL subband inv FHT
f_far_lh = remake_3(f_far_lh, f_fht_lh_ll_uq, f_fht_lh_lh_uq, f_fht_lh_hl_uq, ...
    f_fht_lh_hh_uq, m_vec_ndx, 8);           % LH subband inv FHT
f_far_hl = remake_3(f_far_hl, f_fht_hl_ll_uq, f_fht_hl_lh_uq, f_fht_hl_hl_uq, ...
    f_fht_hl_hh_uq, m_vec_ndx, 8);           % HL subband inv FHT
f_far_hh = remake_3(f_far_hh, f_fht_hh_ll_uq, f_fht_hh_lh_uq, f_fht_hh_hl_uq, ...
    f_fht_hh_hh_uq, m_vec_ndx, 8);           % HH subband inv FHT

f_far_ll_p2 = remake_3(f_far_ll_p2, f_fht_ll_ll_uq, f_fht_ll_lh_uq, ...
    f_fht_ll_hl_uq, f_fht_ll_hh_uq, m_vec_ndx, 8); % LL p2 subband inv FHT
f_far_lh_p2 = remake_3(f_far_lh_p2, f_fht_lh_ll_uq, f_fht_lh_lh_uq, ...
    f_fht_lh_hl_uq, f_fht_lh_hh_uq, m_vec_ndx, 8); % LH p2 subband inv FHT
f_far_hl_p2 = remake_3(f_far_hl_p2, f_fht_hl_ll_uq, f_fht_hl_lh_uq, ...
    f_fht_hl_hl_uq, f_fht_hl_hh_uq, m_vec_ndx, 8); % HL p2 subband inv FHT
f_far_hh_p2 = remake_3(f_far_hh_p2, f_fht_hh_ll_uq, 0, 0, ...
    f_fht_hh_hh_uq, m_vec_ndx, 8);           % HH p2 subband inv FHT

f_far_ll_p1 = remake_3(f_far_ll_p1, f_fht_ll_ll_uq, f_fht_ll_lh_uq, ...
    f_fht_ll_hl_uq, 0, m_vec_ndx, 8); % LL p1 subband inv FHT
f_far_lh_p1 = remake_3(f_far_lh_p1, f_fht_lh_ll_uq, f_fht_lh_lh_uq, ...
    0, 0, m_vec_ndx, 8); % LH p1 subband inv FHT
f_far_hl_p1 = remake_3(f_far_hl_p1, f_fht_hl_ll_uq, 0, ...
    f_fht_hl_hl_uq, 0, m_vec_ndx, 8); % HL p1 subband inv FHT
f_far_hh_p1 = remake_3(f_far_hh_p1, f_fht_hh_ll_uq, 0, ...
    0, f_fht_hh_hh_uq, m_vec_ndx, 8); % HH p1 subband inv FHT

f_3 = remake_3(f_3, f_far_ll, f_far_lh, f_far_hl, ...
    f_far_hh, m_vec_ndx, 16); % frame inv FHT with 3 layers
f_2 = remake_3(f_2, f_far_ll_p2, f_far_lh_p2, f_far_hl_p2, ...
    f_far_hh_p2, m_vec_ndx, 16); % frame inv FHT with 2 layers
f_1 = remake_3(f_1, f_far_ll_p1, f_far_lh_p1, f_far_hl_p1, ...
    f_far_hh_p1, m_vec_ndx, 16); % frame inv FHT with 1 layer

end % ends frame_type discrimination

***** Make Display Size *****

fig_3 = shape_back(f_3); % make display dimensions
fig_2 = shape_back(f_2); % make display dimensions
fig_1 = shape_back(f_1); % make display dimensions

L3 = round(fig_3); % for viewing
L2 = round(fig_2); % for viewing
L1 = round(fig_1); % for viewing

***** Calculates the mean-square-error per frame *****
if mse
    MSE_3L(i+1,1) = (sum(sum((i_present - fig_3).^2)))/176/144;
    MSE_2L(i+1,1) = (sum(sum((i_present - fig_2).^2)))/176/144;
    MSE_1L(i+1,1) = (sum(sum((i_present - fig_1).^2)))/176/144;
end % end if mse

```



```

if display

    % The following lines show the figure with 3 layers
    subplot(2,2,2)
    image(L3)
    axis off
    title('Layers 1, 2, and 3')

    % The following lines show the figure with 2 layers
    subplot(2,2,3)
    image(L2)
    title('Layers 1 and 2')
    axis off

    % The following lines show the figure with 1 layer
    subplot(2,2,4)
    image(L1)
    title('Layer 1 Only')
    axis off
    drawnow

end % ends if display

% closing reconstruction occasionally to conserve memory
if ((i==20)|(i==40)|(i==60)|(i==80)|(i==100)|(i==120)|(i==140)|(i==160)|(i==180)|...
    (i==200)|(i==220)|(i==240)|(i==260)|(i==280))
    close all
end

end % ends looping through frames

% The following lines simply rename variables to be consistent with an off-line
% evaluation program used in the development.

% LL dynamic
BITS_LL_HUFF = bits_ll_zz';

% LL static
BITS_LL_LL_3D = bits_ll_ll_r_3D';
SCAN_LL_LL_22 = ll_ll_r_22';
SCAN_LL_LL_LEN = l_p_ll_ll_r_3D';

BITS_LL_LH_3D = bits_ll_lh_r_3D';
SCAN_LL_LH_22 = ll_lh_r_22';
SCAN_LL_LH_LEN = l_p_ll_lh_r_3D';

BITS_LL_HL_3D = bits_ll_hl_r_3D';
SCAN_LL_HL_22 = ll_hl_r_22';
SCAN_LL_HL_LEN = l_p_ll_hl_r_3D';

BITS_LL_HH_3D = bits_ll_hh_r_3D';
SCAN_LL_HH_22 = ll_hh_r_22';
SCAN_LL_HH_LEN = l_p_ll_hh_r_3D';

% LH both types of slide
BITS_LH_LL_3D = bits_lh_ll_r_3D';
SCAN_LH_LL_22 = lh_ll_r_22';
SCAN_LH_LL_LEN = l_p_lh_ll_r_3D';

BITS_LH_LH_3D = bits_lh_lh_r_3D';
SCAN_LH_LH_22 = lh_lh_r_22';
SCAN_LH_LH_LEN = l_p_lh_lh_r_3D';

BITS_LH_HL_3D = bits_lh_hl_r_3D';
SCAN_LH_HL_22 = lh_hl_r_22';
SCAN_LH_HL_LEN = l_p_lh_hl_r_3D';

BITS_LH_HH_3D = bits_lh_hh_r_3D';
SCAN_LH_HH_22 = lh_hh_r_22';
SCAN_LH_HH_LEN = l_p_lh_hh_r_3D';

% HL both types of slides

```

```

BITS_HL_LL_3D = bits_hl_ll_v_3D';
SCAN_HL_LL_22 = hl_ll_v_22';
SCAN_HL_LL_LEN = 1_p_hl_ll_v_3D';

BITS_HL_LH_3D = bits_hl_lh_v_3D';
SCAN_HL_LH_22 = hl_lh_v_22';
SCAN_HL_LH_LEN = 1_p_hl_lh_v_3D';

BITS_HL_HL_3D = bits_hl_hl_v_3D';
SCAN_HL_HL_22 = hl_hl_v_22';
SCAN_HL_HL_LEN = 1_p_hl_hl_v_3D';

BITS_HL_HH_3D = bits_hl_hh_v_3D';
SCAN_HL_HH_22 = hl_hh_v_22';
SCAN_HL_HH_LEN = 1_p_hl_hh_v_3D';

% HH from dynamic
BITS_HH_3D = bits_hh_r_3D';
SCAN_HH_22 = hh_r_22';
SCAN_HH_LEN = 1_p_hh_r_3D';

% HH from static
BITS_HH_LL_3D = bits_hh_ll_r_3D';
SCAN_HH_LL_22 = hh_ll_r_22';
SCAN_HH_LL_LEN = 1_p_hh_ll_r_3D';

BITS_HH_LH_3D = bits_hh_lh_r_3D';
SCAN_HH_LH_22 = hh_lh_r_22';
SCAN_HH_LH_LEN = 1_p_hh_lh_r_3D';

BITS_HH_HL_3D = bits_hh_hl_r_3D';
SCAN_HH_HL_22 = hh_hl_r_22';
SCAN_HH_HL_LEN = 1_p_hh_hl_r_3D';

BITS_HH_HH_3D = bits_hh_hh_r_3D';
SCAN_HH_HH_22 = hh_hh_r_22';
SCAN_HH_HH_LEN = 1_p_hh_hh_r_3D';

% saves parameters for evaluation later
if write
    s = char('g:\thesis\BR');
    s = strcat(s,num2str(br));
    save(s, 'm_mat_ndx','BITS_*','MSE_*','SCAN_*','layer')
end % if write

```

```

function [output] = dct_of_fht(input,m_vec_ndx)

% performs the 2D DCT of input. m_vec_ndx identifies where this operation needs
% to be performed.

output = zeros(792,8);
offset = -8;

for ndx = 1:99
    offset = offset + 8;

    if m_vec_ndx(ndx)
        output(offset+1:offset+8,:) = dct2(input(offset+1:offset+8,:));
    end
end

end

```

```

function [f_fht_ll,f_fht_lh,f_fht_hl,f_fht_hh] = fht(f_vec,m_vec_ndx,in)

% Performs the FHT of the appropriate IN x IN macroblocks of F_VEC as
% specified by M_VEC_NDX. Returns four sets of 99 IN/2 x IN/2 matrices,
% each stacked into one big 99*IN/2 x IN/2 matrix. The places
% where the fht was not performed are filled with zeroes as place-holders.

half = in/2;
f_fht_ll = zeros(99*half,half);
f_fht_lh = zeros(99*half,half);
f_fht_hl = zeros(99*half,half);
f_fht_hh = zeros(99*half,half);
mask_lh = [1 1;-1 -1];
mask_hl = [1 -1;1 -1];
mask_hh = [1 -1;-1 1];

offset = -in;

for ndx = 1:99
    offset= offset+in;
    oso2 = offset/2;

    if m_vec_ndx(ndx)

        for rndx = 1:half

            for cndx = 1:half
                f_fht_ll(rndx+oso2,cndx) = ...
                    sum(sum(f_vec(rndx*2-1+offset:rndx*2+offset,cndx*2-1:cndx*2)))/4;
                f_fht_lh(rndx+oso2,cndx) = sum(sum(mask_lh .* ...
                    f_vec(rndx*2-1+offset:rndx*2+offset,cndx*2-1:cndx*2)))/4;
                f_fht_hl(rndx+oso2,cndx) = sum(sum(mask_hl .* ...
                    f_vec(rndx*2-1+offset:rndx*2+offset,cndx*2-1:cndx*2)))/4;
                f_fht_hh(rndx+oso2,cndx) = sum(sum(mask_hh .* ...
                    f_vec(rndx*2-1+offset:rndx*2+offset,cndx*2-1:cndx*2)))/4;
            end
        end
    end
end

end

function [bits] = get_bits_Huff(parsed)

% Uses Huffman table to get bits for JPEG-based compression of PARSED.

global HUFF_TABLE

bits = 0;
[r,c] = size(parsed);

for ndx = 1:r

    while(parsed(ndx,1) >= 15)
        bits = bits + 11;
        parsed(ndx,1) = parsed(ndx,1) - 15;
    end

    table_row = find((HUFF_TABLE(:,2) == parsed(ndx,1)) & ...
        (HUFF_TABLE(:,3) == parsed(ndx,2)));
    bits = bits + HUFF_TABLE(table_row,4) + parsed(ndx,2);
end
end

```

```
bits = bits + 99*4;
```

```
function [bits,count] = get_bits2(parsed,kind)
```

```
% Uses PARSED to fetch bits from custom VLC tables  
% KIND will be 1 for static scenes  
% KIND will be 0 for dynamic scenec
```

```
global VLC_DYN VLC_STA
```

```
bits = 0;  
count = 0;  
parsed = abs(parsed);  
[r,c] = size(parsed);
```

```
if kind
```

```
for ndx = 1:r
```

```
    poss_rows = find(VLC_STA(:,2) == parsed(ndx,1));  
    start = poss_rows(1);  
    poss_rows = find(VLC_STA((poss_rows(1):poss_rows(length(poss_rows))),3) ==...  
        parsed(ndx,2));
```

```
    if ~(isempty(poss_rows))  
        poss_rows = poss_rows + start - 1;  
        start = poss_rows(1);  
    end
```

```
    if ~(isempty(poss_rows))  
        poss_rows = find(VLC_STA((poss_rows(1):poss_rows(length(poss_rows))),4) ==...  
            parsed(ndx,3));  
        poss_rows = poss_rows + start - 1;  
    end
```

```
    if ~(isempty(poss_rows))  
        bits = bits + VLC_STA(poss_rows,5);  
    else  
        bits = bits + 22;  
        count = count + 1;  
    end
```

```
end
```

```
else
```

```
for ndx = 1:r
```

```
    poss_rows = find(VLC_DYN(:,2) == parsed(ndx,1));  
    start = poss_rows(1);  
    poss_rows = find(VLC_DYN((poss_rows(1):poss_rows(length(poss_rows))),3) ==...  
        parsed(ndx,2));
```

```
    if ~(isempty(poss_rows))  
        poss_rows = poss_rows + start - 1;  
        start = poss_rows(1);  
    end
```

```
    if ~(isempty(poss_rows))  
        poss_rows = find(VLC_DYN((poss_rows(1):poss_rows(length(poss_rows))),4) ==...  
            parsed(ndx,3));  
        poss_rows = poss_rows + start - 1;  
    end
```

```
    if ~(isempty(poss_rows))  
        bits = bits + VLC_DYN(poss_rows,5);  
    else  
        bits = bits + 22;  
        count = count + 1;  
    end
```

```

        end

    end

end
bits = bits + 99;

function [f] = get_next_image(num)

% Gets next frame as a .bmp file converts to form needed in MATLAB

s = char('g:\pictures\Head');
fn = strcat(s,num2str(num));
f = imread(fn,'bmp');
f = double(f(:,:,1));

function [f] = get_next_image_2(num)

% Gets next frame as a .bmp file converts to form needed in MATLAB

s = char('g:\pictures\ncaa');
fn = strcat(s,num2str(num));
f = imread(fn,'bmp');
f = double(f(:,:,1));

function [Q] = get_Q1_matrix(q1)

% makes the JPEG standard quantization matrix and multiplies it by q1.
% q1 = 16 will result in no scaling of the matrix when coupled with the rest
% of the code. q1 < 16 is finer quantization, i.e. less quantization noise results.

Q = [16 11 10 16 24 40 51 61;
     12 12 14 19 26 58 60 55;
     14 13 16 24 40 57 69 56;
     14 17 22 29 51 87 80 62;
     18 22 37 56 68 109 103 77;
     24 35 55 64 81 104 113 92;
     49 64 78 87 103 121 120 101;
     72 92 95 98 112 100 103 99] .* q1;

function [out] = get_qd_entryf(flag,default,entry,delta_Binter,MBnum,beta)

% selects the appropriate quantizer triplet based on the input parameters
% FLAG implies the first frame following a scene change frame. DEFAULT is the
% choice of triplet based on test sequences and serves as a starting point for a
% new sequence. ENTRY hold the table entry from the previous frame. The remaining
% parameters ara as defined in the thesis.

global QD_TABLE

if (flag)

```

```

    out = min(find(default > QD_TABLE(:,4)));
else
    deltaQ = fix(delta_Binter/MBnum/beta);
    out = entry + deltaQ;
    if (out > 17)
        out = 17;
    end
    if (out < 1)
        out = 1;
    end
end
end

```

```

function [run] = get_run(seq_to_code,len)

```

```

% Called by the parsing functions PARSE_3D and PARSE_HUFF, this function obtains
% the RUN field for RLE.

```

```

run = zeros(len,1);

```

```

count = 0;
place = 1;
mdx = 1;

```

```

while (mdx <= length(seq_to_code))
    if seq_to_code(mdx)
        place = place + 1;
        mdx = mdx + 1;
    else
        while (seq_to_code(mdx) == 0)
            mdx = mdx + 1;
            count = count + 1;
        end
        run(place) = count;
        count = 0;
        place = place + 1;
        mdx = mdx + 1;
    end
end
end

```

```

function [output] = invdct_of_fht(input,m_vec_ndx)

```

```

% Performs the inverse 2D DCT. M_VEC_NDX identifies where this operation needs to be
% performed.

```

```

output = zeros(792,8);
offset = -8;

```

```

for ndx = 1:99
    offset = offset + 8;

```

```

    if m_vec_ndx(ndx)
        output(offset+1:offset+8,:) = idct2(input(offset+1:offset+8,:));
    end
end

```

```

end

```

```

function [m_vec_ndx,byAge,b_count,mb_count] = m_blk_id_xr(f1,f2,T)

% Figures out which 16x16 macroblocks of the 144x176 image need to be further
% processed via an absolute sum of differences between the last frame f1 and
% the current frame f2. m_vec_ndx is 99x1 vector of 0 or 1 raster scanned.
% T is the threshold utilized. byAge is 1 if macroblocks are selected only due
% to aging. byAge is 0 otherwise. b_count and mb_count were used in refining the
% search sequence. b_count is "block count." mb_count is "macroblock count." As
% are artifacts now, they are commented-out.

global LAST RV

%b_count = 0;
%mb_count = 0;
r_count = 0;
m_vec_ndx = zeros(99,1);

for ndx = 1:99
    if (RV(ndx) == 0)
        m_vec_ndx(ndx) = 1;
        RV(ndx) = floor(21*rand);
    else
        RV(ndx) = RV(ndx) - 1;
    end
end

byAge1 = sum(m_vec_ndx);

for rndx = 1:16:1584
    r_count = r_count + 1;

    if (~m_vec_ndx(r_count))
        go = 1;
        if ((LAST(r_count) == 1) & (go))
            for cndx = 1
                f1_8x8 = f1(rndx:rndx+7,cndx:cndx+7);
                f2_8x8 = f2(rndx:rndx+7,cndx:cndx+7);
                asd = abs(sum(sum(f1_8x8-f2_8x8)));

                if (asd > T)
                    m_vec_ndx(r_count) = 1; % ID's position
                    %mb_count = mb_count + 1;
                    %b_count = b_count + 1;
                    LAST(r_count) = 1;
                    go = 0;
                    break; % gets out of the inner loop if justified now
                end

                f1_8x8 = f1(rndx+8:rndx+15,cndx+8:cndx+15);
                f2_8x8 = f2(rndx+8:rndx+15,cndx+8:cndx+15);
                asd = abs(sum(sum(f1_8x8-f2_8x8)));

                if (asd > T)
                    m_vec_ndx(r_count) = 1; % ID's position
                    %mb_count = mb_count + 1;
                    %b_count = b_count + 2;
                    LAST(r_count) = 3;
                    go = 0;
                    break; % gets out of the inner loop if justified now
                end

                f1_8x8 = f1(rndx:rndx+7,cndx+8:cndx+15);
                f2_8x8 = f2(rndx:rndx+7,cndx+8:cndx+15);
                asd = abs(sum(sum(f1_8x8-f2_8x8)));

                if (asd > T)
                    m_vec_ndx(r_count) = 1; % ID's position
                    %mb_count = mb_count + 1;
                    %b_count = b_count + 3;
                    LAST(r_count) = 2;
                end
            end
        end
    end
end

```

```

        go = 0;
        break; % gets out of the inner loop if justified now
    end

    f1_8x8 = f1(rndx+8:rndx+15,cndx:cndx+7);
    f2_8x8 = f2(rndx+8:rndx+15,cndx:cndx+7);
    asd = abs(sum(sum(f1_8x8-f2_8x8)));

    if (asd > T)
        m_vec_ndx(r_count) = 1; % ID's position
        %mb_count = mb_count + 1;
        %b_count = b_count + 4;
        LAST(r_count) = 4;
        go = 0;
    end

end %for cndx
end % if LAST

if ((LAST(r_count) == 2) & (go))
    for cndx = 1
        f1_8x8 = f1(rndx:rndx+7,cndx+8:cndx+15);
        f2_8x8 = f2(rndx:rndx+7,cndx+8:cndx+15);
        asd = abs(sum(sum(f1_8x8-f2_8x8)));

        if (asd > T)
            m_vec_ndx(r_count) = 1; % ID's position
            %mb_count = mb_count + 1;
            %b_count = b_count + 1;
            LAST(r_count) = 2;
            go = 0;
            break; % gets out of the inner loop if justified now
        end

        f1_8x8 = f1(rndx+8:rndx+15,cndx:cndx+7);
        f2_8x8 = f2(rndx+8:rndx+15,cndx:cndx+7);
        asd = abs(sum(sum(f1_8x8-f2_8x8)));

        if (asd > T)
            m_vec_ndx(r_count) = 1; % ID's position
            %mb_count = mb_count + 1;
            %b_count = b_count + 2;
            LAST(r_count) = 4;
            go = 0;
            break; % gets out of the inner loop if justified now
        end

        f1_8x8 = f1(rndx+8:rndx+15,cndx+8:cndx+15);
        f2_8x8 = f2(rndx+8:rndx+15,cndx+8:cndx+15);
        asd = abs(sum(sum(f1_8x8-f2_8x8)));

        if (asd > T)
            m_vec_ndx(r_count) = 1; % ID's position
            %mb_count = mb_count + 1;
            %b_count = b_count + 3;
            LAST(r_count) = 3;
            go = 0;
            break; % gets out of the inner loop if justified now
        end

        f1_8x8 = f1(rndx:rndx+7,cndx:cndx+7);
        f2_8x8 = f2(rndx:rndx+7,cndx:cndx+7);
        asd = abs(sum(sum(f1_8x8-f2_8x8)));

        if (asd > T)
            m_vec_ndx(r_count) = 1; % ID's position
            %mb_count = mb_count + 1;
            %b_count = b_count + 4;
            LAST(r_count) = 1;
            go = 0;
        end
    end
end

```



```

    end %for cndx
end % if LAST

if ((LAST(r_count) == 3) & (go))
    for cndx = 1
        f1_8x8 = f1(rndx+8:rndx+15,cndx+8:cndx+15);
        f2_8x8 = f2(rndx+8:rndx+15,cndx+8:cndx+15);
        asd = abs(sum(sum(f1_8x8-f2_8x8)));

        if (asd > T)
            m_vec_ndx(r_count) = 1; % ID's position
            %mb_count = mb_count + 1;
            %b_count = b_count + 1;
            LAST(r_count) = 3;
            go = 0;
            break; % gets out of the inner loop if justified now
        end

        f1_8x8 = f1(rndx:rndx+7,cndx:cndx+7);
        f2_8x8 = f2(rndx:rndx+7,cndx:cndx+7);
        asd = abs(sum(sum(f1_8x8-f2_8x8)));

        if (asd > T)
            m_vec_ndx(r_count) = 1; % ID's position
            %mb_count = mb_count + 1;
            %b_count = b_count + 2;
            LAST(r_count) = 1;
            go = 0;
            break; % gets out of the inner loop if justified now
        end

        f1_8x8 = f1(rndx+8:rndx+15,cndx:cndx+7);
        f2_8x8 = f2(rndx+8:rndx+15,cndx:cndx+7);
        asd = abs(sum(sum(f1_8x8-f2_8x8)));

        if (asd > T)
            m_vec_ndx(r_count) = 1; % ID's position
            %mb_count = mb_count + 1;
            %b_count = b_count + 3;
            LAST(r_count) = 4;
            go = 0;
            break; % gets out of the inner loop if justified now
        end

        f1_8x8 = f1(rndx:rndx+7,cndx+8:cndx+15);
        f2_8x8 = f2(rndx:rndx+7,cndx+8:cndx+15);
        asd = abs(sum(sum(f1_8x8-f2_8x8)));

        if (asd > T)
            m_vec_ndx(r_count) = 1; % ID's position
            %mb_count = mb_count + 1;
            %b_count = b_count + 4;
            LAST(r_count) = 2;
            go = 0;
        end

    end

end %for cndx
end % if LAST

if ((LAST(r_count) == 4) & (go))
    for cndx = 1
        f1_8x8 = f1(rndx+8:rndx+15,cndx:cndx+7);
        f2_8x8 = f2(rndx+8:rndx+15,cndx:cndx+7);
        asd = abs(sum(sum(f1_8x8-f2_8x8)));

        if (asd > T)
            m_vec_ndx(r_count) = 1; % ID's position
            %mb_count = mb_count + 1;
            %b_count = b_count + 1;
            LAST(r_count) = 4;
        end
    end
end

```

```

        go = 0;
        break; % gets out of the inner loop if justified now
    end

    f1_8x8 = f1(rndx:rndx+7,cndx+8:cndx+15);
    f2_8x8 = f2(rndx:rndx+7,cndx+8:cndx+15);
    asd = abs(sum(sum(f1_8x8-f2_8x8)));

    if (asd > T)
        m_vec_ndx(r_count) = 1; % ID's position
        %mb_count = mb_count + 1;
        %b_count = b_count + 2;
        LAST(r_count) = 2;
        go = 0;
        break; % gets out of the inner loop if justified now
    end

    f1_8x8 = f1(rndx:rndx+7,cndx:cndx+7);
    f2_8x8 = f2(rndx:rndx+7,cndx:cndx+7);
    asd = abs(sum(sum(f1_8x8-f2_8x8)));

    if (asd > T)
        m_vec_ndx(r_count) = 1; % ID's position
        %mb_count = mb_count + 1;
        %b_count = b_count + 3;
        LAST(r_count) = 1;
        go = 0;
        break; % gets out of the inner loop if justified now
    end

    f1_8x8 = f1(rndx+8:rndx+15,cndx+8:cndx+15);
    f2_8x8 = f2(rndx+8:rndx+15,cndx+8:cndx+15);
    asd = abs(sum(sum(f1_8x8-f2_8x8)));

    if (asd > T)
        m_vec_ndx(r_count) = 1; % ID's position
        %mb_count = mb_count + 1;
        %b_count = b_count + 4;
        LAST(r_count) = 3;
        go = 0;
    end

    end %for cndx
end % if LAST

end %if ~m_vec_ndx

end % for rndx

byAge2 = sum(m_vec_ndx);
byAge = (byAge1 == byAge2);

```

```

function [table] = make_HAC_table();

% Generates the Huffman VLC table

vec1 = ones(10,1);
vec2 = (1:10)';

index = (1:162)';
runn = [0;vec1*0;vec1;vec1*2;vec1*3;vec1*4;vec1*5;vec1*6;
vec1*7;vec1*8;vec1*9;vec1*10;vec1*11;vec1*12;vec1*13;
vec1*14;vec1*15;15];
siz = [0;vec2;vec2;vec2;vec2;vec2;vec2;vec2;vec2;vec2;vec2;
vec2;vec2;vec2;vec2;vec2;0;vec2];
cw_len = [0;2;2;3;4;5;7;8;10;16;16;4;5;7;9;11;16;16;16;16];

```

```

16;5;8;10;12;ones(6,1)*16;6;9;12;ones(7,1)*16;6;10;
ones(8,1)*16;8;11;ones(8,1)*16;7;12;ones(8,1)*16;8;
12;ones(8,1)*16;9;ones(9,1)*16;9;ones(9,1)*16;9;
ones(9,1)*16;10;ones(9,1)*16;10;ones(9,1)*16;11;
ones(19,1)*16;11;ones(10,1)*16];
table = [index, runn, siz, cw_len];

```

```

function [a] = make_it_compact(big,index,size)

```

```

% gets rid of trailing zeros in the vector BIG that resulted from scanning 99 matrices
% of dimensions SIZExSIZE. INDEX holds the position of the last non-zero entry in each of
% the 99 matrices.

```

```

entry = size^2;
offset = -entry;
a = [];
for ndx = 1:99
    offset = entry + offset;
    if isinf(index(ndx))
        a = [a ; inf];
    else
        a = [a ; [big(offset+1:offset+index(ndx))]];
    end
end
end

```

```

function [parsed] = parse_3D(vector,index)

```

```

% RLE's VECTOR into the {last,run,level} format. INDEX is the position of the last non
% zero entity in each of the 99 matrices.

```

```

last = [];
level = [];
run = [];

for ndx = 1:99
    if isinf(index(ndx))
        index(ndx) = 1;
    end
    point = sum(index(1:ndx));
    seq_to_code = vector(point-index(ndx)+1:point);
    len = length(seq_to_code);
    if ((len == 1) & isinf(seq_to_code))
        last = [last;0];
        level = [level;0];
        run = [run;0];
    else
        dummy = seq_to_code(find(seq_to_code));
        level = [level;dummy];
        last = [last;zeros(length(dummy)-1,1);1];
        this_run = get_run(seq_to_code,length(dummy));
        run = [run;this_run];
    end
end
end

parsed = [last,run,level];

```

```

function [parsed] = parse_Huff(vector,index)

% Parses VECTOR into the JPEG format. INDEX holds the position of the last non-zero
% value of each of the 99 matrices.

last = [];
level = [];
run = [];

for ndx = 1:99
    if isinf(index(ndx))
        index(ndx) = 1;
    end
    point = sum(index(1:ndx));
    seq_to_code = vector(point-index(ndx)+1:point);
    len = length(seq_to_code);
    if ((len == 1) & isinf(seq_to_code))
        level = [level;0];
        run = [run;0];
    else
        dummy = seq_to_code(find(seq_to_code));
        level = [level;dummy];
        this_run = get_run(seq_to_code,length(dummy));
        run = [run;this_run];
    end
end

level = abs(level);
S = zeros(length(level),1) ;

for mdx = 1:length(level)
    if level(mdx)
        S(mdx) = length(dec2bin(level(mdx)));
    else
        S(mdx) = 0;
    end
end

parsed = [run,S];

```

```

function [ll_q] = quantizer_ll(ll,Q,m_vec_ndx)

% Quantizes matrix ll with quantization matrix Q. M_VEC_NDX identifies
% where this quantization need be performed.
%
% see UNQUANTIZE_LL

ll_q = zeros(792,8);
offset = -8;
ll = ll* 16;

for ndx = 1:99
    offset = offset + 8;

    if m_vec_ndx(ndx)
        ll_q(offset+1:offset+8,:) = round(ll(offset+1:offset+8,:) ./ Q);
    end
end

```

```

function [out,rast] = raster(mat,in)

% Horizontal raster scans the input matrix MAT of dimensions INxIN.

entry = in^2;
offset = -entry;
mat = mat.';
rast = reshape(mat,entry*99,1);

for ndx = 1:99
    offset = offset+entry;
    dummy = max(find(rast(offset+1:offset+entry)));

    if isempty(dummy)
        out(ndx) = inf;
    else
        out(ndx) = dummy;
    end
end

out = out.';

function [out] = remake_3(f_3,f_fht_ll,f_fht_lh,f_fht_hl,f_fht_hh,m_vec_ndx,in)

% Performs the inverse FHT. F_3 is the present content of the reconstructed image.
% The next four parameters are the subbands that update this content as dictated
% by the content of M_VEC_NDX. INxIN is the matrix dimensions.

half = in/2;

if (f_fht_ll == 0)
    f_fht_ll = zeros(99*half,half);
end

if (f_fht_lh == 0)
    f_fht_lh = zeros(99*half,half);
end

if (f_fht_hl == 0)
    f_fht_hl = zeros(99*half,half);
end

if (f_fht_hh == 0)
    f_fht_hh = zeros(99*half,half);
end

B = [1 1 1 1;1 1 -1 -1;1 -1 1 -1;1 -1 -1 1];
x = zeros(4,1);
a = zeros(4,1);
offset = -half;
out = zeros(99*in,in);
f_3 = f_3 /4;

for ndx = 1:99
    offset = offset + half;
    ost2 = offset*2;

    if m_vec_ndx(ndx)

        for rndx = 1:half

            for cndx = 1:half
                x = [f_fht_ll(rndx+offset,cndx);

```

```

        f_fht_lh(rndx+offset,cndx);
        f_fht_hl(rndx+offset,cndx);
        f_fht_hh(rndx+offset,cndx)];
    a = B \ x;
    f_3(rndx*2-1+ost2:rndx*2+ost2,cndx*2-1:cndx*2) = ...
        [a(1) a(2); a(3) a(4)];

    end

end

end

end

out = f_3*4;

```

```

function [f_out] = shape(f_in)

% Shapes the 144x176 f_in into a 1584x16 matrix taken 16 rows at a time
% left to right, top to bottom. (raster scans the macroblocks.)

f_out = [];

for rndx = [1 17 33 49 65 81 97 113 129]
    for cndx = [1 17 33 49 65 81 97 113 129 145 161]
        f_out = [f_out;[f_in(rndx:rndx+15,cndx:cndx+15)]];
    end
end

```

```

function [f_out] = shape_back(f_in)

% Shapes the 1584x16 matrix back into a 144x176 image.

f_out = [];
f_row = [];
offset = -176;

for i = 1:9
    offset = offset + 176;
    for rndx = ([1 17 33 49 65 81 97 113 129 145 161] + offset)
        f_row = [f_row,[f_in(rndx:rndx+15,:)]];
    end
    f_out = [f_out;f_row];
    f_row = [];
end

```

```

function [ll] = unquantize_ll(ll_q,Q,m_vec_ndx)

% Unquantizes ll_q with quantization matrix Q. M_VEC_NDX identifies where this
% unquantization need be performed.
%
% see QUANTIZE_LL

ll = zeros(792,8);
offset = -8;

```

```

for ndx = 1:99
    offset = offset + 8;

    if m_vec_ndx(ndx)
        ll(offset+1:offset+8,:) = ll_q(offset+1:offset+8,:) .* Q;
    end

end

ll = ll / 16;

```

```

function [out,vert] = vertical(mat,in)

```

```

% raster scans vertically top to bottom 99 matrices of size INxIN contained in MAT.

```

```

offset = -in;
offset2 = -in^2;
vert = zeros(offset2*99,1);

```

```

if (in == 8)
    for ndx = 1:99
        offset = offset + 8;
        offset2 = offset2 + 64;
        vert(offset2+1:offset2+64,1)=[mat(offset+1:offset+8,1);mat(offset+1:offset+8,2);
            mat(offset+1:offset+8,3);mat(offset+1:offset+8,4);mat(offset+1:offset+8,5);
            mat(offset+1:offset+8,6);mat(offset+1:offset+8,7);mat(offset+1:offset+8,8)];
        dummy = max(find(vert(offset2+1:offset2+64)));

        if isempty(dummy)
            out(ndx) = inf;
        else
            out(ndx) = dummy;
        end
    end

```

```

end

```

```

else

```

```

    for ndx = 1:99
        offset = offset + 4;
        offset2 = offset2 + 16;
        vert(offset2+1:offset2+16,1)=[mat(offset+1:offset+4,1);mat(offset+1:offset+4,2);
            mat(offset+1:offset+4,3);mat(offset+1:offset+4,4)];
        dummy = max(find(vert(offset2+1:offset2+16)));

        if isempty(dummy)
            out(ndx) = inf;
        else
            out(ndx) = dummy;
        end
    end

```

```

end

```

```

end

```

```

out = out.';

```

```

function [place,out] = zzb(bigmat,M)

```

```

% zigzag scans the 99 matrices of size MxM contained in BIGMAT.

```

```

vec = zeros(M*M,1);
loop = 0;
out = [];

for ndx = 1:M:M*99
    loop = loop + 1;
    mat = bigmat(ndx:ndx+M-1,:);
    vec(1) = mat(1,1);

    % start scan at
    x = 2;
    y = 1;
    index = 2;

    % initial scan direction
    xstep = -1;
    ystep = 1;

    % process each interior diagonal
    for i=2:(2*M-2)

        % determine diagonal length
        if (i > M)
            len = 2*M - i;
        else
            len = i;
        end

        % run the diagonal
        for j = 1:len

            vec(index) = mat(y,x);

            % move to next point
            x = x + xstep;
            y = y + ystep;
            index = index + 1;
        end

        % set up next pass
        xstep = -xstep;
        ystep = -ystep;

        if (x == 0)

            if (y <= M)
                x = 1;
            else
                x = x + 2;
                y = M;
            end

        elseif (x > M)
            x = M;
            y = y + 2;
        end

        if (y == 0)

            if (x <= M)
                y = 1;
            else
                x = M;
                y = y + 2;
            end

        elseif (y > M)
            y = M;
            x = x + 2;
        end

    end
end

```



```
end

vec(M*M) = mat(M,M);
dummy = max(find(vec));

if isempty(dummy)
    place(loop) = inf;
else
    place(loop) = dummy;
end

out = [out;vec];
end

place = place';
```

## LIST OF REFERENCES

- [1] ADM A. Clemins, "IT-21: Information Technology for the 21<sup>st</sup> Century," presented at *AFCEA West '98*, San Diego, CA, Jan. 14-16, 1998.
- [2] Chief of Naval Operations, N60 - Fleet and Allied C4 Requirements Division IT-21 Homepage, <http://copernicus.hq.navy.mil/divisions/n6/n60/it21/>.
- [3] R. Weekly, "Guaranteeing Fair Access for Multimedia Traffic Using the SMART Algorithm for Multicast ATM Connections," Master's Thesis, Naval Postgraduate School, September 1999.
- [4] K. Rao and J. Hwang, *Techniques & Standards for Image, Video & Audio Coding*, Upper Saddle River, NJ: Prentice-Hall, 1996.
- [5] M. Riley and I. Richardson, *Digital Video Communications*, Norwood, MA: Artech House, Inc., 1997.
- [6] M. H. Willebeek-LeMair, Z. Shae, and Y. Chang, "Robust H.263 Video Coding for Transmission Over the Internet," IBM Res. Rep. RC20532, Aug. 1996.
- [7] S. McCanne, M. Vetterli, and V. Jacobson, "Receiver-driven layered multicast," *Proc. SIGCOMM '96*, ACM, Stanford, CA, Aug. 1996.
- [8] V. Rhee and J. D. Gibson, "Rate-Constrained Two-Layer Coding of H.261 Video," *28th Asilomar Conference on Signals, Systems, & Computers*, Pacific Grove, CA, 31 Oct - 2 Nov, 1994.
- [9] R. Parker, "Robust Transmission of Layered Video for Low Bit Rate Tactical Video Conferencing Applications," Ph.D. Dissertation, Naval Postgraduate School, September 1999.
- [10] R. Parker, S. Skretkowicz, and M. Tummala, "Low-Complexity, Adaptive Layered Video Coder for Video Teleconferencing," To be presented at *33rd Asilomar Conference on Signals, Systems, & Computers*, Pacific Grove, CA, 24-27 Oct, 1999.
- [11] C. W. Therrien, *Discrete Random Signals and Statistical Signal Processing*, Upper Saddle River, NJ: Prentice-Hall, 1992.
- [12] Z. Xiong, K. Ramchandran, M. T. Orchard, and Y. Zhang, "A comparative study of DCT and wavelet based coding," *Proc. of the IEEE International Symposium on Circuits and Systems*, Monterey, CA, June 1-3, 1998.

- [13] G. Kaiser, "The Fast Haar Transform," *IEEE Potentials*, vol. 17, no. 2, pp.34-36, 1998.
- [14] S. McCanne, M. Vetterli, and V. Jacobson, "Low-Complexity Video Coding for Receiver-Driven Layered Multicast," *IEEE J. of Select. Areas in Comm.*, vol. 15, no. 6, pp. 983-1001, 1997.
- [15] J. Gibson, T. Berger, T. Lookabaugh, D. Lindbergh, and R. Baker, *Digital Compression for Multimedia: Principles and Standards*, San Francisco, CA: Morgan Kaufmann Publishers, Inc., 1998.
- [16] T. Eude, et al., "On the Distribution of DCT Coefficients," *ICASSP '94*, vol. 5, pp. 365-368, Adelaide, Australia, Apr. 1994.
- [17] M. Vetterli and J. Kovacevic, *Wavelets and Subband Coding*, Upper Saddle River, NJ: Prentice-Hall, 1995.
- [18] R. Frederick, "Experiences with real-time software video compression," *Proc. 6<sup>th</sup> Int. Workshop Packet Video*, Portland, OR, Sept. 1994.
- [19] Telenor Research, *Video Codec Test Model, Tmn5*, Jan. 1995.
- [20] V. Rhee and J. D. Gibson, "Block-Level Refinement of Motion Description in Layered H.261 Video," 29th Annual Asilomar Conference on Signals, Systems and Computers, Pacific Grove, CA, 29 Oct - 1 Nov 1995.
- [21] P. Bahl and W. Hsu, "Adaptive Region-Based Multi-Scaled Motion-Compensated Video Coding for Error Prone, Bandwidth-Limited Communication Channels," *Proc. Conf. Broadband Networking Technologies, SPIE's Int'l Symp. Voice, Video and Data Communications*, Dallas, TX, Nov. 1997.
- [22] Brown, T. B., Cantrell, P. E., and Gibson, J. D., "Multicast Layered Video Teleconferencing: Overcoming Bandwidth Heterogeneity," *1996 Int. Conf. on Image Processing*, Lausanne, Switzerland.
- [23] H. Gharavi and M. H. Partovi, "Video coding and distribution over ATM for multipoint teleconferencing," *Proc. GLOBECOM '93*, Houston, TX, Dec. 1993.
- [24] G. J. Sullivan and T. Wiegand, "Rate-Distortion Optimization for Video Compression," *IEEE Signal Processing Magazine*, vol. 15, no. 6, pp. 74-90, Nov. 1998.
- [25] C. Diab, R. Prost, and R. Goutte, "Block-Adaptive Subband Coding of Images," *ICASSP*, 1990, pp. 2093-2096.

- [26] ITU-T Recommendation H.263, *Video Coding for Low Bitrate Communication*, 1996.



## INITIAL DISTRIBUTION LIST

1. Defense Technical Information Center .....2  
8725 John J. Kingman Rd., Ste 0944  
Ft. Belvoir, VA 22060-6218
2. Dudley Knox Library .....2  
Naval Postgraduate School  
411 Dyer Rd.  
Monterey, CA 93943-5101
3. Chairman, Code EC ..... 1  
Department of Electrical and Computer Engineering  
Naval Postgraduate School  
Monterey, CA 93943-5121
4. Prof. Murali Tummala, Code EC/Tu ..... 4  
Department of Electrical and Computer Engineering  
Naval Postgraduate School  
Monterey, CA 93943-5121
5. LCDR Robert E. Parker, U.S. Navy ..... 1  
2452 Ponte Vedra Way  
Chula Vista, CA 91915
6. Dr. Don Gingras ..... 1  
SPAWAR Systems Center San Diego, Code D8805  
Communication and Information Systems Department  
San Diego, CA 92152-5001
7. LT Steven J. Skretkowicz, U.S. Navy ..... 3  
519 West "L" Street  
North Little Rock, AR 72116